

THESIS

A FLOOR SLAB DAMPER AND ISOLATION HYBRID SYSTEM OPTIMIZED FOR
SEISMIC VIBRATION CONTROL

Submitted by

Travis J. Engle

Department of Civil and Environmental Engineering

In partial fulfillment of the requirements

For the Degree of Master of Science

Colorado State University

Fort Collins, Colorado

Summer 2014

Master's Committee:

Advisor: Hussam N. Mahmoud

Bogusz J. Bienkiewicz
Caroline M. Clevenger

Copyright by Travis Engle 2014

All Right Reserved

ABSTRACT

A FLOOR SLAB DAMPER AND ISOLATION HYBRID SYSTEM OPTIMIZED FOR SEISMIC VIBRATION CONTROL

Damage and fatigue to structures due to earthquake loading has cost millions of dollars in repair and reconstruction over the last century. Limited reduction in seismic excitation has been gained through base isolation and tuned mass damping theories. Both theories have limitations that reduce the effectiveness of the system. Getting around these limitations is necessary to accomplish the goals of the study. An innovative design utilizing aspects of both isolation and tuned mass damping is developed by allowing the floor slabs of the structure to displace relative to the frame of the structure. Equations of motion are developed to model this unique system. This system is then optimized and the efficiency of the design is assessed. The reduction of this response over a range of frequencies is the goal of this optimization and thesis.

Vibration control is achieved in this system by attempting to remove the mass of the floor slabs from the inertia of the system. When excited, the structure moves while the slabs remain stationary. This greatly reduces the stress on the frame. In this way, the design is a friction isolation and damping hybrid system. The relative motion between the frame and the slab has to be controlled. To control its displacement, the slab is supported by a curved support and bumpers are added. These additions utilize aspects of translational and pendulum tuned mass damper systems and force the slab back to its original location after excitation. This system imitates multi-tuned mass damper systems as well by utilizing multiple floor slabs on multiple stories. Because of the large mass of the floor slabs the system is more effective than any of the standard tuned mass damper systems.

The system is optimized for its total response over a range of frequencies compared to a standard composite structure over those same frequencies by adjusting the combination of stories that are activated, the radius of curvature of the slab support, the stiffness of the bumpers, and the coefficient of friction of the contact surface between the support and slab. The response is a normalized multi-objective optimization of the acceleration, global drift, interstory drift, and relative slab drift. The optimized structures can be tested by real seismic records to demonstrate their effectiveness.

ACKNOWLEDGEMENTS

I thank my advisor and committee chair Professor Hussam Mahmoud. He gave the guidance necessary to complete this thesis and the insight and experience to help with any problems. I would like to thank Colorado State University, which has not only been my school for the past six years, but it has been my home. I would again like to thank Professor Criswell, Professor Arabi, and Professor Atadero for the recommendations they wrote. I thank Professor Bogusz Bienkiewicz for the knowledge he provided in his Fundamentals of Vibrations class. I would like to thank Professor Caroline Clevenger for accepting my request to be on my. I would like to thank Professor Paul Heyliger for everything he did for me. He was by far the best *teacher* that I have had at CSU and inspired me. For the time and work he gave to pioneer much of the work I expanded on and for the help he gave me I would like to thank Akshat Chulahwat. Additionally, I would like to thank Zhiming Guo and Mehrdad Memeri for the advice they gave me with wind engineering and seismic design concepts.

I would like to thank Brian and Lynette Engle, they have given me nothing but support and love. My brother Tanner is an inspiration for me. My sister Delaina is my motivation to be at my best to push her. My uncle Roger has shown me leadership, Sharon the importance of God, David gave me home away from home, Sandy has shown me what I can do with what I have achieved, and John for being the source of fun. To my grandpa Engle, I can never forget the experiences we had, and grandma Engle, you are the person we all should be. I thank Ernie for showing that there are important things besides civil engineering, my grandpa Kari for never complaining, and my grandma Kari, who is so understanding.

TABLE OF CONTENTS

ABSTRACT.....	ii
ACKNOWLEDGEMENTS.....	iv
LIST OF TABLES.....	viii
LIST OF FIGURES.....	ix
1. INTRODUCTION.....	1
1.1 Statement of Problem.....	1
1.2 Objectives and Scope of Research.....	4
1.3 Organization of Thesis.....	6
2. BACKGROUND AND LITERATURE REVIEW.....	7
2.1 Introduction.....	7
2.2 Seismic Loading on Structures.....	8
2.3 Base Isolation Systems.....	15
2.3.1 Rubber Bearings.....	16
2.3.2 Sliding System.....	20
2.3.3 Smart Systems.....	22
2.4 Tuned Mass Damping Systems.....	23
2.4.1 Translational System.....	25
2.4.2 Pendulum System.....	26
2.4.3 Active Systems.....	27
2.4.4 Multiple TMD Systems.....	28
2.4.5 Friction Damping.....	30
2.4.6 Innovative Damping.....	30
2.5 Derivation of Equations.....	31
2.5.1 LaGrange Energy Conservation Method.....	31
2.5.2 Newmark Numerical Solver.....	33
2.6 Optimization of Parameters.....	34
2.7 Summary and Results.....	35
3. SYSTEM DEVELOPMENT.....	37
3.1 Introduction.....	37
3.2 Conception of system.....	38
3.3 Development of equations of motion.....	40
3.3.1 Idealization of system.....	41

3.3.2	Lagrange Energy balance.....	42
3.3.3	Friction forces	44
3.3.4	Signum function.....	45
3.4	Modal Analysis	46
3.5	Newmark Numerical Solver.....	50
3.5.1	Response Equations	52
3.6	Verification	53
3.6.1	Newmark Modal Analysis Example	53
3.6.2	Composite System vs Hybrid System imitating a composite	54
3.6.3	Flat versus high radius of curvature	55
3.7	Optimization	56
3.7.1	Covariance Matrix Adaptation.....	57
3.8	Summary and Conclusions.....	59
4.	PUBLICATION.....	62
	Summary	62
4.1	Introduction.....	63
4.2	Proposed Isolated Floor System.....	66
4.3	Single Story System Development	68
4.3.1	Simplification.....	68
4.3.2	Equations of Motion.....	69
4.3.3	Response Equation.....	71
4.4	Multiple Story System	74
4.4.1	Idealization.....	74
4.4.2	Equations of Motion.....	75
4.4.3	Response Equation.....	78
4.4.4	Verification	79
4.5	Optimization	80
4.5.1	Parameters.....	80
4.5.2	Covariance Matrix Adaptation (CMA)	82
4.6	Performance Evaluation	84
4.7	Design Considerations	90
4.7.1	Friction Surface.....	91
4.7.2	Slab Support.....	91
4.7.3	Stiffness Devices.....	92
4.7.4	Damping Devices.....	93

4.8	Conclusions.....	94
5.	SEISMIC EVENTS	95
5.1	Introduction.....	95
5.2	Ground Motion Characteristics	96
5.2.1	Selection.....	96
5.2.2	Normalization.....	97
5.2.3	Maximum Considered Earthquake.....	98
5.2.4	Scaling to MCE.....	98
5.3	Responses of structures.....	100
5.4	Summary and Conclusions.....	110
6.	CONCLUSIONS.....	112
6.1	Summary of Current Work	112
6.2	Summary of Findings.....	113
6.3	Future Research	115
	REFERENCES	118

LIST OF TABLES

Table 3-1 Newmark parameters	51
Table 3-2 Response parameters of interest	52
Table 4-1. Variable definitions	70
Table 4-2 Structural properties of the frames	85
Table 4-3 Optimization Limits.....	85
Table 4-4 Optimized parameters and peak response.....	85
Table 5-1. Characteristics of the ground motion records used in the parametric study	97
Table 5-2 Scale factors of ground motion records	99

LIST OF FIGURES

Figure 1-1 (a) Pendulum damper (b) translational damper	2
Figure 1-2 Base Isolation Example	3
Figure 2-1 (a) Strength reduction after earthquake (b) Damage Index versus peak ground acceleration (c) Damage Index versus maximum interstory drift (Ghobarah et al., 1999).....	11
Figure 2-2 Example of a rubber bearing base isolation system (Kelly, 1986).....	17
Figure 2-3 Friction support fail safe base isolation system from (Kelly & Beucke, 1983)	19
Figure 3-1 Elevation view of two story structure with first story slab isolated	40
Figure 3-2 Idealized single slab system	41
Figure 3-3 Elevation view of multiple story hybrid structure.....	47
Figure 3-4 Idealized multiple story hybrid system	47
Figure 3-5 Verification comparison to Chopra’s El Centro response (Chopra, 1995)	54
Figure 3-6 Verification of composite structure to hybrid structure with rigid connections between slab and frame	55
Figure 3-7 Verification comparison of horizontal translational dampers versus hybrid system with infinite radius of curvature	56
Figure 3-8 Binary representation of activated stories of structure in vector form	57
Figure 3-9 Flowchart of CMA optimization process (Chulahwat, 2013)	58
Figure 4-1. (a) Pendulum Damper (b) Translational Damper: <i>after [8], [15], and [16]</i>	64
Figure 4-2. Elevation view of proposed single story system	67
Figure 4-3. Idealized representation of single story system.....	68
Figure 4-4. Response versus input variables for (a) radius of curvature (b) coefficient of friction (c) stiffness of bumper.....	73

Figure 4-5. Elevation view of multistory system	74
Figure 4-6. Idealized representation of multistory system.....	75
Figure 4-7. Response comparison for validation of calculations.....	79
Figure 4-8. Verification of (a) composite structure to isolated structure with high bumper stiffness, (b) flat support versus curved support with high radius of curvature	80
Figure 4-9. Binary representation of activated stories of structure in vector form	81
Figure 4-10. Flowchart of CMA optimization process [25]	84
Figure 4-11. (a) Global drift and (b) ISD of top story vs frequency ratio of rigid and isolated 4 story structure	87
Figure 4-12. Comparison of acceleration of (a) floor slab and (b) frame vs frequency of composite and isolated 4-story structure.....	87
Figure 4-13. (a) Comparison of the relative slab drift vs frequency of the 4 story hybrid structure versus composite system (b) Effect of damping on response of the hybrid system.....	87
Figure 4-14. Improvement per story for 4 story structure.....	88
Figure 4-15. Improvement per story for 7 story structure.....	89
Figure 4-16 Improvement per story for 10 story structure.....	89
Figure 4-17. Effects of isolating different stories for (a) 4 story (b) 7 story and (c) 10 story structures	90
Figure 5-1 Response spectra of (a) near field records and (b) far field records compared to maximum considered earthquake.....	100
Figure 5-2. (a) Normalized Acceleration and (b) Normalized interstory drift of fourth story of optimized four story hybrid structure compared to composite four story structure under the Imperial Valley, Bonds Corner earthquake of 1979.....	102
Figure 5-3. Percent Improvement of the fourth story of optimized four story hybrid structure versus composite four story structure over various earthquake loads for (a) the average acceleration (b) average interstory drift (c) maximum acceleration (d) maximum interstory drift.....	104

Figure 5-4. (a) Normalized Acceleration and (b) Normalized interstory drift of seventh story of optimized seven story hybrid structure compared to composite seven story structure under the Imperial Valley, Bonds Corner earthquake of 1979 105

Figure 5-5. Percent Improvement of the seventh story of optimized seven story hybrid structure versus composite seven story structure over various earthquake loads for (a) the average acceleration (b) average interstory drift (c) maximum acceleration (d) maximum interstory drift..... 107

Figure 5-6. (a) Normalized Acceleration and (b) Normalized interstory drift of tenth story of optimized ten story hybrid structure compared to composite ten story structure under the Loma Prieta Capitola earthquake of 1989..... 108

Figure 5-7 Percent Improvement of the tenth story of optimized ten story hybrid structure versus composite ten story structure over various earthquake loads for (a) the average acceleration (b) average interstory drift (c) maximum acceleration (d) maximum interstory drift..... 110

1. INTRODUCTION

1.1 Statement of Problem

Earthquakes are one of the most destructive forces on structures. Since the beginning of civilization they have destroyed what man has built. Only recently in history have engineers and researchers understood these forces sufficiently to combat them. For years structures have been designed to withstand the most powerful earthquakes, preventing collapse or harm to occupants. This step was the most important in structural design. The safety of the inhabitants is always the most important consideration when designing a structure. The engineers of the past were able to keep buildings upright during an earthquake, making our world a safer place.

However, seismic loading can do more damage than harming the people in and around buildings. It inflicts millions of dollars' worth of damage onto a structure, even if collapse is prevented. The stresses, fatigue and plastic deformations that are induced through seismic loads are enough to make structures unfit for use. Though structures may not collapse, earthquakes have damaged buildings to the point where even repair and renovation are not viable options. Millions of dollars have been spent on tearing down and rebuilding structures after they have been damaged. In the last century, a very significant amount of time and money has been spent developing methods to reduce the stresses inflicted on structures from seismic loading.

Increased flexibility has been considered by designers in order to reduce the permanent damage applied to structures. However, this allows for greater motion in the structure and can be a safety hazard for those inside the building due to the falling debris during an earthquake. Additionally, the building sways noticeably during high wind or seismic loadings if the lateral

stiffness is too low and could lead to catastrophic failure. Although this design may be viable for some seismic applications, it does not include a mechanism for energy dissipation and therefore does not reduce the damage potential.

Many have applied damping devices to structures in order to reduce the vibrational response during seismic loading. This method involves a damping mass that is allowed to move in order to reduce the response. This damping mass dissipates energy by changing the momentum of the overall system and forcing seismic energy to push the extra mass rather than shaking the structure. Figure 1-1 shows examples of tuned mass damper systems.

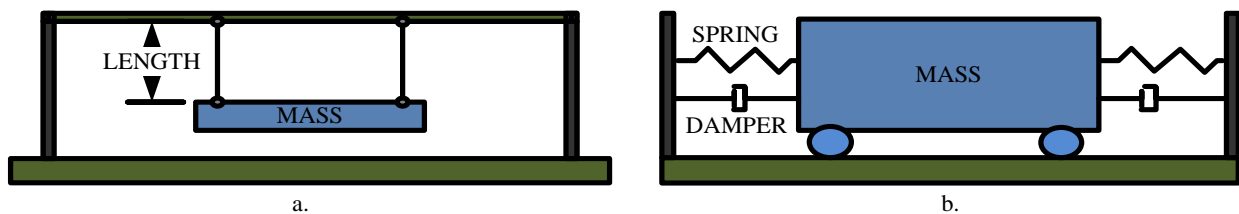


Figure 1-1 (a) Pendulum damper (b) translational damper

This method reduces vibrations for a small range of excitation frequencies due to the small range of mass and translation of the damper. The mass and stiffness of the damper is thus tuned to reduce the predominant resonant vibrations. The more mass used for damping, the more effective the process. But a mass damper large enough to fully reduce the response of an entire building would be overly massive. This extra weight would require a drastic over design of the structure and be very impractical. Because of this, modern tuned-mass dampers (TMD), as they are called, must be relatively small, much too small to have a great effect on the structure. This method is one of the most popular and most effective being used today, however, since earthquake loads are so variable, the extent of their effectiveness is rather questionable.

Another approach of mitigating earthquake excitation is decoupling the motion of the main structural frame from that of the foundation. The largest shear and moment forces in a structure

are most often found near the base. The method described is called “base isolation”. This method involves isolating the structure from the base or foundation. Ideally, the structure’s inertia attempts to keep the structure at rest while the ground moves beneath it under seismic loading. Realistically, the structure must remain on the foundation. Anchors, bearings, or pendulum sloped plates are used to bring the structure back into place after the motion has ceased. Figure 1-2 shows a pendulum sliding base isolation structure.

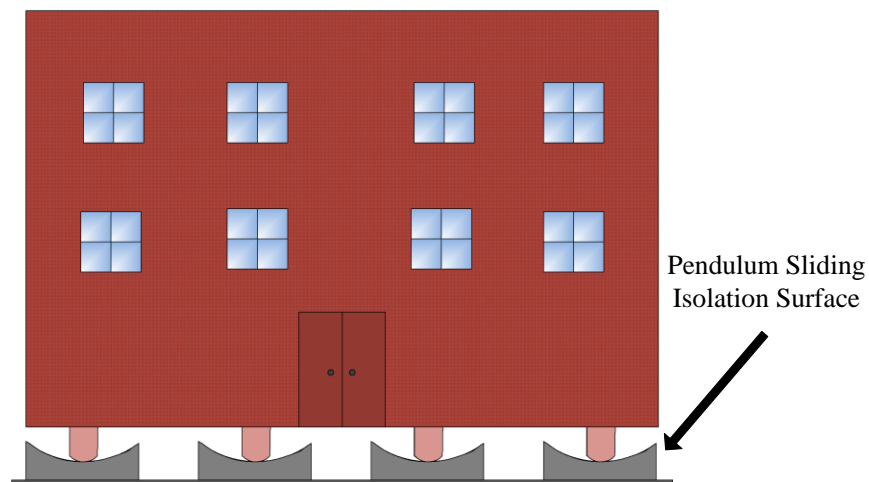


Figure 1-2 Base Isolation Example

These systems allow for the peak displacements to be greatly reduced, but not altogether removed. The method has proven to be very effective in a few cases. But base isolation is only as effective as the amount of isolation allowed. The structure is allowed to move independent of the ground to some degree, but the energy of the earthquake is only partially deflected and not fully dissipated, which eventually transfers to the structure and causes damage.

During high seismic loading the bearings on which the structure rests could be damaged. This could cause collapse, or necessitate replacement of these bearings. Collapse is unacceptable for design. Replacing bearings is much more desirable than rebuilding a structure, but is very costly and difficult since the bearings are supporting the structure. Even if damage is induced, repair is a problem in base isolation.

Thus, the problem remains as to how the demand on a structure under seismic loading can be reduced so permanent damage requiring repair or rebuilding is avoided? Flexible structures are not safe. Damping is not effective enough due to size and feasibility. Base isolation is effective but has drawbacks. Therefore, a new design must be developed to effectively and practically dissipate energy during large earthquake events while being simple to construct and cost effective to repair. Components of both TMD and base isolation theories are utilized by isolating floor slabs throughout the structure. This is tested to meet the goals of this thesis.

1.2 Objectives and Scope of Research

As previously discussed, research and design for mitigating seismic loading focuses on either the application of tuned mass dampers or base isolation systems. Neither of these systems has proven to be completely adequate solutions to the problem of permanent deformation and damage to structures under seismic loading.

The objective of the research being presented is to: Develop an innovative system that effectively reduces the stresses on the structure's main frame during seismic loadings to avoid permanent damage and deformation.

The system that is analyzed in this study is a hybrid isolation-tuned mass damper system that is developed to mitigate the seismic demand for a large range of frequencies. First, the system of equations representing the dynamics of the system is developed. Second, results that show the effectiveness of this system are presented. The tasks listed below highlight the main process followed to develop this model and to analyze its effectiveness. A more detailed discussion is presented in subsequent chapters.

- Task 1. Perform a comprehensive literature review to understand base isolation and tuned mass damper systems and utilize their strengths and avoid their weaknesses for the development of the proposed model.
- Task 2. Characterize the dynamics of the proposed system.
 - Develop the equations of the motion describing the dynamic behavior of the system when subjected to harmonic excitation.
 - Determine the response of the system using the Newmark numerical method.
 - Verify accuracy and validity of calculations
- Task 3. Optimize the design parameters to minimize the response over a range of input ground excitations.
 - Develop nonlinear optimization procedure to optimize the floor at which the new hybrid isolated/TMD slab system should be activated.
 - Develop nonlinear multi objective optimization procedure to optimize multiple design parameters
- Task 4. Interpret results.
 - Compare simulation results to the base-line results of a composite structure.
 - Conduct frequency analysis of proposed system versus composite structure.
 - Compare response of proposed system to individual seismic events.
- Task 5. Provide insight on the effectiveness of system.
 - Discuss the most influential parameter.
 - Discuss feasibility and effectiveness against other systems.
 - Discuss how to improve system response.
- Task 6. Develop guide for design and use of system.

- Explain which design considerations must be taken into account and emphasize which attributes are most important and possible pitfalls of design
- Task 7. Highlight the future research needed to fully implement the proposed system.

1.3 Organization of Thesis

This thesis develops an alternative method to reduce demand on structures during seismic loading by incorporating aspects of tuned mass dampers and base isolation systems. The system is idealized and an equation of motion is developed based on the assumed interaction of the design on the structure and analyzed to optimize the system and its critical components. The performances of the optimized structures are then analyzed and quantified. Design considerations are applied and further research is proposed.

There are six chapters in this document. Chapter 1 provides an introduction to the problem and the objectives of the research. Chapter 2 provides a comprehensive review of previous literature and background. Chapter 3 explains the system development and concepts that govern its behavior. The development of the equations of motion and derivations of the response equations are also explained in this chapter. Chapter 4 provides a full publication, which is submitted to the Journal of Earthquake Engineering and includes system development, optimization, and performance. This chapter also analyzes the results and the feasibility of the system. Chapter 5 compares the response of the proposed design to a composite structure for a variety of earthquake loadings. This chapter also analyzes the results of these tests. Chapter 6 concludes with relevant results and major findings of this study, as well as highlighting future tasks and improvements that can be made.

2. BACKGROUND AND LITERATURE REVIEW

2.1 Introduction

Conventional design for seismic loads on a structure has to ensure the safety of the inhabitants of the building. This has always historically been, and always should be, the focus of design for all structures. But a structure under seismic loads may be severely damaged following a seismic event due to the demand on the structure. If properly designed, when the structure were subjected to large earthquakes it did not topple, but required significant repair to be deemed reusable. Since this was very costly, engineers began to develop ways of reducing the demand that affect buildings in order to reduce the damage. The main focus was to reduce the accelerations and displacements generated by the structure. There are many innovative ideas as to how to do this. Many are used in practice now. Many are still in development. There are two broad methods used to achieve this. One was the use of tuned mass dampers to dissipate energy and reduce acceleration. The second was base isolation which un-couples the structure from its foundation, thus reducing displacements and stresses. Initially, this literature review investigates seismic loading on structures. It then investigates the details of base isolation followed by tuned mass dampers. To complete the literature review, the focus shifts to mathematical concepts and processes that were used to derive and solve the equations that govern the response of these systems.

2.2 Seismic Loading on Structures

In Earthquake Engineering for Structural Design Mark Yashinsky (2006) explained what damages generally occur in structures due to seismic loads. In buildings designed with the most basic design methods, damage did not generally occur until an earthquake approached a magnitude of 5.0 on the Richter magnitude scale. Of course this was a generalization because all earthquakes are unique in how they may affect a structure. In general, the damage was caused by failure of the surrounding soil or the structure itself as a result of the strong shaking. Yashinsky (2006) described failure of foundation connections, shear failure, flexural failure, other connection problems, and other damages that did not necessarily result in failure. Engineers design for the peak accelerations and displacements that are experienced on a probability basis. Areas in high seismicity regions may experience earthquakes every day. Damage can also occur from surface ruptures, failure of nearby lifelines, or collapse of more vulnerable structures nearby. Damage can range from small cracks which occur in smaller earthquakes to failure, but all reduce the integrity of the structure and require repair. Most structures, especially in the past and in areas not known for seismic activity, were designed to prevent collapse. The stronger a building, the more forces it attracted. So it was not necessarily advantageous to have a very stiff, strong structure. For this reason, most structures were designed to be strong in shear but ductile and easy to flex to move with an earthquake. This caused yielding and deformation during loading but these structures were designed to withstand their loads during and after an earthquake. Permanent damage occurred in the elements with the lowest capacity for load. Damage or failure of connections from torsional moments, tension and compression or buckling can also occur. This yielding and damage had to be repaired because it caused the structure to

become progressively weaker. The repairs became very expensive; therefore preventing such damage was very critical to mitigate economic impact.

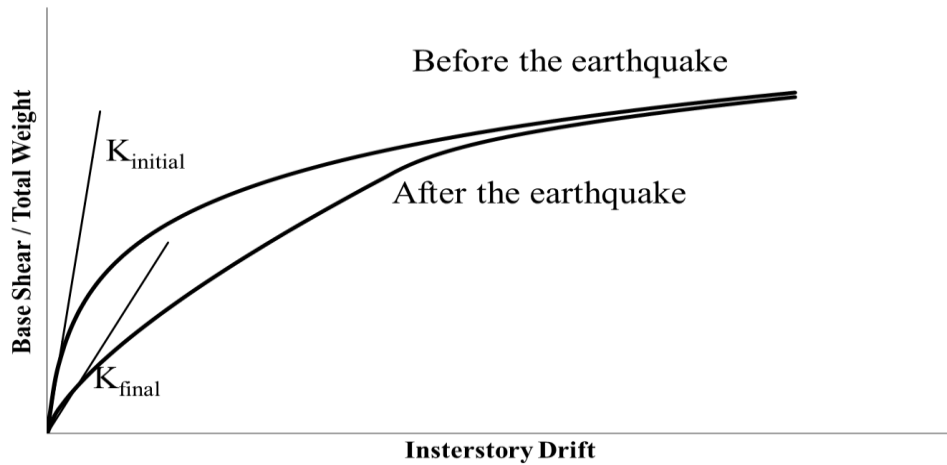
The highest stresses and most damages occurred in the connection of the structure to its foundation. The elements in this region had to have a high flexural capacity in order to prevent failure. Many flexural members throughout a structure were designed to form plastic hinges during seismic loading to allow for energy absorption without compromising the integrity of the structure. Often times the most likely and most catastrophic failure was found in connections. All members may have been designed sufficiently but if they were not effectively attached then the structure could inevitably collapse under large deformation. A single connection failure can progressively cause the failure of an element which can lead to partial or complete the failure of the entire structure.

Elements being used to prevent damage and improve dynamic response must have relatively the same stiffness. Otherwise the stiffer elements take on more load. Yashinsky clearly explained that earthquakes caused damage to structures even if they did not collapse and that most structures were even designed to undergo damages in order to withstand a seismic event without collapse.

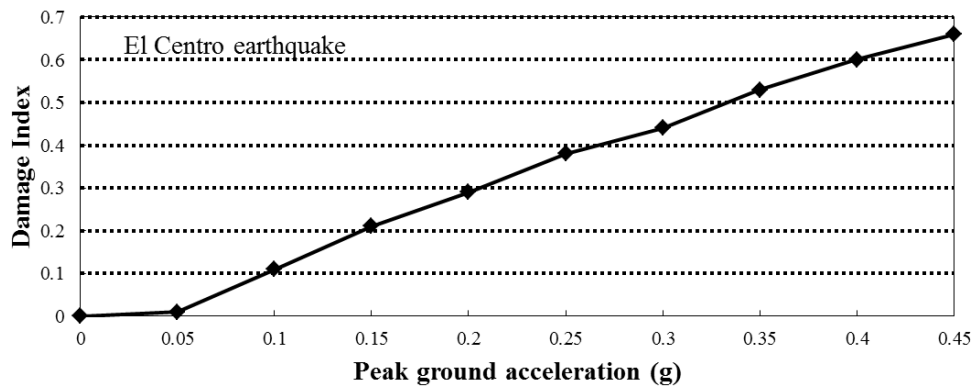
Ghobarah et al. (1999) described what defined the survival of a structure based on seismic damage and what quantified the damage in “Response-Based Damage Assessment of Structures”. The damage was described using damage indices that showed what effects seismic loading had on a structure and why, though a structure did not collapse, seismic loading was still catastrophic to a structure. As explained, a structures ability to survive an earthquake was described by the state of damage of the structure after the earthquake. The study evaluated damage indices and damage states where various strength values were observed before and after

loading in order to determine their applicability to damage assessment of a structure after seismic loading. The method proposed for developing the assessment and determining its effectiveness was based on a simple static pushover analysis to estimate the expected damage under differing seismic loading intensities. The results confirm the applicability of the indicators and show the importance of considering damages to structures under seismic loading even when collapse did not occur.

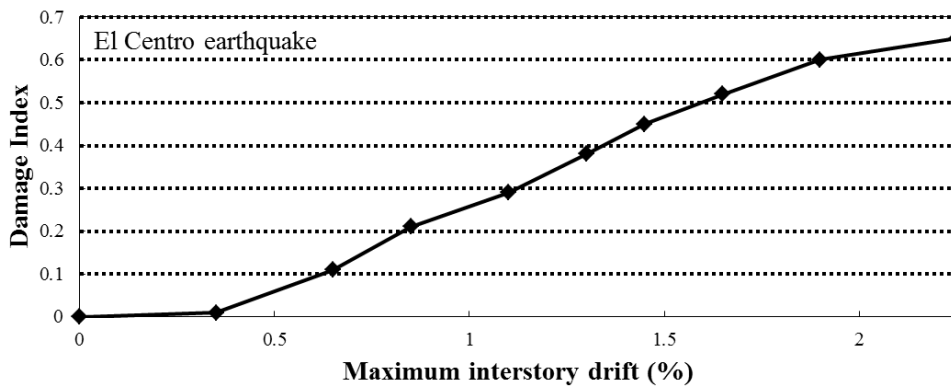
Using various damage indices the experimental work demonstrated the strength of a structure before an earthquake with a pushover test. The state of the structure following the earthquake represented its damage condition. After the first pushover curve, another pushover test was performed again to understand the differences in the strength of a structure before and after an earthquake. Figure 2-1 (a) shows the strength of a structure before and after the El Centro earthquake. This figure was analogous to a stress vs strain curve. It was seen that the earthquake significantly decreased the strength of the structure upon initial excitation. Figure 2-1 (b) and (c) show the damage index that described this behavior as it related to the peak ground acceleration and maximum interstory drift. It was concluded from these experiments that an earthquake can cause significant damage to a structure and this damage must be accounted for when assessing the need for repairs. This conclusion applied for ductile and non-ductile structures as well as maximum deformation versus cumulative damage analyses.



(a)



(b)



(c)

Figure 2-1 (a) Strength reduction after earthquake (b) Damage Index versus peak ground acceleration (c) Damage Index versus maximum interstory drift (Ghobarah et al., 1999)

Stephens and VanLuchene (1994) presented an alternative approach to assessing the damage and safety of structures during seismic loading in “Integrated Assessment of Seismic Damage in Structures”. Their approach was focused on strong-motion earthquakes using several damage

condition indices that were input into an analysis program that assessed the safety parameters of the system using a neural network. Using weighted factors considering the damage conditions and attributes of the system the program ran an assessment based off data collected during past seismic events. The weighted factors and neural network algorithm were developed from gathered data from responses observed in laboratory testing. The data generated was useful in describing how damage was developed in a structure and how much damage was critical. It points to the importance of effectively reducing this damage. As equation 2-1 shows, the damage on a structure was characterized by the maximum displacement versus the ultimate displacement under static loading and dissipated energy. D was the damage, δ_{max} was the maximum displacement, δ_u was the ultimate possible displacement under static load, β and Q_y were physical properties of the structure or member, and $\int dE$ was the cumulative energy of the excitation.

$$D = \frac{\delta_{max}}{\delta_u} + \frac{1}{\delta_u} \frac{\beta}{Q_y} \int dE \quad (2-1)$$

Chai et al. (1995) demonstrated that the displacement ductility factor for damage assessment was insufficient in “Energy-Based Linear Damage Model for High-Intensity Seismic Loading”. This number accounted for the peak displacement during seismic loading and the design of the structure to indicate the severity of damage on a structure after seismic loading. Chai argued that this number did not accurately represent the amount of damage a structure underwent because it did not consider the non-peak or even elastic cycles that the structure may have endured in addition to the peak displacement. This was in contrast to the earlier assessment by Stephens and VanLuchene (1994). Chai et al. (1995) attempted to model the damage of a structure by considering a normalized peak displacement and normalized plastic strain energy. Chai stated

that the damage a structure underwent was greatly dependent on the energy that was dissipated, even under elastic loading caused by smaller earthquakes and was greater than earlier assumed.

The study supported this conclusion by testing many steel cantilevers under cyclic loading below the maximum displacement. The results indicated that a good way to avoid damage was to reduce all stresses, even cyclic loads of low amplitudes, rather than only reducing the maximum stresses.

Saatcioglu and Ozcebe (1989) examined the response of reinforced concrete columns to seismic loading in “Response of Reinforced Concrete Columns to Simulated Seismic Loading”. Full-scale concrete columns were loaded gradually with lateral load reversals. Unidirectional and bidirectional loadings were applied for testing. Various testing parameters were being considered including axial load, shear/confinement reinforcement, and deformation path. The columns were loaded axially ranging from no load to a significant gravity load compared to the column strength. Some columns were even subjected to tension loads during testing. Results showed that gravity loads significantly influenced the hysteretic response of the concrete columns. These results indicated that compression reduced column deformation. Additionally, the study concluded that the bidirectional load cycles caused severe strength and stiffness degradations in the columns.

Lee and Fenves (1998) developed plastic-damage model for concrete subjected to cyclic loading in “Plastic-Damage Model for Cyclic Loading of Concrete Structures”. This model was developed by considering the required energy to create fractures and to degrade the stiffness of the structural elements in continuum damage mechanics. The model incorporated a damage variable for tensile damage and a variable for compression damage along with a yield function that considered hardening for differing damage states. The function that was developed to model

the uniaxial strength was factored into two parts that corresponded to effective stress and degradation of elastic stiffness. Much like the steel examples already explored, cyclic loading, even below the plastic deformations, caused severe strength degradation in a structure.

Elenas and Meskouris (2001) presented a study that laid out the interdependency of seismic acceleration parameters and structural damage indices in “Correlation study between seismic acceleration parameters and damage indices of structures” . The study explored peak ground motions, spectral and energy parameters to describe the seismic excitation. Structural and nonstructural damage was considered in the study as well. Service design should always be considered and thus was useful for research consideration. The damages were expressed by the Park/And overall structural damage index (OSDI), the maximum interstory drift (ISD) and the maximum floor acceleration. Many seismic parameters were numerically evaluated and nonlinear dynamic analyses were performed to understand the damage status of the structure. Correlation coefficients were then developed to relate the seismic parameters to the damage indices. The results of the experimentation indicated that the spectral and energy parameters provided the best correlation, especially with the OSDI. The study recommended using the spectral and energy parameters as descriptors of seismic damage potential. This means the best way to attempt to reduce damage was to reduce the energy applied to the structure and that focusing on reducing the peak motion was not the most critical parameter. This conclusion reinforced the literature previously addressed.

In general, previous studies demonstrated that even after low energy demand that can be induced by earthquake loads, a structural element significantly loses strength. This fact has been reinforced by all of these studies emphasizing the need to avoid the severity of any and all loads in order to maintain a structure’s integrity.

2.3 Base Isolation Systems

Kelly (1986, 1998) described the idea of base isolation as uncoupling a building from the damaging effects of ground motion in “Aseismic base isolation : review and bibliography” and “Base Isolation : Origins and Development”. Base Isolation includes a variety of methods that detach the base of the building from the ground while still providing support and stability from the foundation. The idea has been around for over a century. This method drastically reduces the acceleration in the building itself. Base isolation minimizes building damage and interior damage while still protecting lives. It mainly accounts for horizontal accelerations and vertical accelerations are not often considered. There are two main types of Base Isolation. The first is rubber bearing base isolation. The second is sliding isolation systems.

The review explained that the original base isolation proposals were sliding systems utilizing either rollers or sand to allow isolation from the foundation. In fact, since accelerations increased with each floor of a structure, the goal was to reduce the peak accelerations of the structure to less than that of the ground through base isolation. The first use of the idea of structural isolation was most likely by Frank Lloyd Wright in 1921 when he built the Imperial Hotel in Tokyo, Japan on a layer of soft mud beneath stronger surface soil instead of securing it on solid ground. The cushioning effect of the mud led to the building performing very well in future earthquakes. Engineers attempted to produce this same effect by creating a flexible first floor on which the rest of the floors would be isolated from the ground accelerations. But this caused a very large amount of displacement in the columns of the first floor and thus made collapse and buckling a severe threat. From there, many roller ideas were produced but problems arose with many of them, as well. Lack of resistance to motion or energy dissipation allowed for permanent

movement and large excitations under wind loading. Also, years of rest caused steel rollers to become rigidly fixed to the foundation or structure, thus offering no isolation. The practical use of base isolation did not really exist until the rubber fabrication technology advanced enough to create the rubber bearings seen in rubber isolation systems today that utilized steel reinforcement to offer axial strength to the bearing, while allowing horizontal motion.

Constantinou et al. (1998) confirmed this information regarding base isolation in Passive Energy Dissipation Systems For Structural Design and Retrofit. Seismic isolation was described as partial isolation and partial absorption of energy through flexibility and isolation at the base of a structure. The absorbed energy was then transferred into the structure but overall the structure was required to dissipate less energy and increases the survivability of the structure.

Huang (1993) tested four different base isolated buildings at a near and far distance under three different earthquake loads in “Analysis of Records from Four Base-Isolated Buildings During Low Levels of Ground Shaking”. Peak accelerations, drift and relative drift were all greatly reduced through base isolation. The drifts were much below design code standards. The isolated structures also had slightly increased periods of excitation.

2.3.1 Rubber Bearings

The rubber bearings described by Kelly were the most common form of base isolation (Kelly, 1986). The bearing layer gave the structure a fundamental frequency that was lower than the fixed-base frequency as well as the ground motion frequencies. The first dynamic mode of the isolated structure involves deformation only in the isolation system of the structure. The building above was rigid for all intents and purposes. The isolation systems did not absorb

earthquake energy, they deflected it. This system was beneficial even when the system was undamped.

In the first models, by Kelly (1986) at the University of California, Berkeley, of the rubber bearing systems a low modulus rubber was used to reduce the accelerations. This was for a 20 ton building model on a shake table. It reduced accelerations by as much as ten times. The scale was too small for the rubber to be useful in larger models or for practical use. It would likely fail. The tests also made it clear some damping was likely needed. Higher grade rubber in larger models experienced reductions in acceleration as well. However, as damping was increased, the added mass of the damping systems actually induced responses in higher modes of the structure and so the reductions of acceleration were not achieved. The best method of increasing damping was to provide it in the rubber itself. Figure 2-2 shows how rubber bearings were used to isolate the structure from seismic motion.

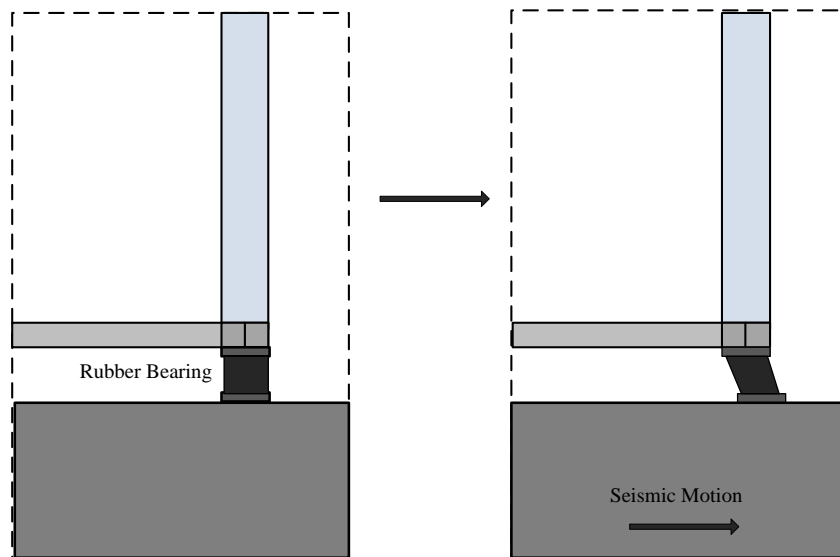


Figure 2-2 Example of a rubber bearing base isolation system (Kelly, 1986)

One trouble that rubber bearings created was the possibility of failure and collapse. Collapse was the very worst possible scenario which was why base isolation took so long to be implemented in the field. If an earthquake significantly larger than the design earthquake struck a

structure with rubber bearings the large horizontal displacements may have caused failure in the bearings and the structure would have no support. Kelly and Beucke (1983) developed a system with a fail-safe to prevent this collapse in the base isolation bearings. The system was tested and both sliding and rubber bearing isolation were used in certain situations. The main isolation system was a rubber bearing system in which the structure rested on four rubber and steel composite bearings that had low horizontal stiffness but high vertical stiffness. The structure then moved back and forth relative to the ground while the actual accelerations experienced by the structure were very low. The fail-safe system was incorporated to prevent collapse and included sliding isolation.

As the bearings displaced horizontally there was an increase in vertical displacement as well. The fail-safe system was a skid system that was anchored to the foundation. When the structure displaced horizontally it then displaced downward as well and came into contact with the fail-safe. While in contact, it was allowed to slide but it did not collapse. When the vertical displacement became so great that the structure came in contact with the fail-safe, friction damping was induced and failure of the structural system was avoided. Figure 2-3 shows the basic design of the friction fail safe base isolation system.

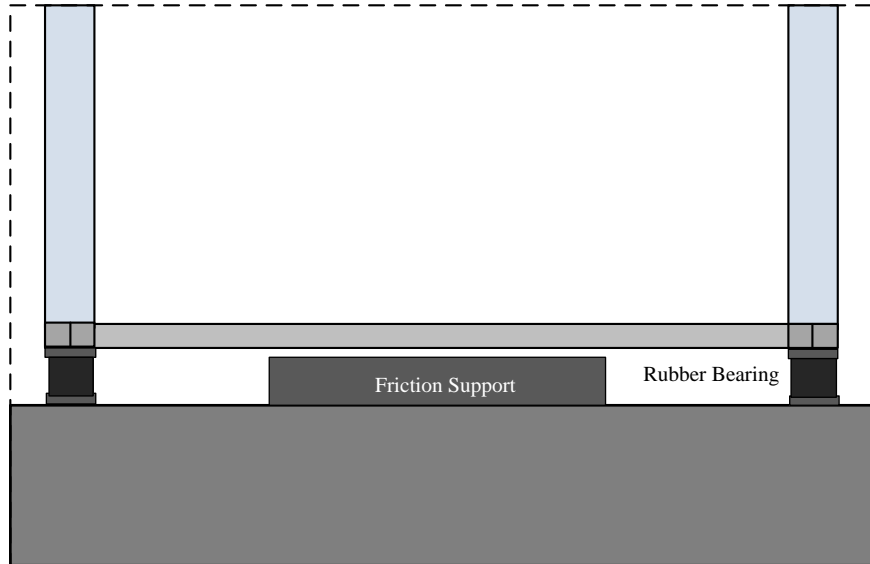


Figure 2-3 Friction support fail safe base isolation system from (Kelly & Beucke, 1983)

This system was tested at four differing fail-safe heights (2 inches from structure, 1 inch from structure, in contact with structure, and fixed base (no isolation)). These four systems were also tested in by four differing earthquakes. These earthquakes used the random vibrations that were induced during the earthquakes. They were originally loaded at a $\sqrt{3}$ time scale and then were loaded at real time. To determine the damping ratio and natural frequency of the system a series of sinusoidal tests were run before-hand. The natural frequency was necessary to know how to induce resonance to force the maximum displacements and failure in the system.

The results of all of these tests confirmed that the base isolation system greatly reduced the accelerations and thus the stresses experienced on the structure. The drawback was that there were large displacements relative to the ground. These large displacements could cause problems, such as failure. The fail-safe also effectively damped the system and prevented failure while still providing additional energy dissipation. The system in which the fail-safe was in contact from the very beginning seemed to be the optimal option. Even though it was in contact and thus had a higher stiffness than the other systems, the isolation was significant enough to greatly reduce the accelerations experienced by the structure, nearly as well as the higher set

systems. What set it apart was the relative displacement of the structure from the ground. These values were lowest with this system as opposed to the others.

Chung et al. (1999) described a series of tests subjected to various seismic earthquake inputs in “Shaking table and pseudodynamic for the evaluation of seismic performance of base-isolated structures”. The study attempted to evaluate the effectiveness of base isolation systems for low-rise structures against severe seismic loads through shaking table tests, and developed an analytical method for predicting earthquake responses of base isolation systems. In the shaking table test, a quarter-scale three-story structure base-isolated by laminated rubber bearings was tested. In the pseudodynamic test, only the laminated rubber bearings were tested using the substructuring technique, whereas the concurrent seismic responses of the superstructure were computed using on-line numerical integration. The results of all of the tests showed that there was significant reduction in floor acceleration, base shear, and overturning moment at rock or stiff soil sites. Rubber bearings offered an effective method of seismic vibration control but the possibility of damage to the bearings and high displacements brought about the possibility of failure.

2.3.2 Sliding System

A sliding base isolation system limits the transfer of the shear force from the ground to the structure. China has at least three buildings utilizing a sand sliding system (Kelly, 1998). A nuclear power plant in South Africa uses an isolation system containing a lead-bronze plate sliding on stainless steel with an elastomeric bearing. Sliding systems inherently allow for the possibility of permanent displacement of the structure from the foundation. This was not acceptable so all systems had some form of centering device. Friction pendulum systems are

being used on several projects in the United States using gravity to pull a structure back to its original location relative to the foundation.

In the “Development of a Friction Pendulum Bearing Base Isolation System for Earthquake Engineering Education,” Kravchuk et al., (2008) demonstrated how a pendulum friction base isolation system performs. Results were presented versus a system without base isolation and it was shown that the accelerations induced on the isolated structure were approximately half that of a structure without isolation. When designing the isolated system, considerations were given to load capacity requirements, earthquake displacement capacity, soil conditions, and the size of the structure. Design parameters included curvature of the concave pendulum systems and diameter of the bearing surface. A low friction surface was used to allow for displacement of the structure when ground movement occurs. This system filtered out earthquake forces through the frictional interface and had a self- centering capability due to the concave surface that the structure rested on. This report did not provide a mathematical solution to the motion of the system but provided results that indicated a very efficient system of vibration control in structures.

The structure essentially rested on a large ball-bearing which was on a low friction concave plate. The structure was designed to be wide enough as to not get caught on the edge of the plate. When the ground (and plate) displaced the ball and building slid relative to the ground. The inertia or tendency to remain motionless for the building moved the bearing relative to the plate. The shape of the plate gave the building a stable system for the foundation. However, this did require that the building moved, somewhat, along with the plate due to the potential energy in the slope of the bearings. The building must always return to the middle of the plate. This system increased the natural period of the structure and slowed the acceleration.

Mokha et al., (1990) tested the physical properties of Teflon as it pertained to base isolation systems in “Teflon Bearings in Base Isolation. I: Testing”. Teflon slide bearings have been used for the past several years to accommodate thermal movement and effects of prestressing, creep, and shrinkage in bridge applications. They have been proposed to be used in seismic base isolation systems. These systems were being used on many buildings such as the Technology Research Center of Taisei Corporation in Tokyo, Japan. The effect of sliding velocity, sliding acceleration, bearing pressure and Teflon type was tested for the Teflon on steel interface. Tests showed that the friction of the Teflon surface was most greatly affected by velocity, not acceleration. Size of Teflon bearings did not affect the material properties, tests on different sized bearings yielded similar results. The coefficient of sliding friction increased rapidly with sliding velocity, up to a certain velocity, after which it remained constant. Difference in maximum and minimum sliding coefficient of friction depended greatly on pressure. The coefficient of friction decreased with increased pressure.

2.3.3 Smart Systems

In “Intelligent Base Isolation Systems” (Johnson, Ramallo, Spencer, & Sain, 1998) and “‘Smart’ Base Isolation Systems” (Ramallo, Johnson, & Jr, 2002), Ramallo and Johnson tested conventional low-damping elastomeric bearings being used with “smart” controllable semi-active dampers, such as magnetorheological fluid dampers. These were compared to lead-rubber bearing isolation systems. These systems showed significant decrease in base drifts while not experiencing any increase in base shear or acceleration compared to passive isolation systems. This system was more applicable to a wider range of ground motions and magnitudes. Active control systems were active devices which reacted to the vibrations. They destabilized the system

if the smart structure was not correctly tuned but as the system was active the response over a large bandwidth of disturbances was better. Semi-active control systems were passive devices in which the properties (stiffness and damping) were varied in real time with a low power input. In conclusion, the “smart” systems outperformed the passive isolation systems in all categories including base and structural displacements, base and structural accelerations, applied forces, and base shear. There were increased costs attributed to active systems as well.

2.4 Tuned Mass Damping Systems

One of the most promising seismic mitigation systems is the tuned mass damper. A tuned mass damper or (TMD) is a simple passive device that can eliminate undesirable motion due to the resonance vibration of the structure (Housner et al., 1997). The main task for a tuned mass damper is to dissipate energy to reduce vibrations through damping. The system generally consists of viscous dampers, a mass/inertia, a restoring mechanism, and an energy dissipation mechanism. The most common type of TMDs is the translational (TTMD) where a mass is mounted atop the roof of a building and allowed to translate horizontally as the primary structure vibrates. The frequency of translation of the added mass is tuned to the resonance frequency of the structure so when that frequency is excited, the added mass resonates out of phase with the structural motion, causing reduction in vibration of the main structure. The concept of TTMD was first developed in 1909 to reduce the rolling motion of ships and mitigate ship hull vibrations (Ormondroyd & Den Hartog, 1928). In 1928, the theory on TMD was presented by Ormondroyd and Den Hartog (Ormondroyd & Den Hartog, 1928) in “The Theory of Dynamic Vibration Absorber”. Following the theoretical development, a detailed discussion on optimal

tuning and damping parameters was discussed in in Den Hartog's book Mechanical Vibrations (Den Hartog, 1940). Significant contributions to understanding the theoretical and practical application of TTMD in civil structures have been made by various researchers (J. Connor, 2003; Randall, Halsted, & Taylor, 1981; Sladek & Klingner, 1993; Spencer & Sain, 1997; Tsai & Lin, 1993; Warburton & Ayorinde, 1980; Warburton, 1982).

As these studies showed TMDs can be very effective in reducing the peak responses of a structure. Their effectiveness did, however, relied on the size of the mass and the amount of energy the TMD can dissipate. The higher the mass of the TMD the more effective it was in dissipating energy (Warburton & Ayorinde, 1980). The mass ratio of the damper to the structure was strongly correlated to the effectiveness of the system. It also made the system more robust and more effective over more excitation frequencies. It was not, however, structurally or economically efficient to place overly massive TMDs in a structure. This would have then required overdesign of the structural components to compensate for the increased mass.

While TMDs effectively limited the peak response of the system, they often had little or no effect on the structure when it was being excited away from resonant frequency. The dampers were tuned to be excited exactly out of phase with the structure at resonance, normally at the first mode of excitation. When excited away from such frequency it translated at its own frequency relative to the structure and may have even translated in phase for some frequencies. This reduced the overall effectiveness of the dampers, as well.

Originally TMDs were designed to mitigate excitation of structures for wind loading. They were adjusted to be very effective for such loadings. They could reduce excitations up to 40% of peak excitations. Sladek and Klingner (1993) worked to test the effectiveness of TMDs on seismic loaded structures in "Effect of Tuned-Mass Dampers on Seismic Response". Seismic

loading occurred at differing and varying frequencies. Structures were excited by their own inertia during seismic events, rather than an external pressure as in wind loads. Their original findings were not promising for seismic loading. It seemed a higher mass ratio between the size of the damper and the structure was necessary. Randall, et al. (1981) showed that an increased mass ratio was ideal and that an increased damping ratio also increases the effectiveness of the system in “Optimum vibration absorbers for linear damped systems”.

2.4.1 Translational System

Translational TMDs are more conventional and utilize a mass that slides or “translates” back and forth opposite of the motion of the building in order to dissipate energy. The damper experiences large relative motion compared to the motion of the actual structure. Its motion is up to 10 times more than that of the structure for a system that only has 2% of the mass of the structure and only 10% for a damping ratio (Feng & Mita, 1995). Translational Tuned Mass Dampers are a type of tuned mass dampers that utilize bearings on which the mass rests. The bearings function as rollers and allow the mass to translate laterally relative to the floor. The John Hancock Tower uses a system similar to this. This high translation is also a problem. If the translation is too high it has to be limited. This limitation reduces the effectiveness of the system. Increased mass ratios reduce the amount of necessary translation without reducing the effectiveness of the TMD.

Tsai and Lin (1993) tested other parameters when optimizing the TMD system in “Optimum Tuned-Mass Dampers for Minimizing Steady-State Response of Support-Excited and Damped Systems”. They demonstrated that the optimum tuning frequency was greatly affected by the internal damping of the structure. However, the optimum damping ratio of the TMD system was

not affected by the internal damping of the structure. They also showed that both damped and undamped structures have similar optimum responses.

2.4.2 Pendulum System

Gerges and Vickery (2005) presented a system that suspended the mass with cables in “Optimum design of pendulum-type tuned mass dampers”. The mass then acted as a pendulum and induced forces opposite in direction to the motion of the floor. This system was limited by the length of the pendulum. Its maximum length was the height of the ceiling. But these dampers were easily tuned by adjusting the length of the pendulum. Compound pendulums have been used to eliminate this problem. Crystal Tower in Japan uses this system. The Crystal Tower is 44,000 ton building (Lourenco, 2011). It uses a 90 ton pendulum that hangs about 4 meters. The heating and cooling systems were used as the mass, making the system cost and mass efficient. The pendulum dampers were also more effective under wind loading than seismic loading. Seismic excitations required less movement from the damper in comparison to the wind loading. Emiliano Matta and Alessandro De Stefano developed the equations of relative motion for a pendulum TMD system under seismic loading and these are given in equations 2-2 and 2-3 (Matta & De Stefano, 2009a).

$$m_1(\ddot{x}_g + \ddot{x}_1) + c_1\dot{x}_1 + k_1x_1 = c_2\dot{x}_2 + (m_2g/R)x_2 \quad (2-2)$$

$$m_2(\ddot{x}_g + \ddot{x}_1 + \ddot{x}_2) + c_2\dot{x}_2 + (m_2g/R)x_2 = 0 \quad (2-3)$$

Almazan et al. (2007) explored the effectiveness of a bidirectional pendulum TMD in “A bidirectional and homogeneous tuned mass damper: A new device for passive control of vibrations”. This system allowed for damping in the two principal directions as well as allowing

for independent tuning for each direction. This system allowed for replacement of damaged parts easily. The study showed that the system was as effective as any standard pendulum TMD system but in both directions.

2.4.3 Active Systems

Active TMD systems utilize sensors to read the input frequency of the earthquake (Spencer & Sain, 1997). These sensors send a signal to an actuator that adjusts the damper to most effectively reduce the frequency of the system. As the structure's response is reduced the sensors continue to read the excitation and adjust the actuator to continue to be most effective. This process helps expand the effective range of a TMD. Another form of active TMD is an adaptive pendulum TMD. An adaptive pendulum TMD is a system developed to improve the performance of a damper by changing factors like length of the damper. Richard Lourenco (2011) performed the initial research on this subject. The improvement of the response through optimization was evaluated. The tuning frequency and the damping ratio were adjusted. The model was a two-story structure subjected to broad and narrow band excitation. A SDOF system was modeled that considered the effects of adjusting the frequency ratio, damping ratio, and mass ratio of the combined system to reduce deflection and find the optimal performance. The vibrational modes were identified in real time and tuned to the desired mode. The system was tuned by moving the pivot point of the pendulum. An external damper was also attached to the pendulum to dissipate energy and to be able to adjust the damping ratio.

2.4.4 Multiple TMD Systems

Chopra's Dynamics of Structures (1995) described many methods to model the behavior of a structure under excitation. A multi-degree of freedom system required modal summation in order to solve the equations of motion. When multiple equations were required to model the behavior of the structural system, they were coupled. Too many coupled equations made the calculations impossible to solve directly and thus modal analysis had to be employed in order to manipulate the equations into solvable independent equations. This was done by converting the system's physical coordinates into modal coordinates. With the use of Eigen analysis the equations can be decoupled and each equation becomes independent and solvable. These concepts were essential when developing equations for large structures and especially for multi-TMD systems.

Moon described how TMDs near the top of a structure were more effective in "Vertically Distributed Multiple Tuned Mass Dampers in Tall Buildings: Performance Analysis and Preliminary Design" (Moon, 2010). However, one of the issues pertaining to the use of TMD was the valuable space it occupied. Moon proposed to spread the mass of the damper throughout multiple stories in multiple dampers. This process made the utilization of space more flexible and efficient. It also provided a means of tuning separate dampers to react to differing frequencies, thus further increasing the effectiveness of the system. The results of the study showed that the effectiveness was only slightly decreased by spreading the mass of the damper throughout the structure. The reliability and range of effectiveness was, however, increased. The damping ratio can be increased as well, due to the smaller masses. The equations of motion for the multi TMD system can be seen in equation 2-4.

2.4.5 Friction Damping

When using friction damping to reduce the response of a system Lee et al. (2008a) showed in “Computation of Optimal Friction of Tuned Mass Damper for Controlling Base-Excited Structures” that the development of the equations and numerical analysis were very different than normal TMD systems. Friction required a different force term and a signum function to adjust the equation based on the relative velocities of the damper to the structure. The adjustment of the friction term meant that the analysis must be in terms of time and not in terms of frequency. The optimum friction value increased with an increased mass ratio but decreases with an increased internal damping in the structure. The performance of the system greatly decreased directly after the friction force became greater than optimum. Gewei and Basu (2010) tested the same principal in “Computation of Optimal Friction of Tuned Mass Damper for Controlling Base-Excited Structures” and discovered that the optimum coefficient of friction and friction force was dependent on the intensity of the excitation. This fact led to possibility of utilizing semi-active friction control of the system.

2.4.6 Innovative Damping

The design presented by Eartherton et al. (2010) in “Hybrid Simulation Testing of a Controlled Rocking Steel Braced Frame System” was characterized by a structural frame that was allowed to shift slightly and between the frame components were energy absorbing fuses that reduce the excitation of the structure. Additionally, when damage occurred it was focused on the fuses which could be replaced after the seismic event. Instead of adding TMDs to the system, this method greatly increases the internal damping of the system. The innovative concept

of this system was focusing damage to small and easily replaced components rather than large structural members.

Li and Zhu (2006) explored the possibilities of a double TMD system in “Estimating double tuned mass dampers for structures under ground acceleration using a novel optimum criterion” where one TDM was a large mass and the other was a smaller mass. It was shown to be more effective with respect to the drift frequency ratio than a multi-TMD system and did not require a damping device between the large device and the structure.

Chulahwat (2013) utilized a new floor slab design with the slabs being suspended from beams above using cables. This system took advantage of the mass of the floor slabs as damping devices in a pendulum behavior. To control translation and energy dissipation, pretensioned cables and damping devices were applied to the system. These components affected the damping ratio and natural frequency of the system. Chulahwat utilized an elitist strategy to optimize these variables and to determine which floor slabs should be suspended in a large structure in order to produce the most efficient structure.

2.5 Derivation of Equations

2.5.1 LaGrange Energy Conservation Method

In the History of Mathematics (Boyer, 1968) the process of the energy conservation developed by Joseph-Louis LaGrange was described. The kinetic and potential energy of each dynamic component of the degrees of freedom were characterized. The partial derivatives in terms of the velocity and displacement were found and then the time derivative of the velocity term was found for each component to reduce the terms into force terms to create an equilibrium

of forces. Tedesco et al. (1999) demonstrated how to analyze the dynamics of a structure under excitations in Structural Dynamics: Theory and Applications and utilized the LaGrange approach for structural dynamics in the derivation of equations of motion. The energy balance terms were then reduced by all energy dissipating terms, such as damping and friction terms when applied to structural dynamics. This process was applied to pendulum dampers and structures (Matta & De Stefano, 2009b) and the derivation of the equations of motion were provided for the pendulum TMD. The LaGrange energy equations can be seen in equations 2-5 through 2-10. Setareh et al. (2006) utilized the same process to develop the equations of motion for the pendulum TMD in “Pendulum Tuned Mass Dampers for Floor Vibration Control”. In these equations x represents horizontal motion, y is vertical motion, θ is angular motion, m is mass, k is stiffness, c is damping coefficient, T is kinetic energy, V is potential energy, and g is gravitational acceleration. Subscript 1 represents the structure and subscript 2 represents the pendulum damper. The dot or double dot represents first (velocity) and second (acceleration) derivative, respectively with respect to time. The prime above some variables represents a derivation with respect to the angular motion.

$$T = \left\{ (m_1 + m_2)(\dot{x}_g + \dot{x}_1)^2 + m_2[(x'_2{}^2 + y'_2{}^2)\dot{\theta}^2 + 2(\dot{x}_g + \dot{x}_1)x'_2\dot{\theta}] \right\} / 2 \quad (2-5)$$

$$V = k_1 x_1^2 / 2 + m_1 g y_1 \quad (2-6)$$

$$\delta W = -c_1 \dot{x}_1 \delta x_1 - c_2 x'_2{}^2 \dot{\theta} \delta \theta \quad (2-7)$$

$$L = T - V \quad (2-8)$$

$$\frac{d}{dt} \left(\frac{\partial L}{\partial \dot{x}_1} \right) - \frac{\partial L}{\partial x_1} = -c_1 \dot{x}_1 \quad (2-9)$$

$$\frac{d}{dt} \left(\frac{\partial L}{\partial \dot{\theta}} \right) - \frac{\partial L}{\partial \theta} = -c_2 x'_{2}{}^2 \dot{\theta} \quad (2-10)$$

2.5.2 Newmark Numerical Solver

Equations of motion that incorporate friction into the calculations require adjustment of the relative velocity of the two degrees of freedom at each time increment. The fact that the equations are not consistent through time means that the peak amplitude cannot be calculated by transfer functions. A numerical time-step solver is required to model the behavior of the system. The Newmark beta method (Newmark, 1959) by Nathan Newmark in “A Method of Computation for Structural Dynamics” is a very popular method used for numerical integration. This method provides two equations that relate the displacement, velocity, and acceleration to the past displacement, velocity, and acceleration over a certain time lapse. Each calculation creates a set of initial conditions for the next time step. Equations 2-11 and 2-12 show the general equations. \dot{U}_{k+1} represents the unknown velocity, \dot{U}_k represents the initial velocity, \ddot{U}_k represents the initial acceleration, \ddot{U}_{k+1} represents the unknown acceleration, δ represents a parameter relating acceleration to velocity, and Δt represents the length of time which is being considered for each step. U_{k+1} represents the unknown displacement, U_k represents the initial displacement, and β represents as parameter relating acceleration to displacement.

$$\dot{U}_{k+1} = \dot{U}_k + \ddot{U}_k(1 - \delta)\Delta t + \ddot{U}_{k+1}\delta\Delta t \quad (2-11)$$

$$U_{k+1} = U_k + \dot{U}_k\Delta t + \ddot{U}_k \left(\frac{1}{2} - \beta \right) \Delta t^2 + \ddot{U}_{k+1}\beta\Delta t^2 \quad (2-12)$$

This process was used for linear functions and nonlinear by using an average prediction process. These equations were traditionally applied to standard coordinate systems. However, when modal analysis was required, these processes were applied to modal coordinates. Tazarv (2011) in “Linear Time History Analysis of MDOF Structure by Mode Superposition Method using Newmark’s Beta Method” utilized the Newmark method on modal coordinates and demonstrated its accuracy by comparing the results to a time history response found in Chopra’s Dynamics of Structures.

2.6 Optimization of Parameters

In Hansen (2011) “The CMA Evolution Strategy : A Tutorial” it was demonstrated how Covariance Matrix Adaptation Evolutionary Strategy can be utilized for optimizing systems. The Covariance Matrix Adaptation (CMA) was a nonlinear optimization procedure. A Gaussian distribution was used to randomly generate vectors for the variables being optimized creating a matrix. The number of vectors generated depended on the number of variables being utilized. Generally, there were more than twice as many generated vectors as variables to ensure a large population of results. Weight factors were generated for the results based on the number of vectors generated. In general, only the vectors with the best “fitness” were given weighted values. After these vectors were created they were filtered to match the limits of the parameter and then input into the governing equation determine the optimization parameter that these combinations produced (Hoshimura, 2005).

The optimization parameter was the end result of the system that was being analyzed. This result was the “fitness” of each particular vector of variables that was sent into the system. The vectors with the best fitnesses were used to create the next generation of variables. The weights

that were created before were then applied to the fittest combinations. These weighted variables were used to create a new mean and standard deviation for each variable. These were then used to create the next generation of vectors. This process was then repeated for multiple generations until an elite generation was created where the vectors were consistent and contained the optimum set of input variables and the optimum fitness of the system.

2.7 Summary and Results

Seismic loading on structures causes damage. Even if the structure is not fatally damaged it may not be fit for use. Even if the structure is still fit for use, the fatigue and deformations cause a reduction in strength. This reduction in strength may require renovation if it is detected or may go undetected and result in unexpected failure in future events. This is the inspiration of research in seismic vibration control. It is also apparent from damage assessment studies that the peak excitations are not the primary damage inducing factors. The total energy applied to the structure, even below peak excitation, is much more indicative of the damage that is assessed to a structure. Excitations of all frequencies and amplitudes must be reduced in order to effectively design a safe structure.

Base Isolation is one method used to reduce the stresses induced on a structure. It is based on the notion of detaching the structure from its foundation and the accelerations of the earthquake. This method is effective by partially deflecting energy and partially absorbing it. The energy that is transferred to the structure is still problematic since the structure has to be anchored to the foundation in some way to return to its original position. These systems show

great improvement but are limited. Many of the same ideas and tools that are utilized in base isolation systems can be applied to other forms of isolation or damping systems.

Tuned Mass Dampers are the primary method being used for vibration control in structures under wind and seismic loading. Translational and pendulum dampers both show effectiveness and have advantages and drawbacks. Active control and multi-tuned mass damper systems both show efficiency and improve on the original TMD ideas. Friction dampers provide the necessary derivation methods needed to describe the system being developed in this document. Many other ideas are being developed in order to increase the effectiveness of damping systems and many of these ideas are useful in other systems as well.

The LaGrange energy method is an efficient and accurate way of deriving equations of motion for dynamic structural systems. This method can be especially useful in pendulum type systems. When a system is developed with a large number of degrees of freedom and coupled equations to model these degrees of freedom, modal analysis is required to effectively manipulate and decouple the equations. This allows them to be solved in terms of modal coordinates. Once the equations are solved in terms of these modal coordinates the system of equations can be analyzed by the Newmark beta numerical solver method. This method is necessary due to the variable equations that are a result of friction forces in the equations of motion.

Optimization of the system is achieved by the Covariance Matrix Adaptation method. This method is an evolutionary method that imitates the survival of the fittest concept. This is a nonlinear optimization process that can optimize multiple parameters quickly and efficiently.

3. SYSTEM DEVELOPMENT

3.1 Introduction

The development of the proposed system began with the concept of isolating the floor slab from the frame. The hypothesis is that such system can be effective since the amount of excited mass is reduced, hence the skeleton frame undergoes small motion since its mass is relatively small. An extensive literature review reveals that no system can be completely isolated. All structural systems must have devices to control the motion of its components relative to the structure and to prevent damage and residual drift due to high displacements of the isolated components. The interaction between the slab and frame is greater when these components are included. The slab begins to move relative to the frame and affect the frame's behavior. These considerations force the slab to act as a TMD system more than an isolation system. In this way, the proposed system is a hybrid system. Literature review is conducted to understand the concepts of TMDs. Many of the dynamic and mathematical analyses that are required to analyze the proposed hybrid system are very similar to other multi-TMD systems. Differences included the friction isolation components and a greatly increased mass ratio due to the size of the floor slabs. The system also combined these aspects with those of pendulum TMDs.

The proposed hybrid system involves isolating the floor slab from the frame. The isolation considered is of the sliding type. Sliding isolation requires the incorporation of friction forces in the derivation. The support surface for the slab is curved as well. The force created by this slope is used to self-center the slab after motion is experienced. Bumpers are also added to protect the frame from the slab during large displacements from the slab.

The equations of motion are derived using the LaGrange Energy conservation. When the equations of motion are completed, modal analysis is required. After the equations are converted into modal coordinates and decoupled the Newmark beta method is utilized. Once the Newmark equations are substituted into the modal equations of motion the unknown variables are found. The modal summation is then completed by converting the coordinates back into the physical coordinates. The complete behavior of the system is then tested and described.

Verification of the derivation of the response equations is achieved by designing a structure to imitate a composite structure modeled in Chopra's Dynamics of Structures. When the system, using Newmark method and modal analysis, is compared to the response of the published structure, the results are identical. Verification of the proposed hybrid system's behavior is confirmed by comparing the floor slab hybrid system with a standard structure without any TMDs. The floor slab system's stiffness is increased greatly to imitate a standard composite floor system to achieve identical results. The final verification of the pendulum TMD derivation is validated by comparing a translational (flat) system to the hybrid system with a very high pendulum arm. These results are also found to be identical.

Once the system is validated the optimization of the system is developed. This is done using the evolutionary theory of Covariance Matrix Adaptation. This is a nonlinear process that optimizes many separate parameters simultaneously. Finally, the optimized the performance of the system is analyzed.

3.2 Conception of system

The development of this concept begins with the idea of isolation. The idea is to isolate as much of the mass of the structure as possible. It is thought that if the frame is split in half and the

slabs isolated, the frame could vibrate out of phase and the slab would not move at all. This would remove all inertia of the slabs from the frame and greatly reduce the stress on the frame. This would require tuning each half of the frame to vibrate out of phase at the resonant frequency. At other frequencies the behavior of the frame halves would not be out of phase and would not perform well. This led to the adjustment to a fixed frame with an isolated floor slab.

The proposed hybrid system comprises of isolated floor slabs that are free to move relative to the frame. The slabs are curved on the bottom and rest on curved supports while conforming to the topology of the supports. The curvature in the supports allows for gravity to reposition the slab back to its original location. Under high excitations large displacements of the slabs may occur during which collisions with the columns and extensive damage are possible. To alleviate such behavior, rubber bumpers are installed between the slab and the frame and their stiffness is relied upon to reduce the potential for such impact. The slab and frame also interact through the contact surface of the support. The friction of the contact surface must be considered and dissipates energy, thus providing damping. However, minimal friction provides better isolation. In doing so, the system acts as a tuned mass damper with large mass ratio. An elevation view of a single story system can be seen in Figure 3-1. The figure shows a 2-story frame with the first story slab that is allowed to move independently from the frame. The slab is curved and rests on curved supports that are used to center the slab after an earthquake. At both ends of the slab, bumpers are installed to prevent contact and damage between the frame and the slab. The stiffness of the frame and the bumpers are represented by k_f and k_b , respectively. The mass of the entire structure, the frame alone, and the slab are designated as, $M_{structure}$, m_1 , and m_2 , respectively. The internal damping of the frame is designated as c_f and the friction coefficient of

the contact surface between the slab and the support as μ . The radius of curvature of the contact surface is represented as R in Figure 3-1.

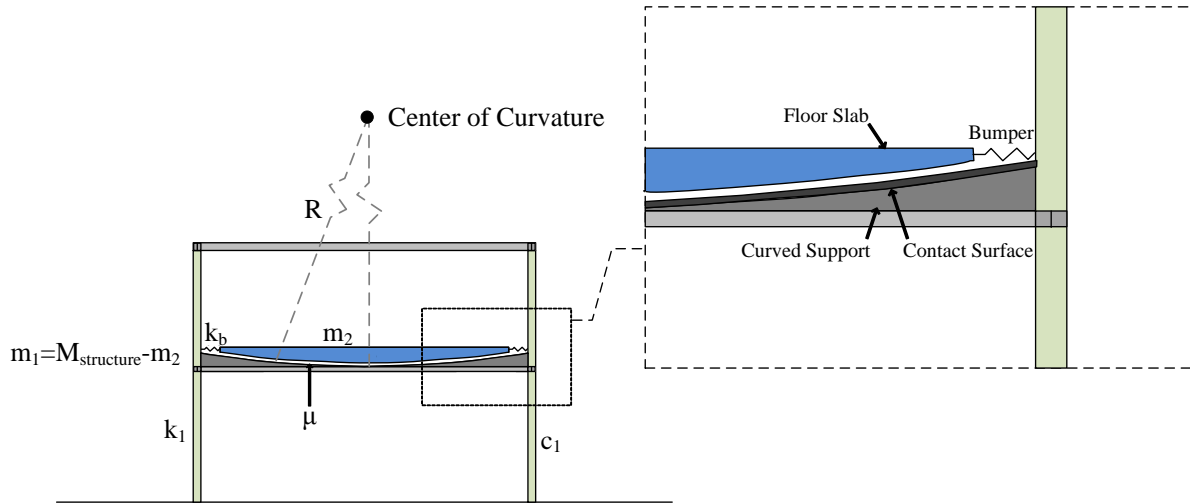


Figure 3-1 Elevation view of two story structure with first story slab isolated

3.3 Development of equations of motion

The hybrid system in Figure 3-1 can be considered a 2 degree-of-freedom (DOF) system, where the mass of the frame is represented as one DOF and the mass floor slab as the second. A coordinate system is set for both degrees of freedom relative to their own original locations. For each story the system has a degree of freedom and an equation of motion. This is also true for every slab that exists on every story. For example, a two story structure will have four degrees of freedom and four governing equations of motion. Each degree of freedom has its own independent coordinate system.

3.3.1 Idealization of system

All components of the proposed hybrid system defined above can be idealized for the development of the equations of motion. Figure 3-2 shows an idealized system representing a single story structure with an isolated floor slab. In Figure 3-2 the bumper stiffness is k_2 instead of k_b . This representation shows a large mass representing the frame of the structure. It is attached to the base by a spring and damper representing the frame properties. The coordinate system for the frame is represented by U_1 and is oriented to the frame's original location. The pendulum behavior and friction are shown for the slab by R and μ . The coordinate system for the slab is in angular coordinates represented by θ_2 . The linearized displacement is U_2 . The linearization is executed with the assumption that angular displacements are small. Equations 3-1 and 3-2 are used to convert to linear coordinates.

$$U_2 = R \sin \theta_2 \quad (3-1)$$

$$y_2 = -R \cos \theta_2 \quad (3-2)$$

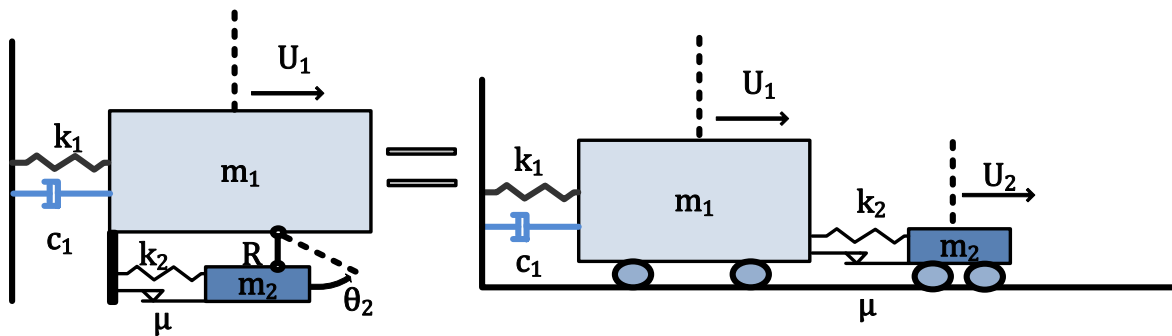


Figure 3-2 Idealized single slab system

3.3.2 Lagrange Energy balance

Each component of the idealized structure has an influence on the energy conservation of the system. Each degree of freedom has its own energy component that must be considered. The frame energy is developed first. The kinetic energy (T_1) consists of the horizontal velocity acting on the mass as in equation 3-3. The potential energy (V_1) of the system is influenced by the displacement and stiffness as shown in equation 3-4.

$$T_1 = \frac{1}{2} m_1 \dot{U}_1^2 \quad (3-3)$$

$$V_1 = \frac{1}{2} k_1 U_1^2 \quad (3-4)$$

The kinetic energy of the slab (T_2) must consider the horizontal and relative vertical velocity of the mass of the slab and is given when equation 3-5 is converted to angular velocity by equation 3-6. The potential energy of the slab (V_2) is influenced by the stiffness of the bumpers as well as the slope of the support. The bumper and slope are only activated, however, by the relative displacement. This means that U_2 must be subtracted from U_1 . This interaction is key in deriving an accurate equation. This can be seen in the potential energy equation 3-7. The derivative of the motion x_2 and y_2 with respect to the angular motion, θ_2 , is denoted with a prime above it, x_2' and y_2' . The second derivative in terms of θ_2 is denoted with a double prime, x_2'' and y_2'' . The equivalent values of these terms can be seen in equations 3-8 through 3-11

$$T_2 = \frac{1}{2} m_2 (\dot{x}_2^2 + \dot{y}_2^2) \quad (3-5)$$

$$T_2 = \frac{1}{2} m_2 [(x_2'{}^2 + y_2'{}^2) \dot{\theta}^2] \quad (3-6)$$

$$V_2 = \frac{1}{2}k_2(x_2 - x_1)^2 - m_2gy_2 \quad (3-7)$$

$$x'_2 = R\cos\theta \quad (3-8)$$

$$x''_2 = -R\sin\theta \quad (3-9)$$

$$y'_2 = R\sin\theta \quad (3-10)$$

$$y''_2 = R\cos\theta \quad (3-11)$$

The kinetic energies and potential energies are combined respectively. The potential energy is then subtracted from the kinetic energy. This new expression is L and represents the balance of energy and can be set to zero. The LaGrange approach now calls for partial derivation of the system to convert the energy terms into force terms. This is done in two steps for the two different coordinate systems. The derivation involves taking the partial derivative of L in terms of the velocity term. The derivative of that expression is found in terms of time to change the velocity terms into acceleration. The partial derivative of L in terms of displacement is then subtracted from the previous term. This process is then repeated for the second coordinate system in the same way. These steps are shown in equations 3-12 through 3-16.

$$L = \frac{1}{2}m_1\dot{x}_1^2 + \frac{1}{2}m_2 \left[(x'_2{}^2 + y'_2{}^2) \dot{\theta}^2 \right] - \frac{1}{2}k_1x_1^2 - \frac{1}{2}k_2(x_2 - x_1)^2 + m_2gy_2 \quad (3-12)$$

$$\frac{d}{dt} \left(\frac{\partial L}{\partial \dot{x}_1} \right) - \frac{\partial L}{\partial x_1} = 0 \quad (3-13)$$

$$\frac{d}{dt} \left(\frac{\partial L}{\partial \dot{\theta}_2} \right) - \frac{\partial L}{\partial \theta_2} = 0 \quad (3-14)$$

$$m_1\ddot{x}_1 + c_1\dot{x}_1 + k_1x_1 + k_2x_1 - k_2x_2 - m_2gy_2' = -m_1\ddot{x}_g + \mu m_2g \quad (3-15)$$

$$m_2 \left[(2x_2'x_2'' + 2y_2'y_2'')\dot{\theta}_2^2 \right] - k_2x_1x_2' - k_2x_2'x_2'' + m_2gy_2' = -m_2\ddot{x}_g - \mu m_2g \quad (3-16)$$

Equations 3-8 through 3-11 are then substituted in for the primed variables. To simplify the equations of motion, it is assumed that the angular displacement of the slab is relatively small. Thus $\cos\theta$ is 1 and $\sin\theta$ is θ .

Now the θ 's can be converted using equation 3-17 to linearize the equations. This substitution finally results in conservative terms of the equations of motion that are desired.

$$\theta_2 = x_2/R \quad (3-17)$$

There are three forcing terms that are not conservative that are also considered. The damping term, the friction term, and the external forcing term are all non-conservative in terms of the closed system of the structure. These terms are included in the equations of motion. The equations of motion are derived through an equilibrium of forces.

3.3.3 Friction forces

Representing friction forces in the equations of motion is a challenge. There are many thoughts on the topic. One method converts the friction force to an equivalent damping term. This is not a simple process and is unnecessarily difficult to derive. It is also not an accurate representation of the system because the friction force is not linearly related to velocity like the damping force. Another approach uses an arcsine representation so as the velocity increases the force approaches the maximum value. This accurately represents the behavior of kinetic friction. However, it is very inefficient to solve in terms of velocity, which is an unknown.

The best option is to assume maximum kinetic friction for any non-zero velocity and utilizing the signum function on the friction term. This function is represented by equation 3-18. This term requires three different equations and three different derivations. But, when the derivations are completed, it can be seen that the only differences in these equations are the signs of the friction terms. The actual friction force is the normal gravitational force of the slab scaled by the coefficient of friction.

$$\text{Signum Function} \Rightarrow \text{sgn}(\dot{x}) = \begin{cases} 1 & \text{if } \dot{x} > 0 \\ 0 & \text{if } \dot{x} = 0 \\ -1 & \text{if } \dot{x} < 0 \end{cases} \quad (3-18)$$

3.3.4 Signum function

The signum function works by applying a certain sign to the terms on which they operate. As it is used in this system, the relative velocity of the floor slab is determined and the signum function acts on that number as seen in equation 3-14. If the argument in the signum function is positive then the function is equal to 1. If the argument is negative then the signum function is -1. If the argument is 0 then the function is 0. This, in effect, does nothing to the friction term other than change its sign. Therefore, if the relative velocity is placed as the argument of the function, then positive velocity would mean positive friction and vice versa. Zero relative velocity would result in no friction. These terms are opposite for the slab versus the frame and this behavior accurately describes the behavior of the system. However, it requires three different sets of equations of motion to solve. These equations are 3-19 through 3-24. Since there are multiple equations describing the behavior, transfer functions cannot be used and a numerical solver is required.

$$m_1\ddot{U}_1 + c_1\dot{U}_1 + \left(k_1 + \left(k_2 + \frac{m_2g}{R}\right)\right)U_1 - \left(k_2 + \frac{m_2g}{R}\right)U_2 = -m_1\ddot{U}_g + \mu m_2g \quad (3-19)$$

$$m_2\ddot{U}_2 - \left(k_2 + \frac{m_2g}{R}\right)U_1 + \left(k_2 + \frac{m_2g}{R}\right)U_2 = -m_2\ddot{U}_g - \mu m_2g \quad (3-20)$$

$$m_1\ddot{U}_1 + c_1\dot{U}_1 + \left(k_1 + \left(k_2 + \frac{m_2g}{R}\right)\right)U_1 - \left(k_2 + \frac{m_2g}{R}\right)U_2 = -m_1\ddot{U}_g - \mu m_2g \quad (3-21)$$

$$m_2\ddot{U}_2 - \left(k_2 + \frac{m_2g}{R}\right)U_1 + \left(k_2 + \frac{m_2g}{R}\right)U_2 = -m_2\ddot{U}_g + \mu m_2g \quad (3-22)$$

$$m_1\ddot{U}_1 + c_1\dot{U}_1 + \left(k_1 + \left(k_2 + \frac{m_2g}{R}\right)\right)U_1 - \left(k_2 + \frac{m_2g}{R}\right)U_2 = -m_1\ddot{U}_g \quad (3-23)$$

$$m_2\ddot{U}_2 - \left(k_2 + \frac{m_2g}{R}\right)U_1 + \left(k_2 + \frac{m_2g}{R}\right)U_2 = -m_2\ddot{U}_g \quad (3-24)$$

3.4 Modal Analysis

The equations of motion can now be determined for all degrees of freedom and the system can be expanded to a four story system with all four stories having activated slabs. This is an initial step for the formation of a generalized equation to be developed to model structures of any size.

Figure 3-3 shows an elevation view of a generalized structure.

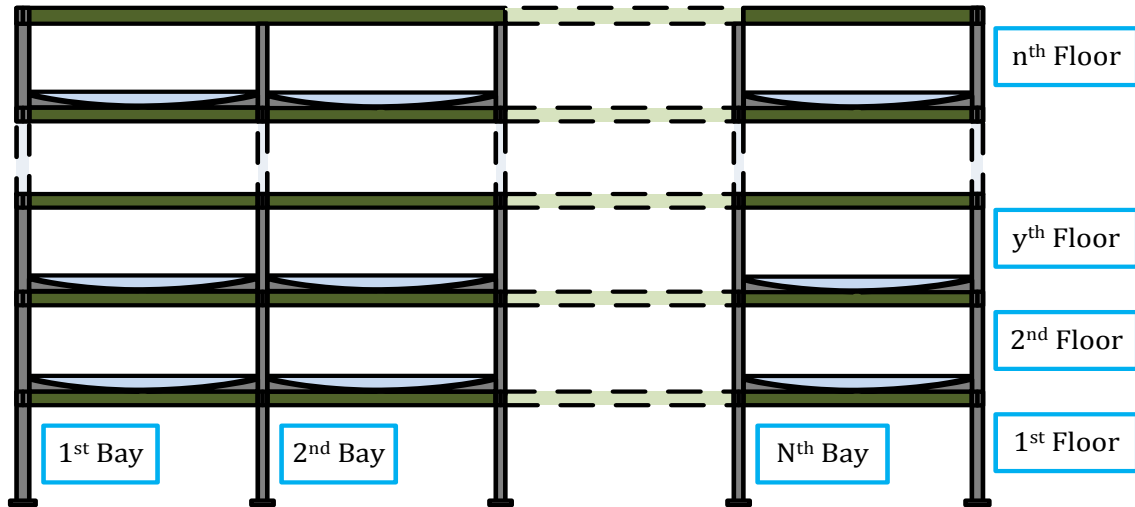


Figure 3-3 Elevation view of multiple story hybrid structure

The derivation of the equations of motion for a four story system allow for the patterns to be seen and the generalized equation to be written. The simplified representation of the generalized structure can be seen in Figure 3-4.

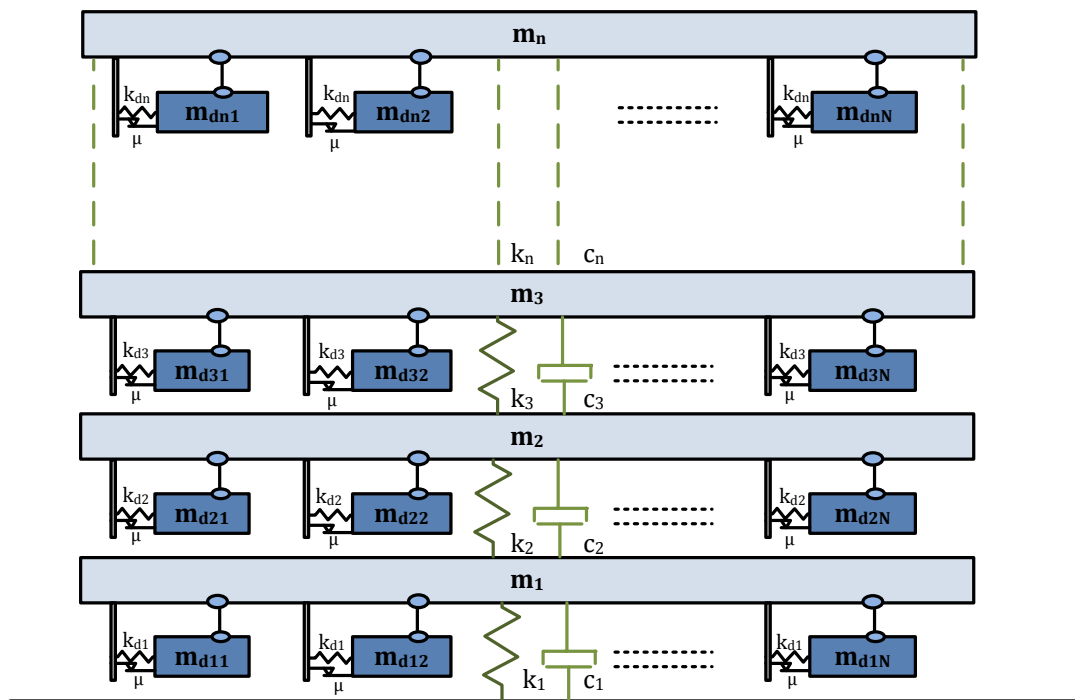


Figure 3-4 Idealized multiple story hybrid system

In the same manner in which the single story equations of motion are derived, the four story structure equations of motion can be seen below. Equation 3-25 is a generalized equation for the frame. Equation 3-26 is a generalized equation for the slabs. Equation 3-27 is the full system of equations for a four story structure. These equations are all coupled and depend on each other. Since the equations are coupled, solving this system of equations requires the Modal Summation method.

$$m_y * \ddot{U}_y + c_y * \dot{U}_y + c_{y+1} * (\dot{U}_y - \dot{U}_{y+1}) + \left(k_y + k_{y+1} + \left(k_{y+n} + \frac{m_{y+n} * g}{R}\right)\right) * U_y - k_{y+1} * U_{y+1} - \left(k_{y+n} + \frac{m_{y+n} * g}{R}\right) * U_{y+n} = \mu * m_{y+n} * g - \ddot{U}_g * m_y \quad (3-25)$$

$$m_{y+n} * \ddot{U}_{y+n} + \left(k_{y+n} + \frac{m_{y+n} * g}{R}\right) * U_{y+n} - \left(k_{y+n} + \frac{m_{y+n} * g}{R}\right) * U_y = -\mu * m_{y+n} * g - \ddot{U}_g * m_{y+n} \quad (3-26)$$

$$\begin{bmatrix} m_1 & 0 & 0 & 0 & 0 & 0 & 0 & 0 \\ 0 & m_2 & 0 & 0 & 0 & 0 & 0 & 0 \\ 0 & 0 & m_3 & 0 & 0 & 0 & 0 & 0 \\ 0 & 0 & 0 & m_4 & 0 & 0 & 0 & 0 \\ 0 & 0 & 0 & 0 & m_5 & 0 & 0 & 0 \\ 0 & 0 & 0 & 0 & 0 & m_6 & 0 & 0 \\ 0 & 0 & 0 & 0 & 0 & 0 & m_7 & 0 \\ 0 & 0 & 0 & 0 & 0 & 0 & 0 & m_8 \end{bmatrix} * \begin{pmatrix} \ddot{U}_{1k+1} \\ \ddot{U}_{2k+1} \\ \ddot{U}_{3k+1} \\ \ddot{U}_{4k+1} \\ \ddot{U}_{5k+1} \\ \ddot{U}_{6k+1} \\ \ddot{U}_{7k+1} \\ \ddot{U}_{8k+1} \end{pmatrix} + \begin{bmatrix} c_1 + c_2 & -c_2 & 0 & 0 & 0 & 0 & 0 & 0 \\ -c_2 & c_2 + c_3 & -c_3 & 0 & 0 & 0 & 0 & 0 \\ 0 & -c_3 & c_3 + c_4 & -c_4 & 0 & 0 & 0 & 0 \\ 0 & 0 & -c_4 & c_4 & 0 & 0 & 0 & 0 \\ 0 & 0 & 0 & 0 & 0 & 0 & 0 & 0 \\ 0 & 0 & 0 & 0 & 0 & 0 & 0 & 0 \\ 0 & 0 & 0 & 0 & 0 & 0 & 0 & 0 \\ 0 & 0 & 0 & 0 & 0 & 0 & 0 & 0 \end{bmatrix} * \begin{pmatrix} \dot{U}_{1k+1} \\ \dot{U}_{2k+1} \\ \dot{U}_{3k+1} \\ \dot{U}_{4k+1} \\ \dot{U}_{5k+1} \\ \dot{U}_{6k+1} \\ \dot{U}_{7k+1} \\ \dot{U}_{8k+1} \end{pmatrix} + \begin{bmatrix} k_1 + k_2 + \left(k_5 + \frac{m_5 g}{R}\right) & -k_2 & 0 & 0 & -\left(k_5 + \frac{m_5 g}{R}\right) & 0 & 0 & 0 \\ -k_2 & k_2 + k_3 + \left(k_6 + \frac{m_6 g}{R}\right) & -k_3 & 0 & 0 & -\left(k_6 + \frac{m_6 g}{R}\right) & 0 & 0 \\ 0 & -k_3 & k_3 + k_4 + \left(k_7 + \frac{m_7 g}{R}\right) & -k_4 & 0 & 0 & -\left(k_7 + \frac{m_7 g}{R}\right) & 0 \\ 0 & 0 & -k_4 & k_4 + \left(k_8 + \frac{m_8 g}{R}\right) & 0 & 0 & 0 & -\left(k_8 + \frac{m_8 g}{R}\right) \\ -\left(k_5 + \frac{m_5 g}{R}\right) & 0 & 0 & 0 & \left(k_5 + \frac{m_5 g}{R}\right) & 0 & 0 & 0 \\ 0 & -\left(k_6 + \frac{m_6 g}{R}\right) & 0 & 0 & 0 & \left(k_6 + \frac{m_6 g}{R}\right) & 0 & 0 \\ 0 & 0 & -\left(k_7 + \frac{m_7 g}{R}\right) & 0 & 0 & 0 & \left(k_7 + \frac{m_7 g}{R}\right) & 0 \\ 0 & 0 & 0 & -\left(k_8 + \frac{m_8 g}{R}\right) & 0 & 0 & 0 & \left(k_8 + \frac{m_8 g}{R}\right) \end{bmatrix} * \begin{pmatrix} U_{1k+1} \\ U_{2k+1} \\ U_{3k+1} \\ U_{4k+1} \\ U_{5k+1} \\ U_{6k+1} \\ U_{7k+1} \\ U_{8k+1} \end{pmatrix} = \begin{pmatrix} -m_1 * \ddot{U}_g + \mu * m_5 * g \\ -m_2 * \ddot{U}_g + \mu * m_6 * g \\ -m_3 * \ddot{U}_g + \mu * m_7 * g \\ -m_4 * \ddot{U}_g + \mu * m_8 * g \\ -m_5 * \ddot{U}_g - \mu * m_5 * g \\ -m_6 * \ddot{U}_g - \mu * m_6 * g \\ -m_7 * \ddot{U}_g - \mu * m_7 * g \\ -m_8 * \ddot{U}_g - \mu * m_8 * g \end{pmatrix} \quad (3-27)$$

This requires an Eigen analysis of the mass and stiffness matrices to determine the mode shapes which can be used to develop the modal equations. The Eigen analysis of the system

yields an Eigen value and an Eigen vector for each degree of freedom. The Eigen values represent the square of the natural frequencies of the structure. There is a modal frequency for each degree of freedom in the system. Each Eigen vector represents the modal contribution factors for each mode and each degree of freedom. The Eigen values and vectors appear as shown in equation 3-28.

$$Eigen\ Values = \begin{bmatrix} \omega_1^2 & 0 & 0 & 0 \\ 0 & \omega_2^2 & 0 & 0 \\ 0 & 0 & \ddots & 0 \\ 0 & 0 & 0 & \omega_{2n}^2 \end{bmatrix} \quad Eigen\ Vectors = \begin{bmatrix} \varphi_{1,1} & \varphi_{1,2} & \cdots & \varphi_{1,2n} \\ \varphi_{2,1} & \varphi_{2,2} & \cdots & \varphi_{2,2n} \\ \vdots & \vdots & \ddots & \vdots \\ \varphi_{2n,1} & \varphi_{2n,2} & \cdots & \varphi_{2n,2n} \end{bmatrix} \quad (3-28)$$

To perform the modal analysis, the global coordinates must be converted to modal coordinates. This is done by a summation of the modal coordinates with the φ values from the modal contribution matrix. Equation 3-29 is used to perform this task. This substitution must be done for all coordinates. The new system of equations is simplified to equation 3-30.

$$U_{1_{k+1}} = \varphi_{11} * q_{1_{k+1}} + \varphi_{12} * q_{2_{k+1}} + \varphi_{13} * q_{3_{k+1}} + \varphi_{14} * q_{4_{k+1}} + \varphi_{15} * q_{5_{k+1}} + \varphi_{16} * q_{6_{k+1}} + \varphi_{17} * q_{7_{k+1}} + \varphi_{18} * q_{8_{k+1}} \quad (3-29)$$

$$[M] * [\varphi] * \{\ddot{q}\} + [C] * [\varphi] * \{\dot{q}\} + [K] * [\varphi] * \{q\} = \{F\} \quad (3-30)$$

The final step in decoupling the equations is to premultiply the entire equation by the transpose matrix of the φ matrix. This system is seen in equation 3-31. By multiplying the mass, damping, stiffness, and forcing values by the transpose of the φ matrix and then the φ matrix again the matrices are converted into diagonal matrices that represent the effective mass, effective damping, effective stiffness, and effective forces. This process is shown by equation 3-32 through 3-35. These matrices only have non-zero values on the diagonal, which results in decoupling of all of the equations. The new decoupled system of equations is shown in equation 3-36.

$$[\varphi]^T * [M] * [\varphi] * \{\ddot{q}\} + [\varphi]^T * [C] * [\varphi] * \{\dot{q}\} + [\varphi]^T * [K] * [\varphi] * \{q\} = [\varphi]^T * \{F\} \quad (3-31)$$

$$[\varphi]^T * [M] * [\varphi] = [M_e] \quad (3-32)$$

$$[\varphi]^T * [C] * [\varphi] = [C_e] \quad (3-33)$$

$$[\varphi]^T * [K] * [\varphi] = [K_e] \quad (3-34)$$

$$[\varphi]^T * \{F\} = \{F_e\} \quad (3-35)$$

$$\begin{bmatrix} m_{e1} & 0 & 0 & 0 & 0 & 0 & 0 & 0 \\ 0 & m_{e2} & 0 & 0 & 0 & 0 & 0 & 0 \\ 0 & 0 & m_{e3} & 0 & 0 & 0 & 0 & 0 \\ 0 & 0 & 0 & m_{e4} & 0 & 0 & 0 & 0 \\ 0 & 0 & 0 & 0 & m_{e5} & 0 & 0 & 0 \\ 0 & 0 & 0 & 0 & 0 & m_{e6} & 0 & 0 \\ 0 & 0 & 0 & 0 & 0 & 0 & m_{e7} & 0 \\ 0 & 0 & 0 & 0 & 0 & 0 & 0 & m_{e8} \end{bmatrix} * \begin{pmatrix} \ddot{q}_{1k+1} \\ \ddot{q}_{2k+1} \\ \ddot{q}_{3k+1} \\ \ddot{q}_{4k+1} \\ \ddot{q}_{5k+1} \\ \ddot{q}_{6k+1} \\ \ddot{q}_{7k+1} \\ \ddot{q}_{8k+1} \end{pmatrix} + \begin{bmatrix} c_{e1} & 0 & 0 & 0 & 0 & 0 & 0 & 0 \\ 0 & c_{e2} & 0 & 0 & 0 & 0 & 0 & 0 \\ 0 & 0 & c_{e3} & 0 & 0 & 0 & 0 & 0 \\ 0 & 0 & 0 & c_{e4} & 0 & 0 & 0 & 0 \\ 0 & 0 & 0 & 0 & c_{e5} & 0 & 0 & 0 \\ 0 & 0 & 0 & 0 & 0 & c_{e6} & 0 & 0 \\ 0 & 0 & 0 & 0 & 0 & 0 & c_{e7} & 0 \\ 0 & 0 & 0 & 0 & 0 & 0 & 0 & c_{e8} \end{bmatrix} * \begin{pmatrix} q_{1k+1} \\ q_{2k+1} \\ q_{3k+1} \\ q_{4k+1} \\ q_{5k+1} \\ q_{6k+1} \\ q_{7k+1} \\ q_{8k+1} \end{pmatrix} = \begin{pmatrix} F_{e1} \\ F_{e2} \\ F_{e3} \\ F_{e4} \\ F_{e5} \\ F_{e6} \\ F_{e7} \\ F_{e8} \end{pmatrix} \quad (3-36)$$

The new independent equations can be directly solved for each unknown variable. Once all of the q values are calculated, the desired unknowns, the U 's, can be calculated using equation 3-29 again.

3.5 Newmark Numerical Solver

As explained before, because of the behavior of the friction terms, transfer functions cannot be used to model the behavior of the structure. Each unknown variable has three different

possible equations. These equations are all used at different points throughout the response of the structure. In addition, each story can have a different sign for the friction term at the same time. Because of this, adjustment of each equation throughout the time response of the system is needed. This requires a numerical time-step solving method. The method of choice among friction based systems is the Newmark-Beta method. This method provides equations to relate the unknown motion variables to the known initial condition motion variables. Equation 3-37 relates the displacement to the acceleration in terms of the initial conditions. Equation 3-38 relates the velocity to the acceleration. β and δ are parameters that represent the interaction of acceleration with the unknown displacement and velocity, respectively, and Δt is the length of time that each time step represents. The mentioned parameters are listed in Table 3-1.

$$\dot{U}_{k+1} = \dot{U}_k + \ddot{U}_k(1 - \delta)\Delta t + \ddot{U}_{k+1}\delta\Delta t \quad (3-37)$$

$$U_{k+1} = U_k + \dot{U}_k\Delta t + \ddot{U}_k\left(\frac{1}{2} - \beta\right)\Delta t^2 + \ddot{U}_{k+1}\beta\Delta t^2 \quad (3-38)$$

β	0.25
δ	0.5
Δt	0.02

When the parameters in Table 3-1 are substituted into the equations of motion the only remaining unknown is the acceleration. Once it is determined, the acceleration can be substituted back into the displacement and velocity equations. This results in the initial conditions for the equations of the next time step. From these new initial conditions, the new equations of motion can be adjusted to match the relative motion of the slab versus the frame. This is how the Newmark method can be used to move through the time response of a system and accurately model the friction in a system.

3.5.1 Response Equations

After substituting the Newmark equations into the decoupled equations of motion the unknown variables can be solved by hand. The resulting equations are 3-39 through 3-41. The modal coordinates (q 's) are then summed using the modal contribution factors (ϕ) in equation 3-29 to find the physical coordinates (U 's). From these U 's the values of interest are shown below. These values are found for an entire time history for each story. The maximum for each story over the entire time response is critical. The maximum response for all the stories is critical among these. This is then tested over many frequencies. The maximum value over all of the frequencies is the peak response of the structure. This value is a component of the total response value of the structure that is optimized. Table 3-2 represents the parameters that are incorporated in the response value of the optimization.

$$\ddot{q}_{y_{k+1}} = \frac{-\dot{q}_{y_k} * [c_{ey} * (1 - \delta) * \Delta t + k_{ey} * (0.5 - \beta) * \Delta t^2] - \dot{q}_{y_k} * [c_{ey} + k_{ey} * \Delta t] - q_{y_{k+1}} * k_{ey} + F_{ey}}{[m_{ey} + c_{ey} * \delta * \Delta t + k_{ey} * \beta * \Delta t^2]} \quad (3-39)$$

$$\dot{q}_{y_{k+1}} = \dot{q}_{y_k} + \ddot{q}_{y_k} * (1 - \delta) * \Delta t + \ddot{q}_{y_{k+1}} * \delta * \Delta t \quad (3-40)$$

$$q_{y_{k+1}} = q_{y_k} + \dot{q}_{y_k} * \Delta t + \ddot{q}_{y_k} * (0.5 - \beta) * \Delta t^2 + \ddot{q}_{y_{k+1}} * \beta * \Delta t^2 \quad (3-41)$$

Table 3-2 Response parameters of interest

Response Parameter	Variable Equivalent
Interstory Drift	$U_y - U_{y-1}$
Global Drift	U_y
Relative Slab Drift	$U_{y+n} - U_y$
Acceleration	\ddot{U}_y

3.6 Verification

The behavior and accuracy of this system had to be verified to ensure the validity of the results. Verification does not only validate that the calculations are accurate and do not contain errors but also prove that the structure is behaving conceptually and physically correctly.

3.6.1 Newmark Modal Analysis Example

The response of a structure to the El Centro earthquake of 1979 in the Imperial Valley of California is found in Chopra's Dynamics of Structures. The building is 5 stories and the structural properties are 45.34×10^3 kg for the mass, 5.52×10^3 kN/m for the stiffness of the frame, and 5% for the damping ratio for each story of the structure. These properties are put into the equations of the hybrid system. To achieve matching results and standard behavior the stiffness of the bumper between the structure and slab is increased exponentially to induce composite behavior. This behavior is confirmed because each story had identical acceleration, velocity, and displacement as its floor slab. The radius is also increased exponentially to imitate a flat structure and so the stiffness created by slope would not affect the results. The friction term is reduced to zero so it did not affect the response of the structure. Once this is done the structure is tested with the El Centro earthquake just as the Chopra structure is. The responses of the structures are virtually identical confirming the accuracy of the Modal analysis and Newmark calculations. No errors can exist with these results and the application of any assumptions made through the derivation of these equations can now be validated. As expected, the verification is seen in Figure 3-5.

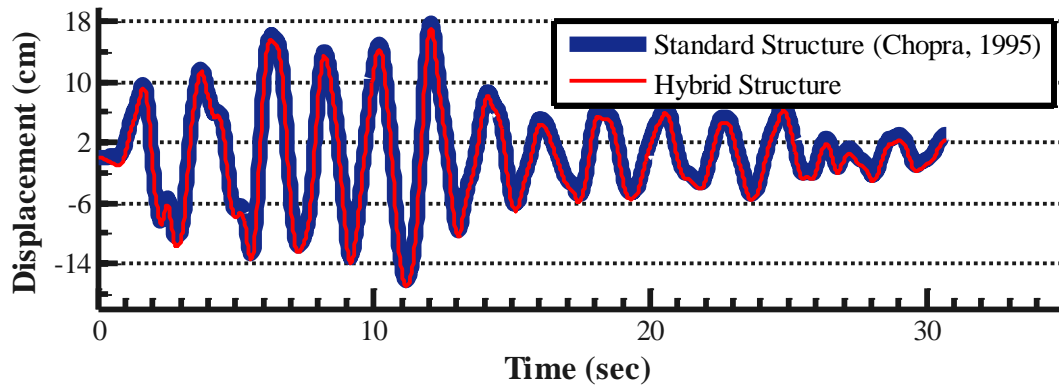


Figure 3-5 Verification comparison to Chopra's El Centro response (Chopra, 1995)

3.6.2 Composite System vs Hybrid System imitating a composite

The conceptual behavior of the system is tested next. This is done by deriving the simple equations of motion for a standard composite structure. No dampers or slabs are added and only the structural degrees of freedom are included. A four story structure is designed and tested over a range of frequencies to find the peak amplitudes of the response of the system. This structure is then tested against the proposed hybrid structure. As previously conducted, this hybrid structure's bumper stiffness and radius are increased exponentially and the friction is reduced to zero. This should produce identical results over the same range of frequencies if the behavior of the system is accurate and the equations of motion are derived properly. In Figure 3-6 the responses are again virtually identical and validated the derivation of the system.

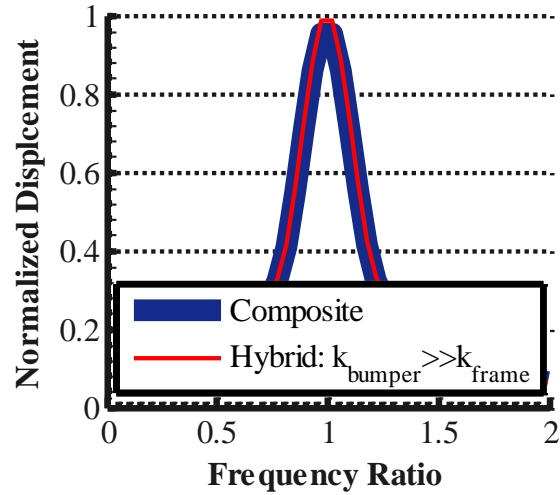


Figure 3-6 Verification of composite structure to hybrid structure with rigid connections between slab and frame

3.6.3 Flat versus high radius of curvature

The final verification step is taken to validate the physical behavior of the curvature of the structure. Theoretically, as the radius of curvature is increased, the system should act as though the damper is on a flat surface. In theory, it should become a translational system. To verify this theory, a hybrid damping system is derived with translational slabs on flat surfaces. Otherwise friction and bumper stiffness are kept consistent and allow for displacement of the slabs. This is then compared to the hybrid system with a curved support. The radius of this curvature is increased exponentially. Both structures are then tested over a range of frequencies. Both responses should be identical, and Figure 3-7 shows that they are. This validates the derivation of the equations of motion.

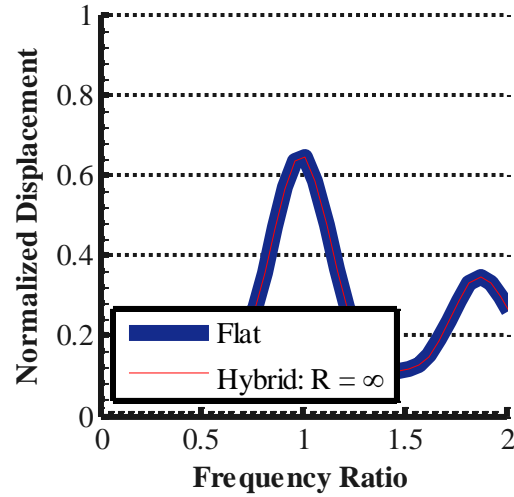


Figure 3-7 Verification comparison of horizontal translational dampers versus hybrid system with infinite radius of curvature

3.7 Optimization

Many of the parameters, such as the size of beams and columns, are dictated by design codes and are not optimized. However the parameters of the hybrid system need to be optimized to minimize the response of the structure. The parameters of the system include the stories at which the hybrid slabs are activated (S_y), the radius of curvature (R), the stiffness between the slab and the frame (k_{y+n}) and the coefficient of friction (μ). S is a binary vector that indicates which stories have activated slabs shown in Figure 3-8. All slabs on each story are activated so a single vector can describe a structure. An activated story is represented by a 1. A rigid story is represented by a 0. The conditional function in equation 3-42 demonstrates the effect of S on the frame parameters.

$$\begin{array}{l}
 \text{if } S = 1 \rightarrow \begin{array}{l} k_{y+n} = k_{y+n} \\ R = R \\ \mu = \mu \end{array} \\
 \text{if } S = 0 \rightarrow \begin{array}{l} k_{y+n} = \infty \\ R = \infty \\ \mu = 0 \end{array}
 \end{array} \tag{3-42}$$

As the size of the structure increases, possible S combinations increase exponentially. These possibilities required robust optimization procedures to ensure an efficient method of finding the best configuration of the system. At least one story has a suspended slab for all combinations. The other optimized variables' physical limits and design requirements dictated their values.

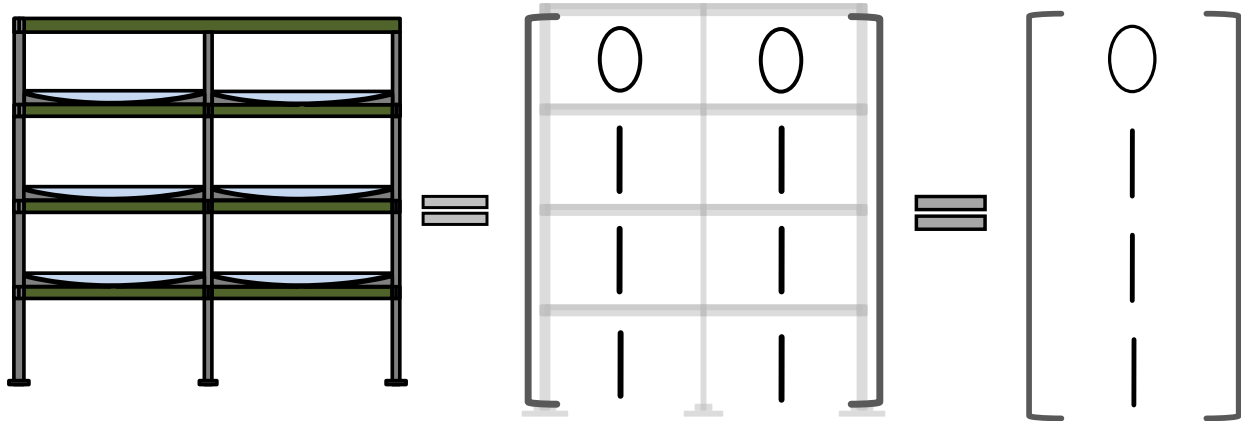


Figure 3-8 Binary representation of activated stories of structure in vector form

3.7.1 Covariance Matrix Adaptation

The Covariance Matrix Adaptation (CMA) is a nonlinear optimization procedure (Hansen, 2011). A CMA optimization code is built in 2 layers. The 1st finds the optimal positions for activated slabs (S) and the 2nd finds the optimal radius (R), stiffness of bumper (k_{y+n}), and coefficient of friction (μ). Figure 3-9 demonstrates how the CMA code functions. The second layer behaves in the same manner. A Gaussian distribution is used to randomly generate vectors for S , creating an S matrix. The number of vectors generated depends on the size of the structure. Weight factors are generated for the results based on the number of combinations generated. After these combinations are created they are filtered to yield binary terms and match any other limits of the parameter and then sent to the inner code. This code does the same for the frame

parameters and put all of these variables into the system response code to retrieve the response of the structure (Hoshimura, 2005).

The optimum frame parameters and responses are found by the inner code and sent back to the combination code. This optimum response is the “fitness” for that combination. Once the fitness’s are found for the generated combinations, they are sorted based on fitness and then the weight factors are applied to the better fitnesses and a new mean and a new standard deviation are created for each. With the new mean and new standard deviation a new group of possible combinations are generated by a new normal distribution (Hansen, 2011). A section of code is included so after a particular combination is optimized its results are stored in a separate matrix. If a duplicate combination is generated then those previous results are called upon instead of optimizing again. This is done to streamline the calculations. This process is repeated for many new generations until a consistent mean is found which represented the best combination of isolated slabs (Hansen, 2011).

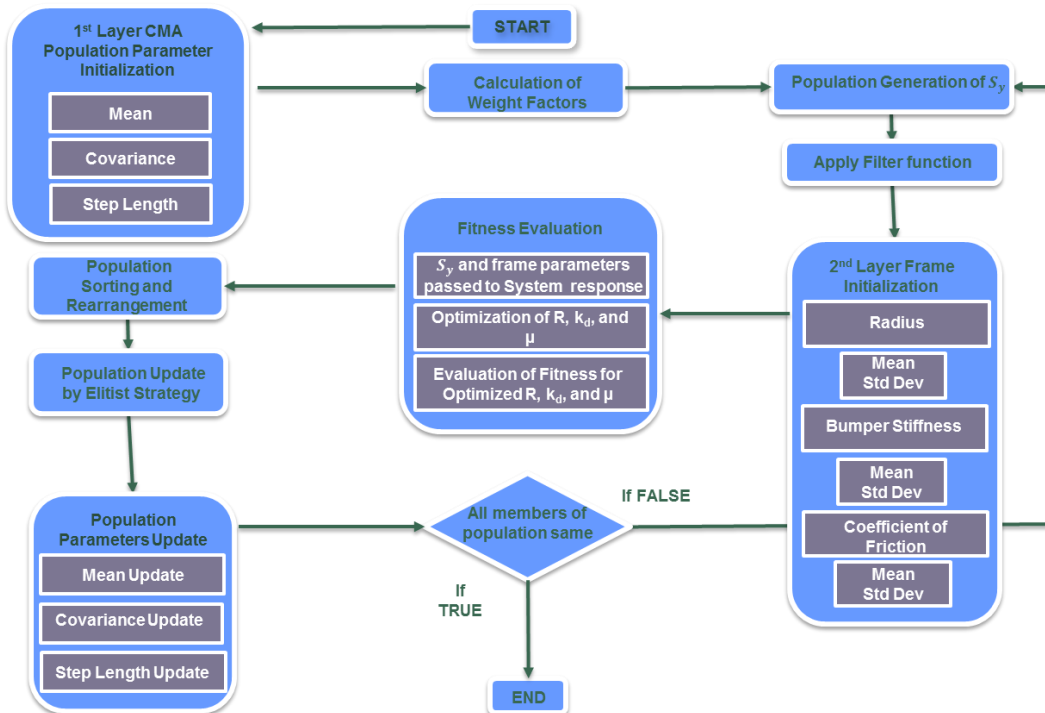


Figure 3-9 Flowchart of CMA optimization process (Chulahwat, 2013)

3.8 Summary and Conclusions

The hybrid system is developed as nothing more than isolating floor slabs from excitation. It soon transformed into a combination of isolation, multi-TMD, pendulum TMD, friction TMD, and large mass ratio TMD systems. Many of the principles needed for these processes have to be incorporated simultaneously to model the hybrid system. The derivation of all the components of the system is completed using the LaGrange energy conservation method. Once these equations of motion are developed the process can be set up in a program to run the calculations.

MATLAB is used for the numerical integration of the system. After the size and structural properties of the system are read into the system response function, the mass and stiffness matrices are built from the equations of motion. These are then used to perform an Eigen analysis on the system to retrieve the natural frequencies and the modal contribution factors. Once the natural frequencies are found the damping coefficients are calculated using the damping ratios. These are used to build the damping matrix. The global coordinates are then converted to modal coordinates by multiplying the mass, damping, and stiffness matrices by the phi matrix and its transpose. This left the equations decoupled with the effective mass, effective damping, and effective stiffness matrices. The known terms of the forcing ground accelerations and friction terms are set up for each individual equation and time step. The frictions of the equations are adjusted based on the initial conditions of the relative velocity of the slabs. These terms are then multiplied by the transpose of the ϕ matrix to keep the two sides of the equations balanced.

The response equations that are calculated earlier are then set up based on the sign of the friction term. These are used to solve for all modal coordinates (q). Once the modal coordinate

terms are found, the physical coordinates (U) are solved through summation with the mode shapes (φ) terms. Once the U terms are found they are set to the initial conditions of the next time step. The loop is then repeated for all time steps. The maximum values throughout the time histories are then found. The maximum of each unknown over all stories is then found. The maximum over all frequencies tested is then found. The sum of the squares of these parameters of interest is found and this value is used to optimize the system.

The optimization code is also built into MATLAB. The number of stories is read into the program. The number of generations and weights of each fitness are initialized. The different generations are then produced and filtered to be useful vectors of binary combinations that represented activated and non-activated stories. These combinations are then sent down into a second layer of optimization. This second layer does the same process with other parameters to be optimized; k_b , R , and μ . This layer then sends all of these parameters to the system response code described above. This code builds the equation of motion matrices from these parameters. It runs the response and gets the sum of the squares described before that represents the total response.

This value is sent back to the second optimization layer. These response values are linked to the combinations put into the system. These combinations are ranked based on the best responses. The mean and standard deviation of each parameter are adjusted separately based on the weighting factors applied to the best responses. A new generation of combinations is produced and tested in the same way. This process is repeated until a consistent mean and standard deviation is found around the optimum combination of parameters. These optimum parameters and the optimum response are sent back to the first layer of the optimization for each activation vector. The same process is followed for each activation vector until the combination

of activation vector and optimum parameters is found with the “fittest” response. This survival of the fittest value represents the structure with the optimized parameters and is subject to a performance evaluation. This process can be done for a structure of any size. Time is the only limitation to the calculations.

4. PUBLICATION¹

Summary

Base isolation and tuned mass dampers are known to be highly effective for earthquake mitigation. However their effectiveness is limited to a specific domain of cases and is confined by various constraints that have to be met. In this study, a hybrid floor slab tuned mass damper and isolation system is introduced whereby the floor slabs are allowed to move relative to the main frame. The floor slabs are resting on curved supports to allow for self-centering of the slabs upon the conclusion of the seismic event. An optimized design of the curved supports and friction between the supports and the slabs can reduce the response of the structure by up to 40%. The optimization strategy is employed over a range of frequencies in order to reduce the response for any input. The results show an improved system with decreased displacement, acceleration and inter-story drift. The proposed hybrid system is shown to not only be quite effective, but also much more robust than conventional isolation strategies. The floor slab mass is uncoupled from that of the main frame through isolation while emulating the function of a tuned mass damper system with inherently much higher mass ratio; hence the improved response.

1. An Innovative Hybrid Tuned Mass Damper and Isolation Floor Slab System Optimized for Vibration Control
By Travis Engle, Hussam Mahmoud, and Akshat Chulahwat

4.1 Introduction

Seismic events are not only a source of concern due to their threat to human life but also due to their affinity for large scale destruction. Recent seismic events including the 1994 Northridge and 1995 Kobe earthquakes demonstrated the potential for earthquakes to inflict billions of dollars' worth of damage to structures (Ghobarah et al., 1999; Kelly, 1998). The plastic deformations that are induced through energy dissipation are significant to classify the structures as unfit for use (Chai et al., 1995; Stephens & VanLuchene, 1994; Suidan & Eubanks, 1971). In the last decade, attention has been shifted towards achieving a sustainable built environment that is less vulnerable to seismic hazard. This resulted in a recent shift in the philosophy outlining structural performance during large magnitude earthquakes from preventing collapse to providing high resiliency structures that are easier to repair after a major event. The change in the performance philosophy requires the development of new and innovative structural systems that are capable of performing as desired. Therefore, it is necessary to create new seismic force resisting systems that satisfy higher performance goals and can be easily repaired, with minimal cost, after major seismic events. Recent research along this theme has demonstrated superior performance of systems employing replaceable elements when compared to conventional structural systems. Examples of such systems include rocking frames with fuses and frames employing scorpion braces (Eartherton et al., 2010; Gray et al., 2012). Tuned mass dampers (TMDs) have proven to be effective in mitigating the potential for earthquake damage on structural systems. A TMD is a simple passive device that can eliminate undesirable motion due to the resonance vibration of the structure (Spencer & Sain, 1997). The system generally consists of dampers, a mass/inertia, a restoring mechanism, and an energy dissipation mechanism. The

most common type of TMDs is the translational one (TTMD) where a mass is mounted atop the roof of a building and allowed to translate horizontally as the primary structure vibrates. The frequency of translation of the added mass is tuned to the resonance frequency of the structure so when the structure is excited at its fundamental frequency, the added mass resonates out of phase with the structural motion, causing reduction in vibration of the main structure. The concept of TTMD was first developed in 1909 to reduce the rolling motion of ships and mitigate ship hull vibrations (Ormondroyd & Den Hartog, 1928). In 1928, the theory on TMD was presented by Ormondroyd and Den Hartog (Ormondroyd & Den Hartog, 1928). Following the theoretical development, a detailed discussion on optimal tuning and damping parameters was discussed in Den Hartog's book on mechanical vibrations (Den Hartog, 1940). Significant contributions to understanding the theoretical and practical application of TTMD in civil structures have been made by various researchers (Randall et al., 1981; Tsai & Lin, 1993; Warburton & Ayorinde, 1980; Warburton, 1982). Figure 1 shows two types of dampers including a pendulum TMD system (Figure 4-1a) and a translational TMD (Figure 4-1b) (J. J. Connor, 2003; Sladek & Klingner, 1993; Spencer & Sain, 1997).

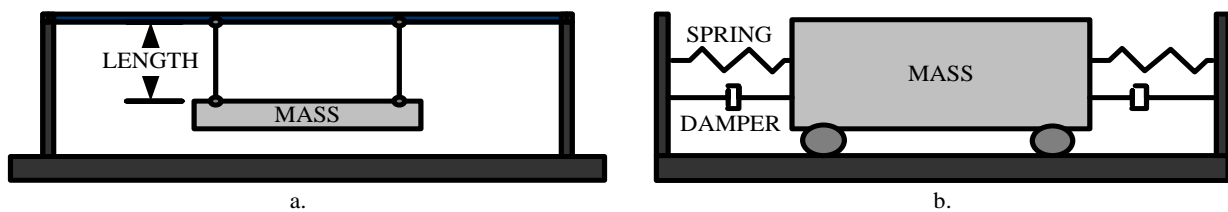


Figure 4-1. (a) Pendulum Damper (b) Translational Damper: *after [8], [15], and [16]*

These TMD systems are effective over a small domain of input frequencies due to their small mass ratio (Almazán et al., 2007; Chopra, 1995). The larger the tuned mass, the more effective it would be in reducing response (Li & Zhu, 2006; Moon, 2010). However, due to design limitations the size of tuned mass was typically restricted since an extra weight would require

larger structural elements to be used, making the system impractical. Standard TMDs, although have a relatively small mass ratio, have a profound effect on the performance of the structure by reducing the motion to an allowable limit (Joshi & Jangrid, 1997). Although their effectiveness have been recognized, the limitation on the mass size have shown to hinder their applicability in certain cases (Mohebbi et al., 2012).

Another popular approach to earthquake mitigation is base isolation, in which the supporting frame of the structure is detached all together from the foundation (Constantinou et al., 1998). In doing so, the entire structure is uncoupled from the base or foundation. Ideally, the structure's inertia attempts to keep it at rest while the ground moves beneath it under seismic loading. In practice, the structure still must remain on the foundation. Bearings or pendulum sloped plates are used to bring the structure back into place after the motion has ceased to prevent any residual drift.

One of the drawbacks of base isolations was that although they allow for the peak displacements to be greatly reduced, a complete elimination of the displacement was not possible. This displacement essentially transfers to the structure through attachments used and can potentially cause some damage to the structure (Kelly & Beucke, 1983). An additional drawback of this system was that the bearings on which the structure rested could be damaged over time from the energy dissipated. While this was more desirable than damage to the main structure, these elements support the entire structure and therefore are difficult to replace (Kelly & Beucke, 1983; Kelly, 1998). Thus, the question remains as to how the demand induced on a structure can be minimized under seismic loading in order to reduce permanent damage while allowing easy repairs?

The objective of this study is to develop a hybrid floor isolation-TMD system that effectively reduces the seismic demand for a wide range of loading frequencies with the ultimate goal of avoiding permanent damage and deformation. The paper first discusses the components of the proposed hybrid system, followed by its respective equations of motion, which are used to describe the dynamics of the proposed hybrid system. The performance of the system is then verified against published data. Finally, a suitable optimization strategy is implemented to obtain the design parameters of the system and to compare its effectiveness against a typical composite steel frame.

4.2 Proposed Isolated Floor System

The merit of the proposed system hinges on the concept of isolating a percentage of the structural mass of the system to effectively reduce the inertia mass and hence decrease the seismic demand. This stems from the fact that floor slabs contribute to a significant percentage of the total structure mass; therefore isolating the floor slabs from the structure leaves only the frame of the structure to be dynamically excited. Similar to the principle of base isolation, this induces relatively less demand on the structure and thus, a reduced response can be obtained (Chulahwat, 2013).

The proposed hybrid floor slab TMD isolation system comprises of isolated floor slabs that are free to move relative to the frame. The slabs are curved at their ends and rest on curved supports while conforming to the topology of the supports. The curvature in the supports allows for gravity to reposition the slab back to its original location. Under large excitations large displacements of the slabs may occur during which collisions with the columns and extensive

damage are possible. To alleviate such behavior, rubber bumpers are installed between the slab and the frame and their stiffness is relied upon to reduce the potential for such impact. The slab and frame also interact through the contact surface of the pendulum supports. The friction of the contact surface can be used to dissipate energy, thereby providing some damping to the system. In doing so, the system acts as a tuned mass damper with large mass ratio. An elevation view of a single story system can be seen in Figure 4-2. The figure shows a 2-story frame with the first story slab that is allowed to move independently from the frame. The slab is curved and rests on curved supports that are used to center the slab after an earthquake. At both ends of the slab, bumpers are installed to prevent contact and damage between the frame and the slab. The stiffness of the frame and the bumpers are represented by k_1 and k_b , respectively. The mass of the entire structure, the frame alone, and the slab are designated as $M_{structure}$, m_1 , and m_2 , respectively. The internal damping of the frame is designated as c_1 and the friction coefficient of the contact surface between the slab and the support as μ . The radius of curvature of the contact surface is represented as R in Figure 4-2.

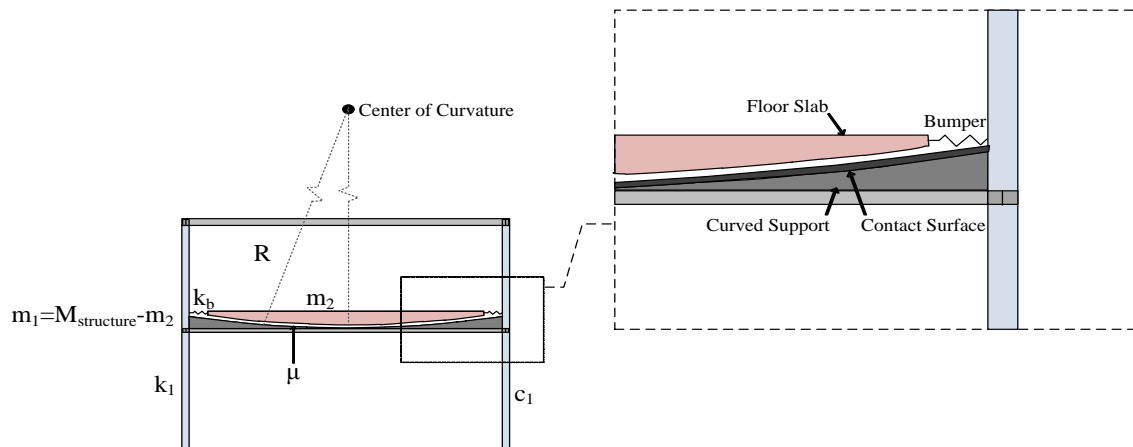


Figure 4-2. Elevation view of proposed single story system

4.3 Single Story System Development

4.3.1 Simplification

The hybrid system in Figure 4-2 can be considered a 2 degree-of-freedom (DOF) system, where the mass of the frame is represented as a one DOF and the mass floor slab as the second. A coordinate system is set for both degrees of freedom relative to their own original locations. The motion of the slab relative to the structure is determined by subtracting the displacement of the slab from the global displacement of the structure at any given point in time. The governing equations of motion for both DOFs are determined using the Lagrange energy balance approach (Boyer, 1968; Matta & De Stefano, 2009a; Setareh et al., 2006; Tedesco et al., 1999). Figure 4-3 shows the idealized representation and linearization of the system. The displacement of the frame and the slab is defined as U_1 and U_2 , respectively. The stiffness of the frame and the bumpers are represented by k_1 and k_2 , respectively. The mass of the slab and the frame alone are designated as m_2 and m_1 , respectively. The internal damping coefficient of the frame is defined as c_1 . The friction coefficient of the contact surface between the slab and the support is shown as μ . The rotation of the slab is θ_2 . The radius of curvature of the contact surface is represented as R as demonstrated in Figure 4-2.

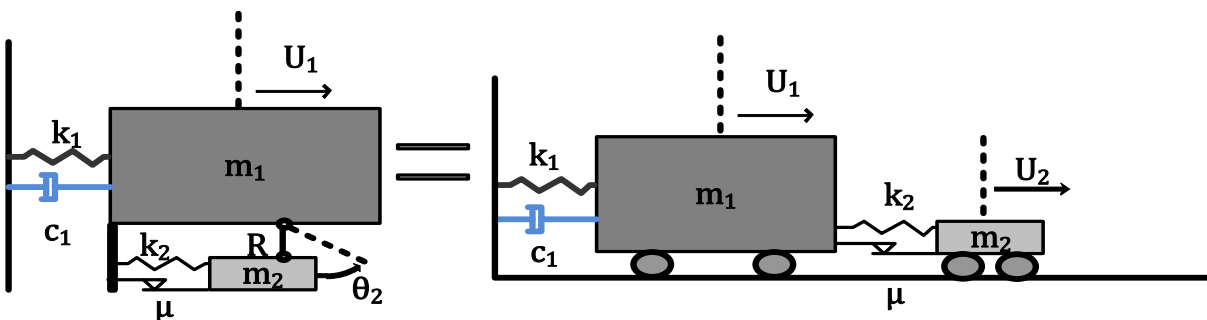


Figure 4-3. Idealized representation of single story system

4.3.2 Equations of Motion

Equation 1 represents the motion of the frame alone while Equation 2 represents the motion of the slab. In the proposed hybrid system, the floor slab moves in a curved path, thus its motion is a function of angle (θ_2) where θ_2 is the angular motion of the slab (shown in Figure 3).

Equation 3 is used to convert the rotational motion of the slab into translational motion.

Equations 1 and 2 are then linearized based on the assumption that the motion of the slab (θ) is small. Thus $\cos(\theta)$ is 1 and $\sin(\theta)$ is θ . Following the linearization of Equation 4-1 and 4-2, Equation 4-3 is substituted into these two equations to obtain the linearized response as shown in Equation 4-4 and 4-5. Table 4-1 defines all variables in the equations.

$$m_1\ddot{U}_1 + c_1\dot{U}_1 + k_1U_1 + \left(k_2 + \frac{m_2g}{R}\right)U_1 - \left(k_2 + \frac{m_2g}{R}\right)R\sin\theta_2 = -m_1\ddot{U}_g + \mu m_2g \quad (4-1)$$

$$m_2R\ddot{\theta}_2 - \left(k_2 + \frac{m_2g}{R}\right)U_1\cos\theta_2 + \left(k_2 + \frac{m_2g}{R}\right)R\cos\theta_2\sin\theta_2 = -m_2\ddot{U}_g - \mu m_2g \quad (4-2)$$

$$U_2/R = \theta_2 \quad (4-3)$$

$$m_1\ddot{U}_1 + c_1\dot{U}_1 + \left(k_1 + \left(k_2 + \frac{m_2g}{R}\right)\right)U_1 - \left(k_2 + \frac{m_2g}{R}\right)U_2 = -m_1\ddot{U}_g + \mu m_2g \quad (4-4)$$

$$m_2\ddot{U}_2 - \left(k_2 + \frac{m_2g}{R}\right)U_1 + \left(k_2 + \frac{m_2g}{R}\right)U_2 = -m_2\ddot{U}_g - \mu m_2g \quad (4-5)$$

Table 4-1. Variable definitions

Known Variables		Unknown Variables	
m_1	mass of the structure	U_1	global displacement of the structure
c_1	damping coefficient of the structure	\dot{U}_1	global velocity of the structure
k_1	stiffness of the structure	\ddot{U}_1	global acceleration of the structure
m_2	mass of floor slab	θ_2	angular displacement of the floor slab
k_2	stiffness of bumper	$\dot{\theta}_2$	angular velocity of the floor slab
μ	coefficient of friction of the contact surface	$\ddot{\theta}_2$	angular acceleration of the floor slab
R	radius of curvature	U_2	global displacement of floor slab
g	gravitational constant	\dot{U}_2	global velocity of floor slab
\ddot{U}_g	ground acceleration	\ddot{U}_2	global acceleration of floor slab

The sign of the friction term in Equation 4-4 and 4-5 above depends on the relative motion of the slab to the frame, which ultimately changes throughout the time-history response of the structure; causing a change in the equations. A time step numerical solver is required so the equations can be adjusted at any time. The Newmark Beta method is most often used in friction – damping systems and is chosen for constructing the system of equations (Bhaskararao & Jangid, 2006; Gewei & Basu, 2010; S. Lee et al., 2008). Equation 4-6 and Equation 4-7 relate velocity (\dot{U}) to acceleration (\ddot{U}), and displacement (U) to acceleration (\ddot{U}) respectively, according to the Newmark Method. In these equations, k represents the values at k^{th} instance of time and $k+1$ at the $(k + 1)^{th}$ instance. In equation 4-6 and 4-7, β and δ are parameters that represent the interaction displacement and velocity in a given step with the acceleration in the prior step, respectively, and Δt is the length of time that each time step represents.

$$\dot{U}_{1_{k+1}} = \dot{U}_{1_k} + \ddot{U}_{1_k} * (1 - \delta) * \Delta t + \ddot{U}_{1_{k+1}} * \delta \Delta t \quad (4-6)$$

$$U_{1_{k+1}} = U_{1_k} + \dot{U}_{1_k} * \Delta t + \ddot{U}_{1_k} * (0.5 - \beta) * \Delta t^2 + \ddot{U}_{1_{k+1}} * \beta * \Delta t^2 \quad (4-7)$$

Similarly, Equations 4-6 and 4-7 can be modified to represent the motion of the floor slab as well. The slab response is shown in Equations 4-8 and 4-9.

$$\dot{U}_{2_{k+1}} = \dot{U}_{2_k} + \ddot{U}_{2_k} * (1 - \delta) * \Delta t + \ddot{U}_{2_{k+1}} * \delta * \Delta t \quad (4-8)$$

$$U_{2_{k+1}} = U_{2_k} + \dot{U}_{2_k} * \Delta t + \ddot{U}_{2_k} * (0.5 - \beta) * \Delta t^2 + \ddot{U}_{2_{k+1}} * \beta * \Delta t^2 \quad (4-9)$$

The Newmark method provided the equations necessary to solve the system of equations. For each time step the unknown variables are solved. After these values are determined the relative motions of the slab and frame are re-evaluated and the friction terms are adjusted accordingly for future calculations. The next time step is then evaluated and the process is repeated for the entire time history of inputs (Newmark, 1959).

4.3.3 Response Equation

The system of equations is solved using the substitution method and the response equations are developed for each unknown variable. These equations model the behavior of the complete system. The numerical integration for the system of equations is performed in MATLAB [34] which is a high-level language and interactive environment for numerical computation, visualization, and programming. Equations 4-10, 4-11 and 4-12 represent the acceleration, velocity and displacement for the structural frame. Equations 4-13, 4-14 and 4-15 represent the acceleration, velocity and displacement for the floor slab.

$$\begin{aligned} \ddot{U}_{1_{k+1}} = & \left\{ \left[- \left[\left(k_2 + \frac{m_2 g}{R} \right) (U_{2_k} + \dot{U}_{2_k} \Delta t + \ddot{U}_{2_k} (0.5 - \beta) \Delta t^2) \right] + \left[\left(k_2 + \frac{m_2 g}{R} \right) (U_{1_k} + \dot{U}_{1_k} \Delta t + \right. \right. \right. \\ & \left. \left. \ddot{U}_{1_k} (0.5 - \beta) \Delta t^2) \right] - [\mu m_2 g + m_2 \ddot{U}_g] \right\} * \left[- \left(k_2 + \frac{m_2 g}{R} \right) \beta \Delta t^2 \right] + \left\{ [c_1 (\dot{U}_{1_k} + \ddot{U}_{1_k} (1 - \delta) \Delta t)] + \right. \\ & \left. \left[\left(k_1 + \left(k_2 + \frac{m_2 g}{R} \right) \right) (U_{1_k} + \dot{U}_{1_k} \Delta t + \ddot{U}_{1_k} (0.5 - \beta) \Delta t^2) \right] - \left[\left(k_2 + \frac{m_2 g}{R} \right) (U_{2_k} + \dot{U}_{2_k} \Delta t + \ddot{U}_{2_k} (0.5 - \right. \right. \right. \\ & \left. \left. \beta) \Delta t^2) \right] - [\mu m_2 g] + [m_1 \ddot{U}_g] \right\} \left[m_2 + \left(k_2 + \frac{m_2 g}{R} \right) \beta \Delta t^2 \right] / \left\{ \left[- \left(k_2 + \frac{m_2 g}{R} \right) \beta \Delta t^2 \right] \left[- \left(k_2 + \right. \right. \right. \\ & \left. \left. \frac{m_2 g}{R} \right) \beta \Delta t^2 \right] - \left[m_1 + c_1 \delta \Delta t + \left(k_1 + \left(k_2 + \frac{m_2 g}{R} \right) \right) \beta \Delta t^2 \right] \left[m_2 + \left(k_2 + \frac{m_2 g}{R} \right) \beta \Delta t^2 \right] \right\} \end{aligned} \quad (4-10)$$

$$\dot{U}_{1_{k+1}} = \dot{U}_{1_k} + \ddot{U}_{1_k} (1 - \delta) \Delta t + \ddot{U}_{1_{k+1}} \delta \Delta t \quad (4-11)$$

$$U_{1_{k+1}} = U_{1_k} + \dot{U}_{1_k} \Delta t + \ddot{U}_{1_k} \left(\frac{1}{2} - \beta \right) \Delta t^2 + \ddot{U}_{1_{k+1}} \beta \Delta t^2 \quad (4-12)$$

$$\begin{aligned} \ddot{U}_{2_{k+1}} = & \left\{ \left[\left[\left(k_2 + \frac{m_2 g}{R} \right) (U_{2_k} + \dot{U}_{2_k} \Delta t + \ddot{U}_{2_k} (0.5 - \beta) \Delta t^2) \right] + [\mu m_2 g] - [c_1 (\dot{U}_{1_k} + \ddot{U}_{1_k} (1 - \delta) \Delta t)] - \right. \right. \\ & \left. \left[\left(k_1 + \left(k_2 + \frac{m_2 g}{R} \right) \right) (U_{1_k} + \dot{U}_{1_k} \Delta t + \ddot{U}_{1_k} (0.5 - \beta) \Delta t^2) \right] - [m_1 \ddot{U}_g] \right\} \left[- \left(k_2 + \frac{m_2 g}{R} \right) \beta \Delta t^2 \right] + \\ & \left\{ \left[\left(k_2 + \frac{m_2 g}{R} \right) (U_{2_k} + \dot{U}_{2_k} \Delta t + \ddot{U}_{2_k} (0.5 - \beta) \Delta t^2) \right] - \left[\left(k_2 + \frac{m_2 g}{R} \right) (U_{1_k} + \dot{U}_{1_k} \Delta t + \ddot{U}_{1_k} (0.5 - \beta) \Delta t^2) \right] - \right. \\ & \left. [\mu m_2 g + m_2 \ddot{U}_g] \right\} \left[m_1 + c_1 \delta \Delta t + \left(k_1 + \left(k_2 + \frac{m_2 g}{R} \right) \right) \beta \Delta t^2 \right] / \left\{ \left[- \left(k_2 + \frac{m_2 g}{R} \right) \beta \Delta t^2 \right] \left[- \left(k_2 + \right. \right. \right. \\ & \left. \left. \frac{m_2 g}{R} \right) \beta \Delta t^2 \right] - \left[m_1 + c_1 \delta \Delta t + \left(k_1 + \left(k_2 + \frac{m_2 g}{R} \right) \right) \beta \Delta t^2 \right] \left[m_2 + \left(k_2 + \frac{m_2 g}{R} \right) \beta \Delta t^2 \right] \right\} \end{aligned} \quad (4-13)$$

$$\dot{U}_{2_{k+1}} = \dot{U}_{2_k} + \ddot{U}_{2_k} (1 - \delta) \Delta t + \ddot{U}_{2_{k+1}} \delta \Delta t \quad (4-14)$$

$$U_{2_{k+1}} = U_{2_k} + \dot{U}_{2_k} \Delta t + \ddot{U}_{2_k} \left(\frac{1}{2} - \beta \right) \Delta t^2 + \ddot{U}_{2_{k+1}} \beta \Delta t^2 \quad (4-15)$$

The system of equations (Equations 4-10 through 4-15) is solved in terms of the response variables. The effect of the system variables including the radius of curvature, the friction between the slab and curved supports, and the stiffness of the bumper on the performance under sinusoidal excitation over a range of frequencies is shown in Figure 4-4. To accurately predict the motion of the system, the time step is kept smaller than that of the input excitation values. The motion of this system varies by the instant in a non-linear behavior, thus the average acceleration method of Newmark Method is chosen instead of the linear acceleration method

(Newmark, 1959). The time stepping interval (Δt) and the parameters β and δ are selected as 0.02, 0.5, and 0.25, respectively. As shown in the figure, as the radius of curvature increases the response of the system decreases initially and then increases. Low friction offers isolation from the system, yet friction is also a method of dissipating energy. As friction increases, the response decreases and approaches a minimum response. The effect of the stiffness between the frame and the slab (bumper) is also tested and it can be seen that as the stiffness increases the response initially decreases and then increases, much like the radius of curvature. This is because both the bumper and the curvature affect stiffness between the slab and frame. All of these variables must be optimized simultaneously in order to develop the most efficient and robust design for the hybrid system.

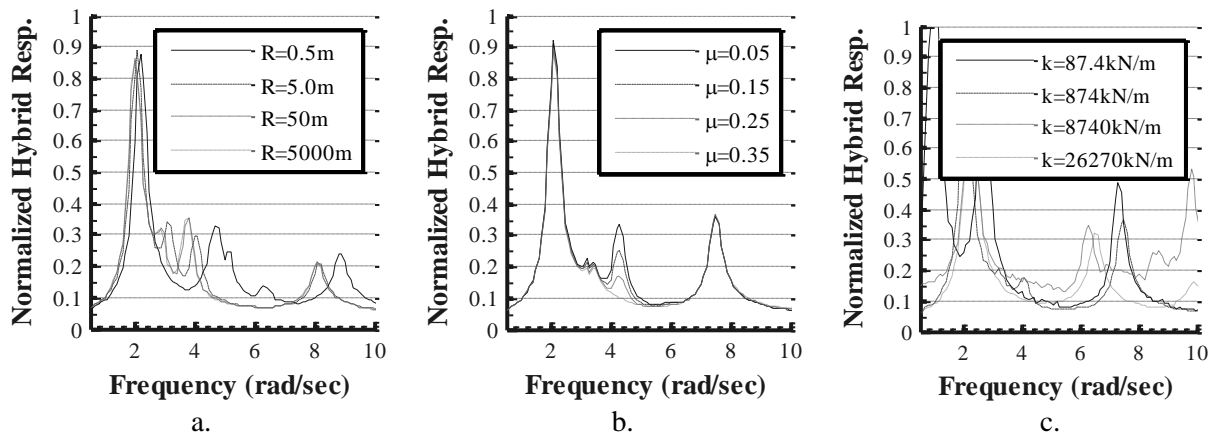


Figure 4-4. Response versus input variables for (a) radius of curvature (b) coefficient of friction (c) stiffness of bumper

4.4 Multiple Story System

4.4.1 Idealization

To extend the proposed hybrid system to a (MDOF) system, the equations of motion need to be generalized. Figure 4-5 shows the elevation view of a multi-story structure with all floor slabs isolated for an N number of bays and n number of stories. The equations governing the response of the slabs are expanded to include multiple floor slabs per story and to account for isolated slabs presented on specific floors. The stiffness, friction, and radius, though to be optimized, are assumed to be consistent throughout the structure. The idealized system is seen in Figure 4-6.

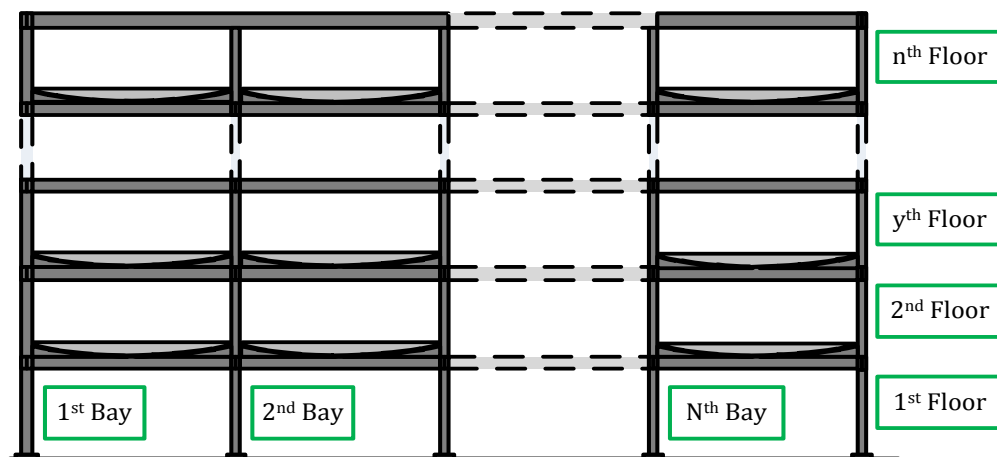


Figure 4-5. Elevation view of multistory system

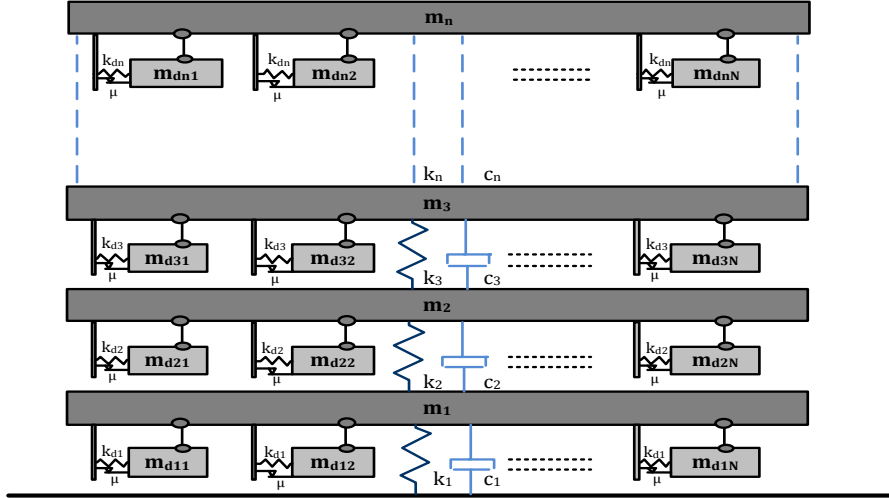


Figure 4-6. Idealized representation of multistory system

4.4.2 Equations of Motion

The equation of motion for each story can be seen by the generalized equation below (Equation 4-16). The equation of motion for each floor slab is the same as that of Equation 4-17 for the single story floor slab, where the floor number is represented by “y” and “n” is the total number of stories.

$$m_y * \ddot{U}_y + c_y * \dot{U}_y + c_{y+1} * (\dot{U}_y - \dot{U}_{y+1}) + \left(k_y + k_{y+1} + \left(k_{y+n} + \frac{m_{y+n} * g}{R} \right) \right) * U_y - k_{y+1} * U_{y+1} - \left(k_{y+n} + \frac{m_{y+n} * g}{R} \right) * U_{y+n} = \mu * m_{y+n} * g - \ddot{U}_g * m_y \quad (4-16)$$

$$m_{y+n} * \ddot{U}_{y+n} + \left(k_{y+n} + \frac{m_{y+n} * g}{R} \right) * U_{y+n} - \left(k_{y+n} + \frac{m_{y+n} * g}{R} \right) * U_y = -\mu * m_{y+n} * g - \ddot{U}_g * m_{y+n} \quad (4-17)$$

To generalize the response equations for the MDOF system, the response is first derived for a four story structure. Using a matrix form, the dynamics of the system is represented by Equation 4-18. All motion terms with subscripts 1-4 represent the motion of the frame at a given story level for a 4 story structure. All motion terms with subscripts 5-8 represent the motion of the floor slabs.

As the case for the single floor system, the response of the MDOF system is represented using the Newmark-Beta numerical integration method. For the single story structure, direct substitution is used to solve the equations. However, for the MDOF system, the equations are coupled. Therefore, modal coordinates are used to decouple the DOFs. The decoupled equations are then used with modal summation to determine the system response (Chopra, 1995; Elgamal, n.d.; Feng & Mita, 1995). The motion variables are converted into modal coordinates using Equation 4-19. Equation 4-19 is substituted into the system of equations in Equation 4-16 for all the motion variables and the result is Equation 4-20, which is shown in a simplified format. The q terms represent the modal coordinates. The ϕ vectors are the modal shapes of the structure.

$$\begin{bmatrix} m_1 & 0 & 0 & 0 & 0 & 0 & 0 & 0 \\ 0 & m_2 & 0 & 0 & 0 & 0 & 0 & 0 \\ 0 & 0 & m_3 & 0 & 0 & 0 & 0 & 0 \\ 0 & 0 & 0 & m_4 & 0 & 0 & 0 & 0 \\ 0 & 0 & 0 & 0 & m_5 & 0 & 0 & 0 \\ 0 & 0 & 0 & 0 & 0 & m_6 & 0 & 0 \\ 0 & 0 & 0 & 0 & 0 & 0 & m_7 & 0 \\ 0 & 0 & 0 & 0 & 0 & 0 & 0 & m_8 \end{bmatrix} * \begin{pmatrix} \ddot{U}_{1k+1} \\ \ddot{U}_{2k+1} \\ \ddot{U}_{3k+1} \\ \ddot{U}_{4k+1} \\ \ddot{U}_{5k+1} \\ \ddot{U}_{6k+1} \\ \ddot{U}_{7k+1} \\ \ddot{U}_{8k+1} \end{pmatrix} + \begin{bmatrix} c_1 + c_2 & -c_2 & 0 & 0 & 0 & 0 & 0 & 0 \\ -c_2 & c_2 + c_3 & -c_3 & 0 & 0 & 0 & 0 & 0 \\ 0 & -c_3 & c_3 + c_4 & -c_4 & 0 & 0 & 0 & 0 \\ 0 & 0 & -c_4 & c_4 & 0 & 0 & 0 & 0 \\ 0 & 0 & 0 & 0 & 0 & 0 & 0 & 0 \\ 0 & 0 & 0 & 0 & 0 & 0 & 0 & 0 \\ 0 & 0 & 0 & 0 & 0 & 0 & 0 & 0 \\ 0 & 0 & 0 & 0 & 0 & 0 & 0 & 0 \end{bmatrix} * \begin{pmatrix} \dot{U}_{1k+1} \\ \dot{U}_{2k+1} \\ \dot{U}_{3k+1} \\ \dot{U}_{4k+1} \\ \dot{U}_{5k+1} \\ \dot{U}_{6k+1} \\ \dot{U}_{7k+1} \\ \dot{U}_{8k+1} \end{pmatrix} + \begin{bmatrix} k_1 + k_2 + (k_5 + \frac{m_5 g}{R}) & -k_2 & 0 & 0 & -(k_5 + \frac{m_5 g}{R}) & 0 & 0 & 0 \\ -k_2 & k_2 + k_3 + (k_6 + \frac{m_6 g}{R}) & -k_3 & 0 & 0 & -(k_6 + \frac{m_6 g}{R}) & 0 & 0 \\ 0 & -k_3 & k_3 + k_4 + (k_7 + \frac{m_7 g}{R}) & -k_4 & 0 & 0 & -(k_7 + \frac{m_7 g}{R}) & 0 \\ 0 & 0 & -k_4 & k_4 + (k_8 + \frac{m_8 g}{R}) & 0 & 0 & 0 & -(k_8 + \frac{m_8 g}{R}) \\ -(k_5 + \frac{m_5 g}{R}) & 0 & 0 & 0 & (k_5 + \frac{m_5 g}{R}) & 0 & 0 & 0 \\ 0 & -(k_6 + \frac{m_6 g}{R}) & 0 & 0 & 0 & (k_6 + \frac{m_6 g}{R}) & 0 & 0 \\ 0 & 0 & -(k_7 + \frac{m_7 g}{R}) & 0 & 0 & 0 & (k_7 + \frac{m_7 g}{R}) & 0 \\ 0 & 0 & 0 & -(k_8 + \frac{m_8 g}{R}) & 0 & 0 & 0 & (k_8 + \frac{m_8 g}{R}) \end{bmatrix} * \begin{pmatrix} U_{1k+1} \\ U_{2k+1} \\ U_{3k+1} \\ U_{4k+1} \\ U_{5k+1} \\ U_{6k+1} \\ U_{7k+1} \\ U_{8k+1} \end{pmatrix} = \begin{pmatrix} -m_1 * \ddot{U}_g + \mu * m_5 * g \\ -m_2 * \ddot{U}_g + \mu * m_6 * g \\ -m_3 * \ddot{U}_g + \mu * m_7 * g \\ -m_4 * \ddot{U}_g + \mu * m_8 * g \\ -m_5 * \ddot{U}_g - \mu * m_5 * g \\ -m_6 * \ddot{U}_g - \mu * m_6 * g \\ -m_7 * \ddot{U}_g - \mu * m_7 * g \\ -m_8 * \ddot{U}_g - \mu * m_8 * g \end{pmatrix} \quad (4-18)$$

$$U_{1k+1} = \phi_{11} * q_{1k+1} + \phi_{12} * q_{2k+1} + \phi_{13} * q_{3k+1} + \phi_{14} * q_{4k+1} + \phi_{15} * q_{5k+1} + \phi_{16} * q_{6k+1} + \phi_{17} * q_{7k+1} + \phi_{18} * q_{8k+1} \quad (4-19)$$

$$[M] * [\phi] * \{\ddot{q}\} + [C] * [\phi] * \{\dot{q}\} + [K] * [\phi] * \{q\} = \{F\} \quad (4-20)$$

Both sides of Equation 4-20 are pre-multiplied by the transpose of the φ matrix as shown in Equation 4-21 for the evaluation of the effective mass (M_e), damping (C_e), and stiffness (K_e) matrix as well as the forcing vector (F_e), where M_e , C_e , K_e , and F_e are shown in Equations 4-22 through 4-25. The resulting equation of motion is shown in Equation 4-26 and is further described in Equation 4-27.

$$[\varphi]^T * [M] * [\varphi] * \{\ddot{q}\} + [\varphi]^T * [C] * [\varphi] * \{\dot{q}\} + [\varphi]^T * [K] * [\varphi] * \{q\} = [\varphi]^T * \{F\} \quad (4-21)$$

$$[\varphi]^T * [M] * [\varphi] = [M_e] \quad (4-22)$$

$$[\varphi]^T * [C] * [\varphi] = [C_e] \quad (4-23)$$

$$[\varphi]^T * [K] * [\varphi] = [K_e] \quad (4-24)$$

$$[\varphi]^T * \{F\} = \{F_e\} \quad (4-25)$$

$$[M_e] * \{\ddot{q}\} + [C_e] * \{\dot{q}\} + [K_e] * \{q\} = \{F_e\} \quad (4-26)$$

$$\begin{bmatrix} m_{e1} & 0 & 0 & 0 & 0 & 0 & 0 & 0 \\ 0 & m_{e2} & 0 & 0 & 0 & 0 & 0 & 0 \\ 0 & 0 & m_{e3} & 0 & 0 & 0 & 0 & 0 \\ 0 & 0 & 0 & m_{e4} & 0 & 0 & 0 & 0 \\ 0 & 0 & 0 & 0 & m_{e5} & 0 & 0 & 0 \\ 0 & 0 & 0 & 0 & 0 & m_{e6} & 0 & 0 \\ 0 & 0 & 0 & 0 & 0 & 0 & m_{e7} & 0 \\ 0 & 0 & 0 & 0 & 0 & 0 & 0 & m_{e8} \end{bmatrix} * \begin{pmatrix} \ddot{q}_{1k+1} \\ \ddot{q}_{2k+1} \\ \ddot{q}_{3k+1} \\ \ddot{q}_{4k+1} \\ \ddot{q}_{5k+1} \\ \ddot{q}_{6k+1} \\ \ddot{q}_{7k+1} \\ \ddot{q}_{8k+1} \end{pmatrix} + \begin{bmatrix} c_{e1} & 0 & 0 & 0 & 0 & 0 & 0 & 0 \\ 0 & c_{e2} & 0 & 0 & 0 & 0 & 0 & 0 \\ 0 & 0 & c_{e3} & 0 & 0 & 0 & 0 & 0 \\ 0 & 0 & 0 & c_{e4} & 0 & 0 & 0 & 0 \\ 0 & 0 & 0 & 0 & c_{e5} & 0 & 0 & 0 \\ 0 & 0 & 0 & 0 & 0 & c_{e6} & 0 & 0 \\ 0 & 0 & 0 & 0 & 0 & 0 & c_{e7} & 0 \\ 0 & 0 & 0 & 0 & 0 & 0 & 0 & c_{e8} \end{bmatrix} * \begin{pmatrix} \dot{q}_{1k+1} \\ \dot{q}_{2k+1} \\ \dot{q}_{3k+1} \\ \dot{q}_{4k+1} \\ \dot{q}_{5k+1} \\ \dot{q}_{6k+1} \\ \dot{q}_{7k+1} \\ \dot{q}_{8k+1} \end{pmatrix} + \begin{bmatrix} k_{e1} & 0 & 0 & 0 & 0 & 0 & 0 & 0 \\ 0 & k_{e2} & 0 & 0 & 0 & 0 & 0 & 0 \\ 0 & 0 & k_{e3} & 0 & 0 & 0 & 0 & 0 \\ 0 & 0 & 0 & k_{e4} & 0 & 0 & 0 & 0 \\ 0 & 0 & 0 & 0 & k_{e5} & 0 & 0 & 0 \\ 0 & 0 & 0 & 0 & 0 & k_{e6} & 0 & 0 \\ 0 & 0 & 0 & 0 & 0 & 0 & k_{e7} & 0 \\ 0 & 0 & 0 & 0 & 0 & 0 & 0 & k_{e8} \end{bmatrix} * \begin{pmatrix} q_{1k+1} \\ q_{2k+1} \\ q_{3k+1} \\ q_{4k+1} \\ q_{5k+1} \\ q_{6k+1} \\ q_{7k+1} \\ q_{8k+1} \end{pmatrix} = \begin{pmatrix} F_{e1} \\ F_{e2} \\ F_{e3} \\ F_{e4} \\ F_{e5} \\ F_{e6} \\ F_{e7} \\ F_{e8} \end{pmatrix} \quad (4-27)$$

The ϕ matrix is found using an Eigen analysis on the mass and stiffness matrices. The Eigen values represent the square of the natural frequency of the system and the Eigen vectors represent the ϕ vectors for each degree of freedom.

4.4.3 Response Equation

Once the decoupled modal systems of equations are formulated, the Newmark time-stepping algorithm is utilized for the numerical solution. The response equations for the acceleration, velocity, and displacement for the modal coordinates are listed in Equations 4-28, 4-29 and 4-30, respectively, in a generalized form for both the frame and the slab with y representing the degree of freedom.

$$\ddot{q}_{y_{k+1}} = \frac{-\dot{q}_{y_k} * [c_{ey} * (1 - \delta) * \Delta t + k_{ey} * (0.5 - \beta) * \Delta t^2] - \dot{q}_{y_k} * [c_{ey} + k_{ey} * \Delta t] - q_{y_{k+1}} * k_{ey} + F_{ey}}{[m_{ey} + c_{ey} * \delta * \Delta t + k_{ey} * \beta * \Delta t^2]} \quad (4-28)$$

$$\dot{q}_{y_{k+1}} = \dot{q}_{y_k} + \ddot{q}_{y_k} * (1 - \delta) * \Delta t + \ddot{q}_{y_{k+1}} * \delta * \Delta t \quad (4-29)$$

$$q_{y_{k+1}} = q_{y_k} + \dot{q}_{y_k} * \Delta t + \ddot{q}_{y_k} * (0.5 - \beta) * \Delta t^2 + \ddot{q}_{y_{k+1}} * \beta * \Delta t^2 \quad (4-30)$$

The equations of motion can be easily written for any floor slab or structural story using these generalized equations. At the conclusion of each time step, once each unknown modal motion term is determined, the desired global motion terms are calculated using modal summation and equation 4-17. Once the response at a given time step is determined, the equations in the next time step are solved while adjusting the equations to account for the sign of the friction term for each slab on each particular story. The results of this method and the direct substitution method are identical what has been presented for a single story system.

4.4.4 Verification

In order to verify the response formulation of the hybrid system the parameters governing the response (i.e., the mass, damping, and stiffness) of the structure are adjusted to match that of a reference structure in Chopra's Dynamics of Structures (Chopra, 1995; Tazarv, 2011). The stiffness between the slab and frame is increased exponentially to render the system as a standard composite structure. The reference structure is then considered for comparison. The reference structure is a five-story structure with story masses of 45.34×10^3 kg, damping ratios of 5%, and frame stiffnesses of 5.52×10^3 kN/m. As Figure 4-7 shows, the results are practically identical, verifying the accuracy of modal summation and Newmark calculations for the hybrid system.

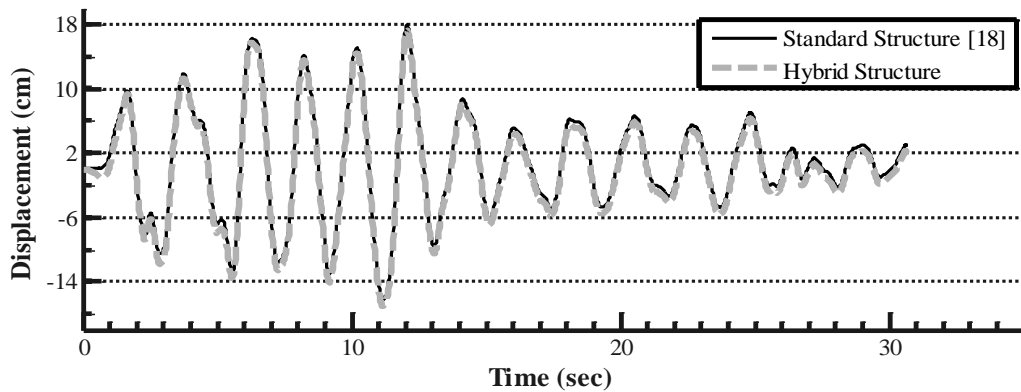


Figure 4-7. Response comparison for validation of calculations

To verify other aspects of the design, the bumper stiffness between the frame and slab is also increased by many orders of magnitude to imitate a composite structure. The comparison response to that of an identically designed composite structure is shown in Figure 4-8 a. The system is also tested with a radius of curvature of the supports that are orders of magnitude higher and its response is compared to that of a composite system as shown in Figure 4-8 b. This is done to imitate the condition where the slabs are resting on a flat surface. This response is different from Figure 4-8 a. because Figure 4-8 b. represents the hybrid system with slabs in

motion while Figure 4-8 a. represents the composite system with rigid slabs. But, as seen below in Figure 4-8 b, the responses are exactly the same between the flat system and the hybrid system with a large radius of curvature. This confirms the physical behavior of the derivation of the equations.

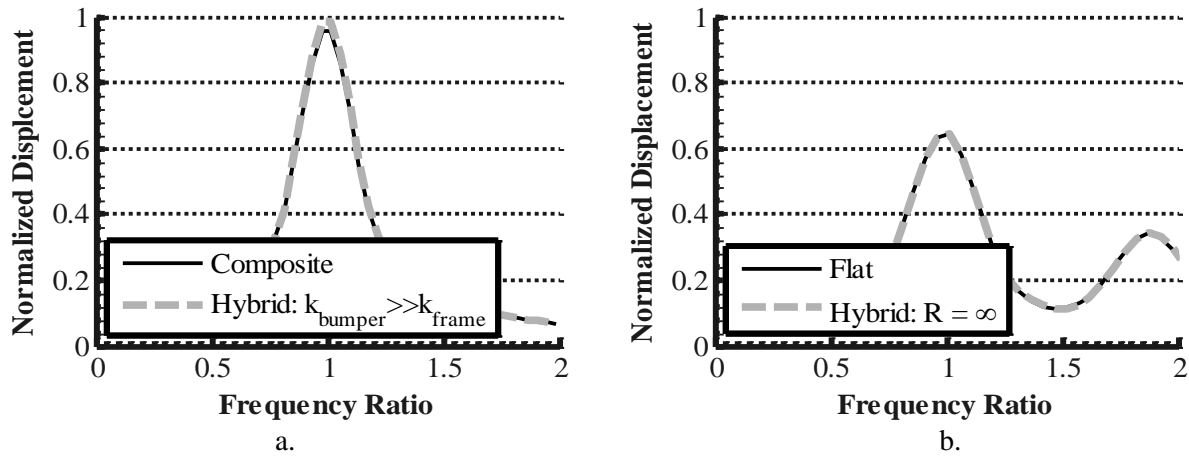


Figure 4-8. Verification of (a) composite structure to isolated structure with high bumper stiffness, (b) flat support versus curved support with high radius of curvature

4.5 Optimization

4.5.1 Parameters

Many of the parameters such as the size of beams and columns are dictated by design codes and cannot be optimized. However other parameters that are unique to the proposed hybrid system need to be optimized to minimize the response of the structure. The parameters of the system include – the stories at which the hybrid slabs are activated, represented by a binary vector (S), the radius of curvature (R), the stiffness between the slab and the frame (k_{y+n}) and the coefficient of friction (μ). The representation of parameter S in a matrix and then to a vector form is shown in Figure 4-9. All slabs on each individual story behave the same (active or not)

so a single value can describe each story. An activated story is represented by the numeric 1 and a story where the slab is composite is represented by 0. As the size of the structure increases, possible S combinations increase exponentially. These possibilities require robust optimization procedures to ensure an efficient method of finding the best configuration of the system. The conditional function in equation 4-31 indicates how the S term affects the response equations of the structure. The bumper stiffness is increased to form a rigid connection between the frame and slab. The radius of curvature is increased so the stiffness created by its term is reduced to zero. The coefficient of friction is reduced to zero so the friction term does not affect the behavior since friction affects a slab by not allowing it to move (Hoshimura, 2005). Every combination has at least one story activated. The other optimized variables' physical limits and design considerations dictated their values.

$$\begin{aligned}
 \text{if } S = 1 \rightarrow & \begin{aligned} & k_{y+n} = k_{y+n} \\ & R = R \\ & \mu = \mu \end{aligned} & \text{if } S = 0 \rightarrow & \begin{aligned} & k_{y+n} = \infty \\ & R = \infty \\ & \mu = 0 \end{aligned}
 \end{aligned}
 \tag{4-31}$$

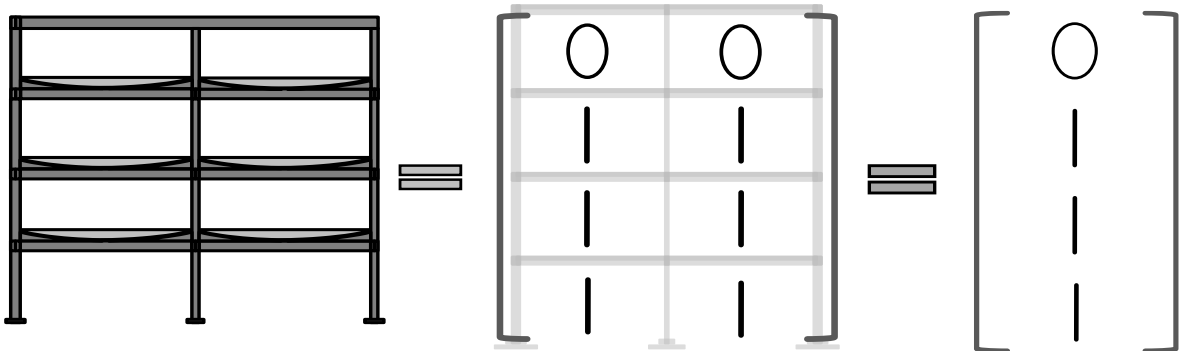


Figure 4-9. Binary representation of activated stories of structure in vector form

4.5.2 Covariance Matrix Adaptation (CMA)

The Covariance Matrix Adaptation (CMA) is a nonlinear optimization procedure (Hansen, 2011). A CMA optimization code is built in 2 layers. The 1st finds the optimal positions for activated slabs (S) and the 2nd finds the optimal radius (R), stiffness of bumper (k_{y+n}), and coefficient of friction (μ). Figure 4-10 demonstrates how the CMA code functions. A Gaussian distribution is used to randomly generate vectors for S , creating an S matrix. The number of vectors generated depends on the size of the structure. Weight factors are generated based on the number of combinations. These weights are applied to the results after the fitnesses of each generation of combinations are found. The combinations are then randomly created. They are filtered to match the limits of the parameter and then sent to the second layer of the optimization. This layer does the same for the frame parameters and puts all of these variables into the system response code to retrieve the response of the structure. The normalized response value of these structures is a summation of the squares of these normalized dependent variables: acceleration of the structure and slab, the global drift of the structure, relative drift of the slab and the ISD between stories. These values are normalized against the response of a composite structure under loading at resonance frequency. Thus each is a dimensionless ratio to a standard response. This forces the optimization code to reduce all of the dependent variables. All of those variables are maxima for any story over the entire response of the structure for each and every frequency tested. Equation 4-32 is used to calculate the response evaluation of the system performance against a conventional composite system. The response of a composite structure at resonant frequency would be 1. All responses below that value show an improvement in the design of the structure.

$$\begin{aligned}
 Resp = & \left(\left(\frac{Max\ Acc.\ Slab_i}{Resonant\ Acc.\ Slab_c} \right)^2 + \left(\frac{Max\ Acc.\ Frame_i}{Resonant\ Acc.\ Frame_c} \right)^2 + \left(\frac{Max\ Global\ Drift_i}{Resonant\ Global\ Drift_c} \right)^2 \right. \\
 & \left. + \left(\frac{Max\ Rel.\ Slab\ Drift_i}{Resonant\ Slab\ Drift_c} \right)^2 + \left(\frac{Max\ ISD_i}{Resonant\ ISD_c} \right)^2 \right)^{1/2}
 \end{aligned}
 \tag{4-32}$$

The optimum frame parameters and responses are found by the second layer of the optimization code and sent back to the first layer. This optimum response is the “fitness” for that combination. Once the fitnesses are found for the generated combinations, they are sorted based on fitness and then the weight factors are applied to the superior fitnesses and a new mean and a new standard deviation are created for each. With the new mean and new standard deviation a new group of possible combinations are generated using a new normal distribution. After a particular combination is optimized, its results are stored in a separate matrix. If a duplicate combination is generated then those previous results are called upon instead of optimizing again. This is done in order to streamline the calculations. This process is repeated for many new generations until a consistent mean is found which represented the best combination of hybrid slab system (Hansen, 2011).

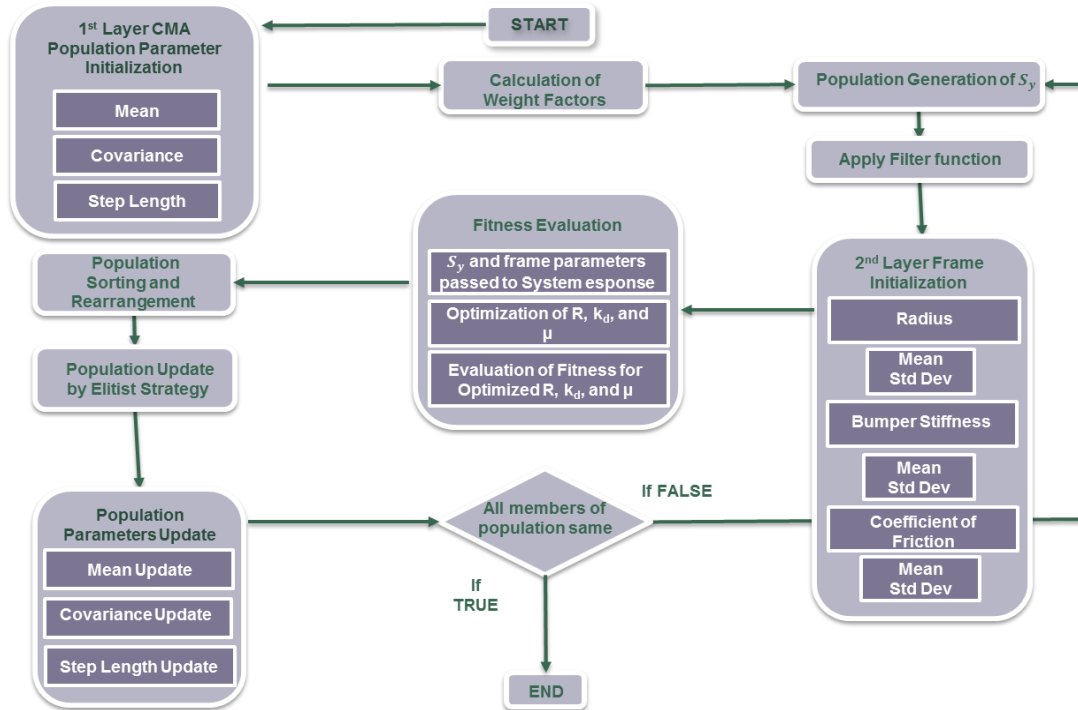


Figure 4-10. Flowchart of CMA optimization process [25]

4.6 Performance Evaluation

To evaluate the effectiveness of the system three multistory structures are designed and optimized using the CMA procedure. The responses of these structures are then compared to a traditionally composite slab system. The three structures that are considered are a four-story two-bay structure, a seven-story three-bay structure, and a ten-story five-bay structure. For all structures the floor slabs are designated to have a mass of 42.9×10^3 kg. The internal damping ratio of the frame of the structure is 5%. The width of the floor bays is 4.57 m. These structures are optimized over a range of sinusoidal excitations with frequencies ranging from 4 rad/sec to 20 rad/sec. For the four-story structure the height of each story is 3.96 m. For the other two the height of each story is 4.57 m. The frame values for each structure are shown in the Table 4-2 below. The limits of the input design variables, including the curvature of the slab, the bumper

stiffness, and the coefficient of friction are listed in Table 4-3. These values are dictated by and described in the design considerations. In this study, relatively large radii of curvature are used to demonstrate the extreme case where a flat surface may be used. The minimum is based on the size of the structure. The maximum bumper stiffness is an arbitrary value that is determined by the stiffness of the frame while keeping the bumper stiffness less than that of the frame. The minimum is an arbitrary value set very close to zero. The friction limits are set based on reasonable materials to be used for the contact surface. Table 4-4 displays the results of the optimization process. As shown in Table 4, the optimization process resulted in the hybrid slab system being installed on all stories for the best performance in the 4 and 7 story structures. The 10 story optimization called for the 4th and 5th stories to be rigid.

Table 4-2 Structural properties of the frames

Floor Number	Mass (kg)	Stiffness (kN/m)
Structural Properties of 4-Story 2-Bay Structure		
Floor 1	108.2*10 ³	13.2*10 ³
Floor 2 and 3	106.5*10 ³	13.2*10 ³
Floor 4	95.8*10 ³	13.2*10 ³
Structural Properties of 7-Story 3-Bay Structure		
Floor 1	157.2*10 ³	19.7*10 ³
Floor 2 to 6	156.3*10 ³	19.7*10 ³
Floor 7	138.8*10 ³	19.7*10 ³
Structural Properties of 10-Story 5-Bay Frame		
Floor 1	256.4*10 ³	33.0*10 ³
Floor 2 to 9	252.9*10 ³	33.0*10 ³
Floor 10	227.7*10 ³	33.0*10 ³

Table 4-3 Optimization Limits

	Radius (m)	Bumper Stiffness (kN/m)	Coefficient of Friction
Max	3000*	35*10 ³ **	0.3
Min	7.6	0.001*10 ³	0.05

* An arbitrarily large value to imitate a flat surface

** An arbitrary value that can be adjusted as needed

Table 4-4 Optimized parameters and peak response

Structure	Isolation Combination	Radius (m)	Bumper Stiffness (kN/m)	Coefficient of Friction	Normalized Peak Response
4 Story	1 1 1 1	7.60	437	0.30	0.66
7 Story	1 1 1 1 1 1 1	7.60	245	0.30	0.70
10 Story	1 1 1 0 0 1 1 1 1 1	7.60	87.4	0.30	0.69

Figure 4-11 a. shows the peak global drift of the proposed hybrid system for a 4-story structure, with structural properties based on the optimization of the 4-story system, compared to that of an identically designed composite structure. Figure 4-11 b. shows the interstory drift (ISD) of the composite structure. The responses are normalized to the peak response of the composite structure. The figure shows that the hybrid slab system causes the maximum global drift of all stories (Figure 4-11 a.) and maximum ISD of all stories (Figure 4-11 b.) of the frame to be reduced by approximately 45%. Since there is minor energy dissipation, much like a base isolation system, the motion is transferred to the isolated slabs. Figure 4-12 b shows approximately a 60% reduction in the maximum frame acceleration of all stories. The maximum acceleration of all slabs is reduced by only 10%. The maximum displacement of all slabs relative to the displacement of the frame is equal to the maximum displacement of all slabs of a composite structure, shown below in Figure 4-12 a. This system has no form of damping or energy dissipation other than friction. These responses, theoretically, could be even further reduced by the addition of a damping device between the frame and slab used with the bumpers. A demonstration of this possibility can be seen below in Figure 4-13 b. Figure 4-13 a. shows a comparison of the relative slab drift vs frequency of the 4 story hybrid structure versus composite system while Figure 4-13 b. shows the effect of damping on response of the hybrid system.

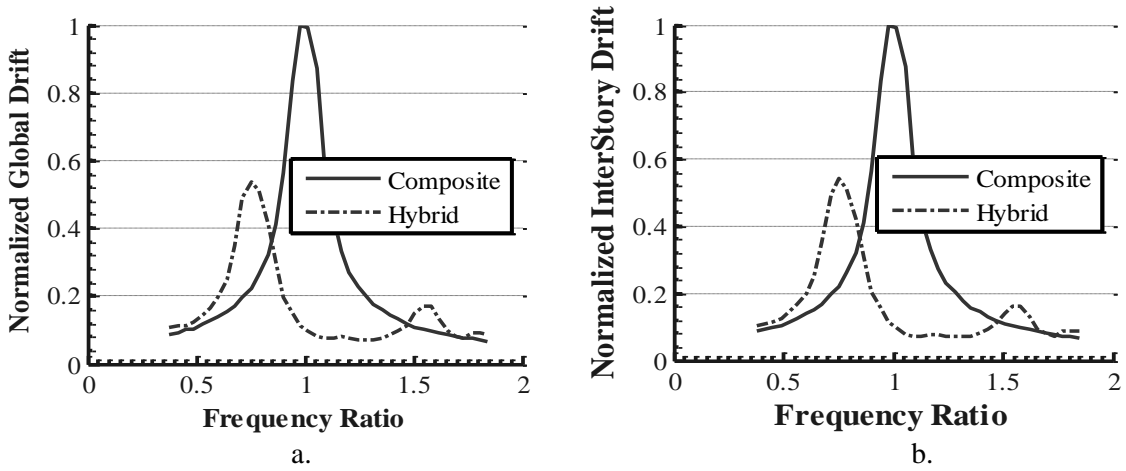


Figure 4-11. (a) Global drift and (b) ISD of top story vs frequency ratio of rigid and isolated 4 story structure

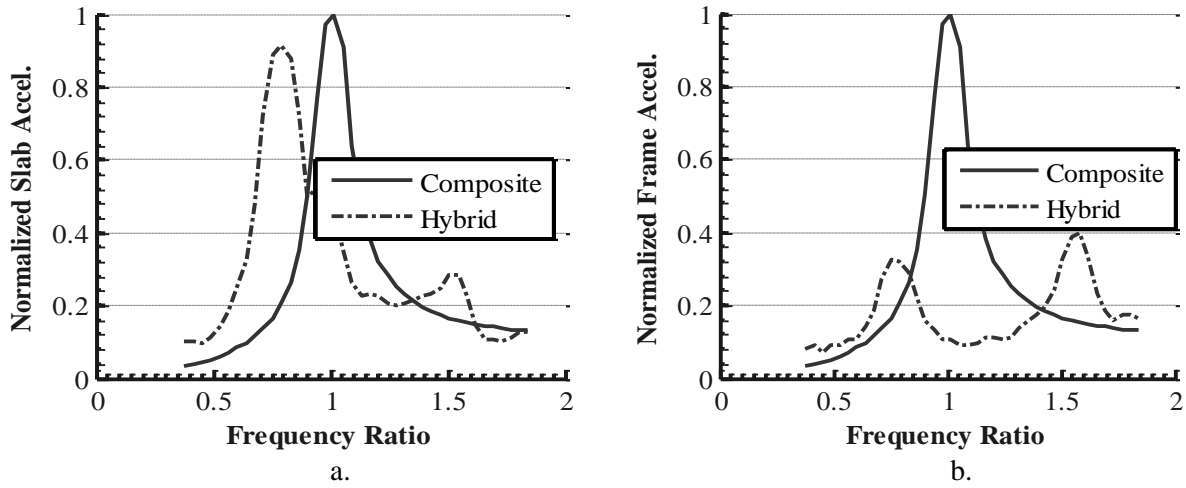


Figure 4-12. Comparison of acceleration of (a) floor slab and (b) frame vs frequency of composite and isolated 4-story structure

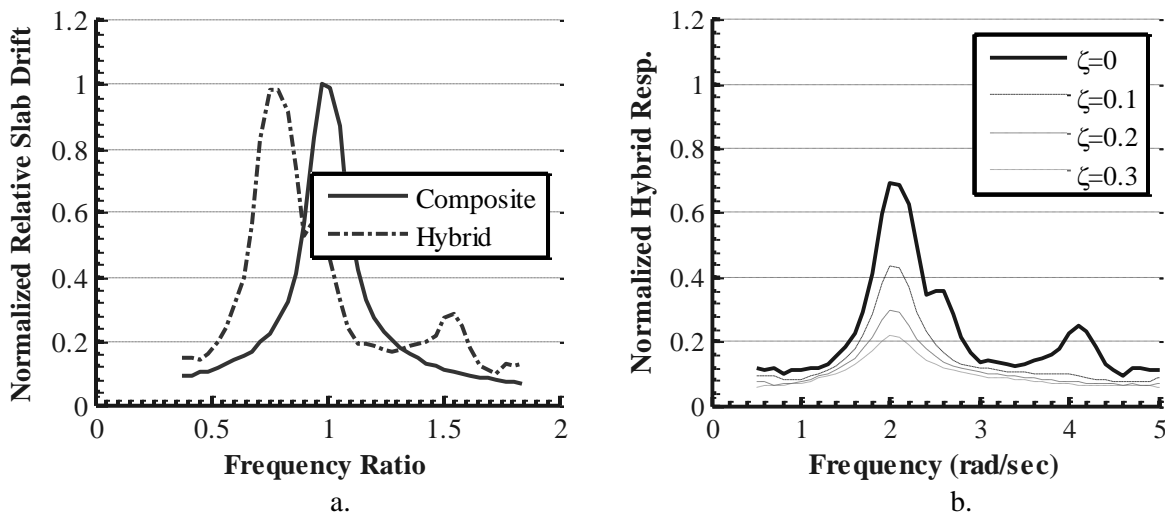


Figure 4-13. (a) Comparison of the relative slab drift vs frequency of the 4 story hybrid structure versus composite system (b) Effect of damping on response of the hybrid system

An assessment of the extent of improvement in response per story can be seen below in Figures 4-14, 4-15, and 4-16 for the 4-story 2-bay, 7-story 3-bay, and 10-story 5 bay structures, respectively. These values are measured at a composite structure's resonant frequency versus the isolated structure's resonant frequency in order to obtain a true assessment of the improvement. The percent improvement is calculated using Equation 4-33. Because the uppermost stories experience the most motion, their improvement is most crucial. The figures show that the story drift and interstory drift of the proposed hybrid system are always better than that of the composite system while the slab acceleration of the lower stories is in some cases much worse than that of the composite structure.

$$\% \text{ Improvement} = \left(1 - \frac{\text{Hybrid System Response}}{\text{Composite Frame Response}} \right) * 100 \quad (4-33)$$

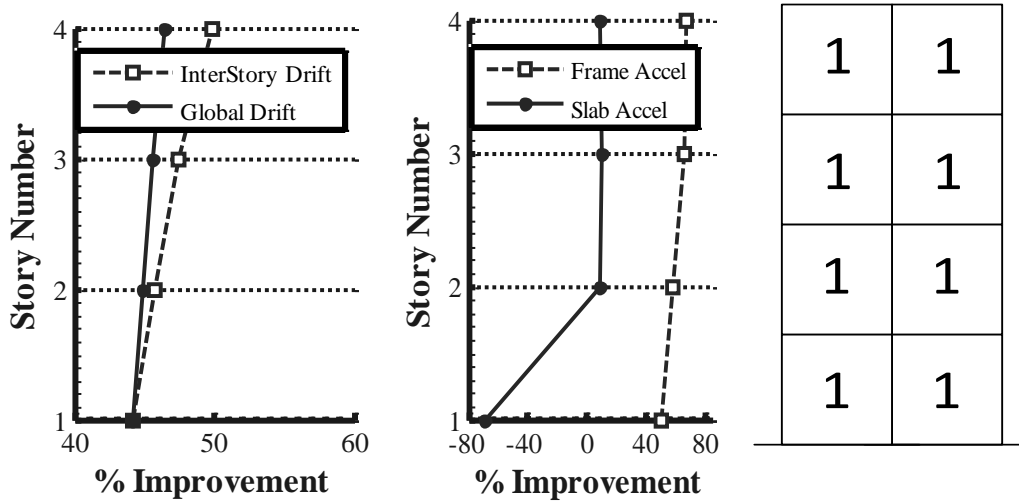


Figure 4-14. Improvement per story for 4 story structure

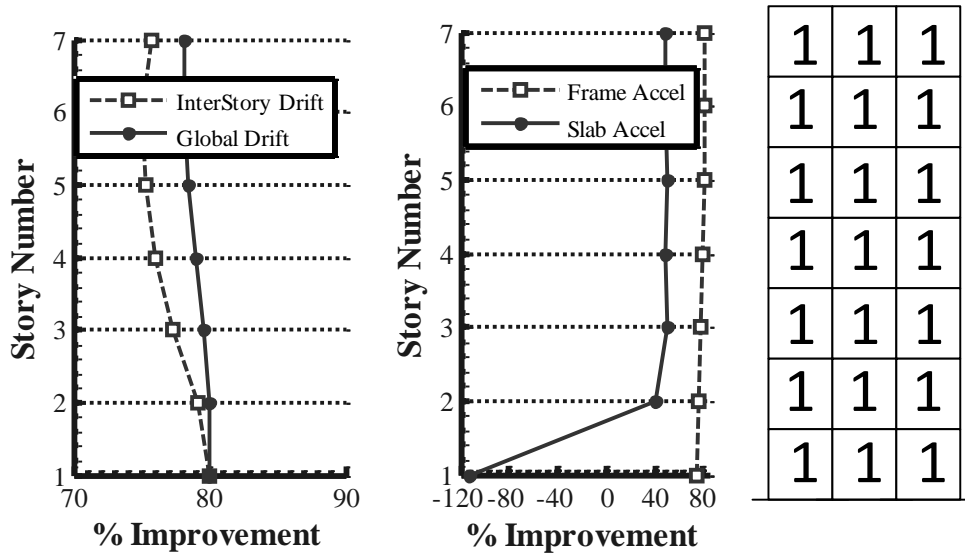


Figure 4-15. Improvement per story for 7 story structure

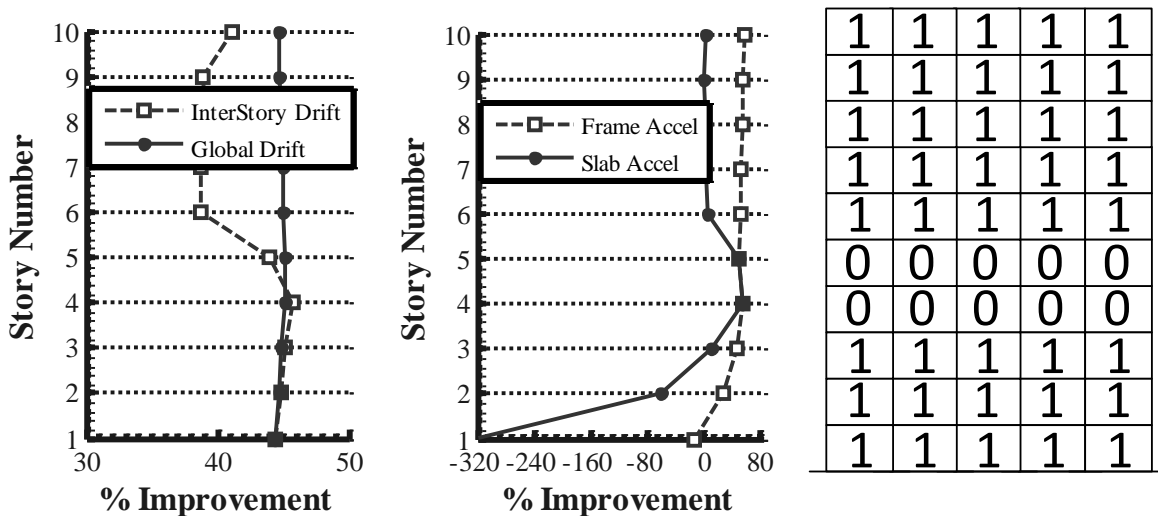


Figure 4-16 Improvement per story for 10 story structure

The responses shown in Figure 4-14, 4-15, and 4-16 represent the effect of a greatly increased mass ratio. Most tuned mass damping systems have mass ratios between 1% and 10%. The mass ratios for this system are as high as 80%. This is one of the main reasons for such improvement in performance without any significant energy dissipation. Increased mass ratios reduce the response of the structure and the response of the slabs.

Since Table 4-4 indicates that with the exception of the 10-story structure, implementing the slab system on almost all floors is the most optimum solution, the next natural step in the

investigation is to evaluate the response of the structure when the implementation is applied to specific floors. Figure 4-17 shows how isolating different stories affects the response. The figure shows that applying the system to most of the floor slabs offers the optimum response, which is in agreement with the optimization results. In addition, when implemented on the upper stories, the maximum response reduces at the resonant frequency and increases the response at other excitation frequencies away from the resonant frequency. The application of the proposed hybrid system on the lower stories is not as effective at resonant frequency but results in reduction in the response more effectively at other frequencies. By utilizing both upper and lower stories for the system, much of the benefits from both are seen.

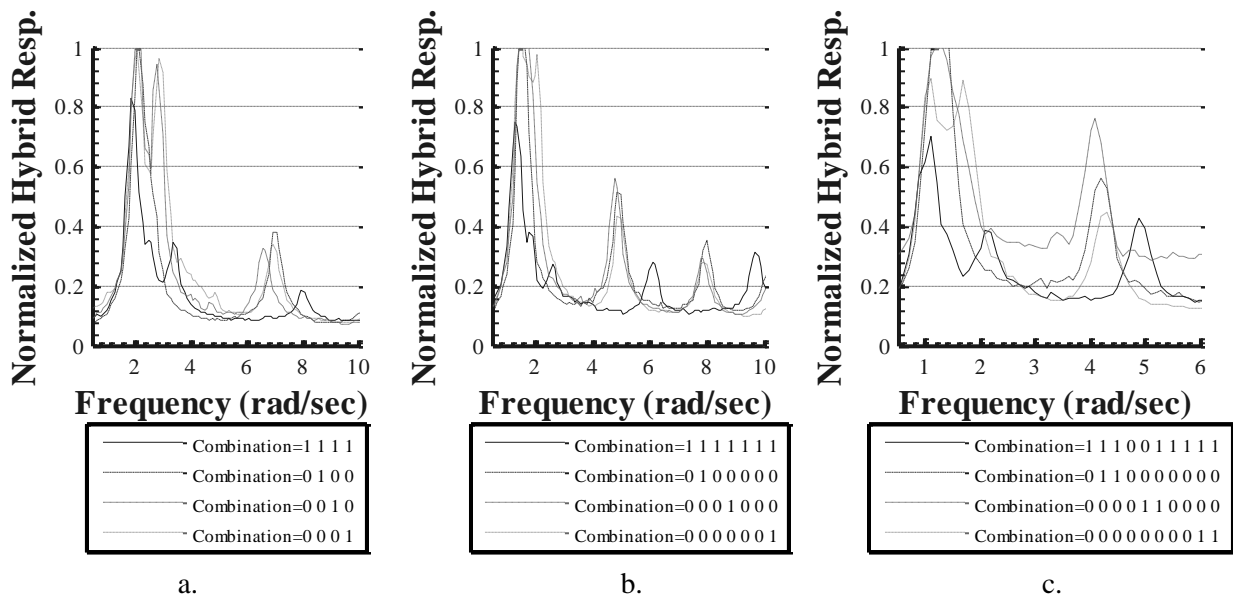


Figure 4-17. Effects of isolating different stories for (a) 4 story (b) 7 story and (c) 10 story structures

4.7 Design Considerations

This system is developed to prevent damage and excitation in the system. However, if the proposed system cannot be constructed then it is not worth anything. Feasibility and design considerations are important to the effectiveness of the proposed hybrid system. An advantage of

the slab isolation concept is that if damage is experienced it would likely be because of large displacements in the slab. This response would likely cause damage to the bumpers and possibly the support surface. When these relatively manageable and isolated slabs are damaged they could be easily replaced and the structure repaired. Repair cost would be greatly reduced even if damage was experienced.

4.7.1 Friction Surface

The friction surface could be made of a variety of materials and even a combination of many materials. The possibilities offer a range of feasible values that can be used for the surface. The optimization indicates that lower friction values are desired. Teflon materials used with chrome plates or other Teflon surfaces are being tested for base isolation applications. In the same way it may be possible for them to be utilized in this system. Teflon surfaces have very low friction values and under the right circumstances could be ideal for application in the proposed hybrid system(M. Constantinou, Mokha, & Reinhorn, 1990; Mokha, Constantinou, & Reinhorn, 1990).

4.7.2 Slab Support

The curvature of the slab is one of the more challenging design aspects of the proposed hybrid system. The curvature shown in the derivation of the system spans the length of the floor bay. The application of this consideration incorporates a curved support along each of the four edges of the bay. The slab rests in these supports with its own curvature matching that of the supports. The materials used are any building materials that can be formed. This may require pre-made pieces to be taken to the construction site.

The limitations of this design have a minimum radius of curvature. If the radius is too small, the supports either won't span the entire bay or create too steep of edges on the sides and too much vertical motion. During the optimization process, a minimum radius value is set to twice the width of the floor bay to avoid those situations.

An advantage of the proposed hybrid system is that if the curvature needs to be adjusted for design purposes, it can while still achieving optimum results. This is possible because two of the adjustable parameters affect the stiffness between the slab and the frame. One parameter is the curvature and the other being the bumpers. This redundancy allows either parameter to be adjusted by making up the difference with the other.

The final design consideration for the radius of curvature is to utilize bearing plates, much like some base isolation systems, along a flat support surface or diaphragm, instead. The bearing plates are smaller, curved, and placed at multiple locations to support the slab. This allows any radius to be used and keeps the slab level throughout its motion. The bearing plates are assumed to be easier to construct, as well.

4.7.3 Stiffness Devices

The bumper between the slab and the frame is considered to be a rubber pad. Rubber has been used as a construction material with relatively low stiffness to allow for motion in other structural designs as well (Kelly & Beucke, 1983; Kelly, 1986, 1998). The proposed system assumes that a bumper is in contact with the slab and frame and resists motion at all times. This may mean only one side of the slab is in contact. The limitations for design of this parameter are the material property possibilities of the material used as the bumper. Since contact is assumed at all times, these bumpers would also provide some self-centering capabilities to the slab.

The second design possibility of this parameter is to have actual spring devices in place of bumpers. This increases the range of possible stiffness values of the bumpers and ensures constant engagement of the bumper device. As explained before, this parameter is a redundant feature in terms of the dynamics of the system and can be adjusted for design accordingly while achieving optimum results.

4.7.4 Damping Devices

The derivation of this system includes no damping devices. Energy dissipation and damping is only found in the internal damping of the structure and the friction between the slab and the support. The proposed hybrid system is evaluated on its capabilities to mitigate vibration as primarily an isolation system.

The addition of damping devices between the slab and the frame for the proposed hybrid system has been developed. Preliminary results of a system that utilizes damping devices show that, in addition to the gains seen by the proposed hybrid system, damping devices increase the ability of the system to mitigate excitations in structures for both wind and seismic loads. The range of possible damping values is dependent on the capabilities of the devices and is not explored in the scope of this document. The large mass of the floor slabs may limit the possible damping ratios. However, any damping has the possibility to improve the performance of the proposed hybrid system.

4.8 Conclusions

In this study, a hybrid system is proposed and comprises of a slab resting on a curved support. The curvature creates stiffness between the slab and the frame and also utilizes gravity to keep the slab in place. Bumpers between the slab and the frame are applied to protect both components from damage during excitation. The proposed system is unique in that it combines the concept of base isolation with TMDs to achieve the desired performance. This design has shown that by isolating the slab's mass and using it as a translational tuned mass damper, vibrations can be mitigated in structures under seismic loading. It shows the ability to reduce the displacement and inter-story drift by up to 45% in comparison to standard composite slab and frame structures. The acceleration of the slabs in the proposed hybrid system is also improved except for the lowest stories. This improvement is due to the large percentage of mass that acts as a damper. This increased mass ratio offers improvement and flexibility in the design. Without significant energy dissipation the demand on the frame of the structure are still greatly reduced.

The development of this system can easily be adjusted to account for wind loading as well. Multi-hazard design consideration for this system could be a promising prospect as future research. With design considerations in mind, the range of effectiveness should be tested against various earthquake inputs to demonstrate how the system would behave for a given seismic excitation.

5. SEISMIC EVENTS

5.1 Introduction

After confirming the effectiveness of the design through a frequency versus response analysis the next step of demonstrating the applicability of the system is to test its performance using actual earthquake records. This is done by using earthquake acceleration event histories as ground accelerations for the optimized structures. The response of the structure is then calculated. In this section the acceleration and interstory drift of the optimized structure are presented. Complete response histories are given for events in which the structures performed well. A comprehensive compilation of the performance of the structures for all of the selected events is also given. Most show improvement while others do not. This behavior is discussed in this section.

A variety of seismic histories are gathered from the Pacific Earthquake Engineering Research Center (“PEER Ground Motion Database,” 2010). Event histories are chosen from both near and far field earthquakes. This offers a range of earthquakes that should adequately test the structure under a wide range of frequencies. The structure is assumed to be in a certain location and the earthquake data is scaled to match the design code for that location according to ASCE 7 (ASCE, 2005a) and FEMA P-695 (Mahoney & Hanson, 2009). This scaling process is standard to ensure the magnitudes of the accelerations for structures of different fundamental periods are at proper design values to design a structure to withstand a 2500 year earthquake (ASCE, 2005a).

Meeting design codes is not the focus of the assessment, but the proper procedure for design is followed to understand the considerations in seismic design. The optimized responses are

compared to a composite structure of the same structural properties. The design of these composite structures is very basic for the sake of comparison. The focus of this section is on demonstrating that after optimization using sine waves, the proposed hybrid structure would perform better under a variety of seismic loads.

5.2 Ground Motion Characteristics

5.2.1 Selection

In general, ground motions used for assessment of structures are selected based on magnitude, epicenter distance, and site conditions. In this study, the distance is used as a selection parameter such that both near-field and far-field records are used. In doing so, a wide range of earthquake behaviors can be captured.

Five near-field earthquakes are selected to ensure a range of frequencies are represented for events less than 10 km in distance from the structure. Five far-field earthquakes are selected to do the same for earthquakes whose epicenter would be over 10 km in distance. This provides a relatively large population to pull data from and to test the structures over many different loading situations

Other important considerations in selection are the magnitude, the source of the earthquake, and the site conditions. Large magnitudes offer possibility of collapse. Smaller are likely to cause damage but not collapse. Strike-slip versus reverse (thrust) earthquakes cause different types of ground motions. The soil type of the ground being excited also effects the behavior of the ground motion. Many records can be found for a single earthquake. For near and far field designations,

respectively, no more than two records for a single earthquake should be chosen. The earthquakes should have high enough peak ground accelerations and velocities to cause damage (Mahoney & Hanson, 2009). All of these factors are considered when selecting events. Table 5-1 shows the selected ground motion records and properties of each record.

Table 5-1. Characteristics of the ground motion records used in the parametric study

Mw	Year	Earthquake Name	Station ID	Reference Name	Distance (km)	PGA
6.5	1979	Imperial Valley	Bonds Corner (HBCR230)	IV-HBCR	2.7	0.775
6.9	1989	Loma Prieta	Corralitos (CLS000)	LP-CLS	3.9	0.644
6.7	1992	Erzincan	Erzincan (ERZEW)	EZ-ERZ	4.4	0.496
7.5	1999	Kocaeli	Izmit (IZT090)	KC-IZT	7.2	0.22
6.7	1994	Northridge	Arleta (ARL360)	NR-ARL	8.7	0.308
7.1	1999	Duzce	Bolu (BOL000)	DZ-BOL	12	0.728
6.7	1994	Northridge	Canyon County WLC (LOS000)	NR-LOS	12.4	0.41
6.9	1989	Loma Prieta	Capitola (CAP090)	LP-CAP	15.2	0.443
6.9	1995	Kobe	Shin Osaka (SHI090)	KB-SHI	19.2	0.212
6.7	1994	Northridge	Century City CC North (CCN360)	NR-CCN	25.7	0.222

5.2.2 Normalization

After the records are selected and the data is procured from Pacific Earthquake Engineering Research Center (“PEER Ground Motion Database,” 2010) the records must be normalized. They are normalized to the median peak ground velocity. This is done to ensure consistency of influence of each individual event. Some earthquakes may be weaker due to inherent magnitude or distant factors, so these must be scaled up to equalize its influence to other events. This process still maintains the individual variability of each event and its unique collapse risk. The peak ground velocity values are calculated by finding the geometric mean of the peak ground velocities of the two primary horizontal directions according to the PEER database.

5.2.3 Maximum Considered Earthquake

The maximum considered earthquake (MCE) is used as the design spectrum to ensure the structures being tested are being loaded by earthquakes with 2% probability of exceedance in 50 years (ASCE, 2005a). The MCE represents the spectral acceleration versus the fundamental period of a structure. It is found using the seismic design criteria found in Chapter 11 of the ASCE 7 code. The factors found are based on the assumed location of the structure and the site conditions (soil type). For this experiment the location is assumed to be a seismically active location with a standard soil type. Los Angeles, California is chosen and the site is assumed to have Soil Type D. Using ASCE 7 chapter 11 these assumptions provide the points to develop the design spectrum for the location. This spectrum is then scaled up by a factor of 1.5 to find the MCE.

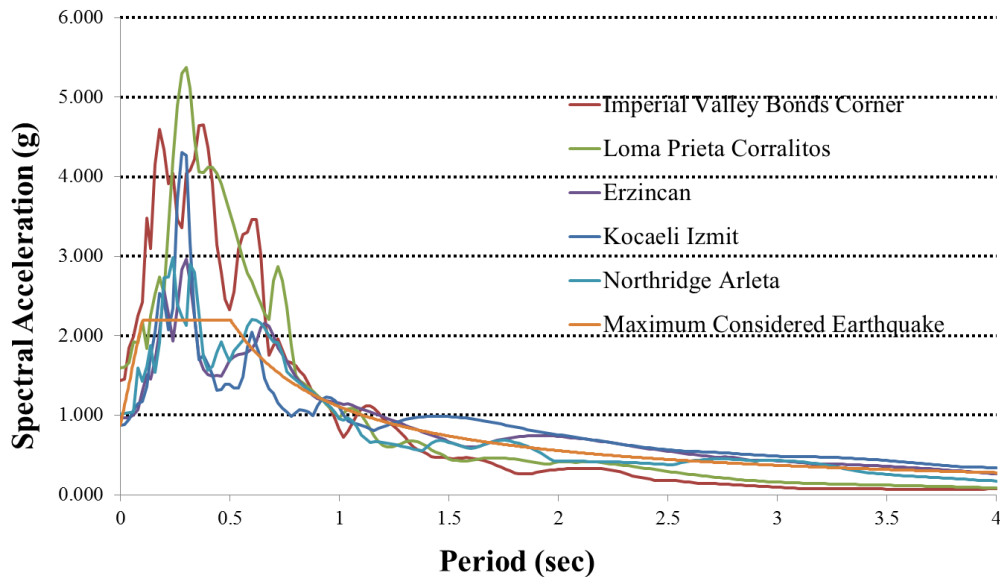
5.2.4 Scaling to MCE

After the MCE is found, spectral analysis of each selected earthquake is required. This is done by applying the earthquake to “structures” with a large range of fundamental periods. This creates a spectrum of peak accelerations versus the period of the structure. This can be done efficiently by applying the earthquakes to Seismosignal software by Seismosoft (SeismoSoft, 2013). This gives the spectral analysis for each earthquake. Once all are found, they are compared to the MCE spectrum. They are then scaled to match the MCE at a certain fundamental period for the structure being designed. This fundamental period is found by using the ASCE 7 design code found in chapter 12, (ASCE, 2005b). The fundamental period of the structure being designed is affected by the height of the structure, the location and site

assumptions mentioned before in the design spectrum calculations. Once the fundamental period is found for each structure, the scale factor for each seismic event can be found. This scale factor can be used to scale each seismic event to match the MCE for the fundamental period of each structure. Now the histories are normalized and scaled. They are ready to be applied to the structures to test the responses. Table 5-2 shows the scale factors found for each record for each structure being tested. Figure 5-1 shows the spectral acceleration of the records versus the period of the structure being designed for near and far field records.

Table 5-2 Scale factors of ground motion records

Earthquake Name	Scale Factor		
	4-Story	7-Story	10-Story
Imperial Valley Bonds Corner	1.857	2.788	2.882
Loma Prieta Corralitos	2.545	3.941	3.138
Erzincan	4.203	4.809	3.142
Kocaeli Izmit	2.661	1.919	1.977
Northridge Arleta	2.125	2.446	2.624
Duzce Bolu	2.302	3.766	3.458
Northridge Canyon County WLC	3.177	2.535	2.198
Loma Prieta Capitola	3.254	3.843	5.734
Kobe Shin Osaka	4.054	2.890	5.145
Northridge Century City CC North	0.408	0.670	0.714



(a)

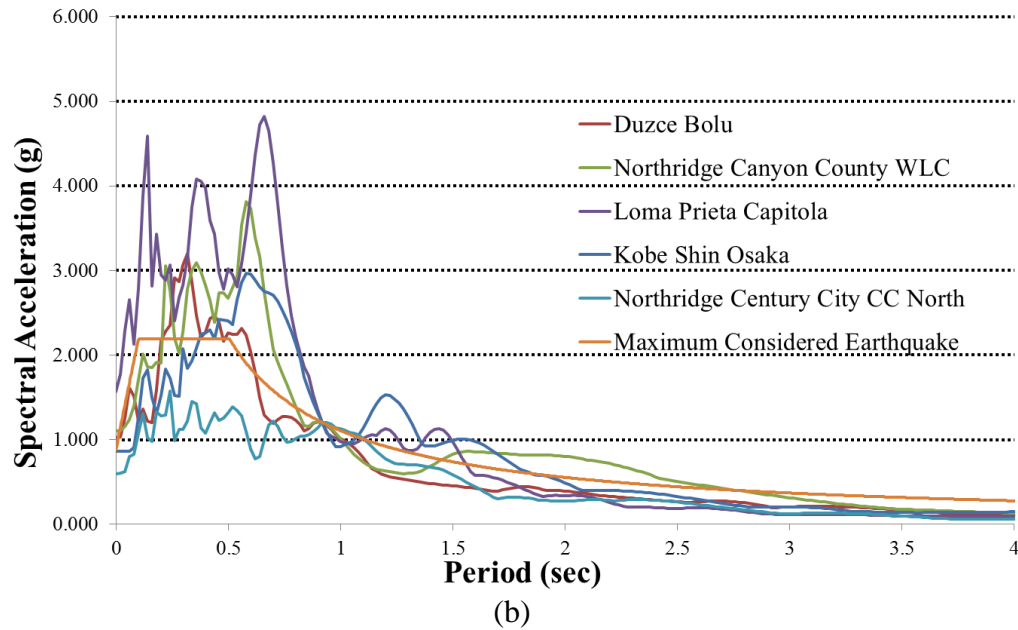
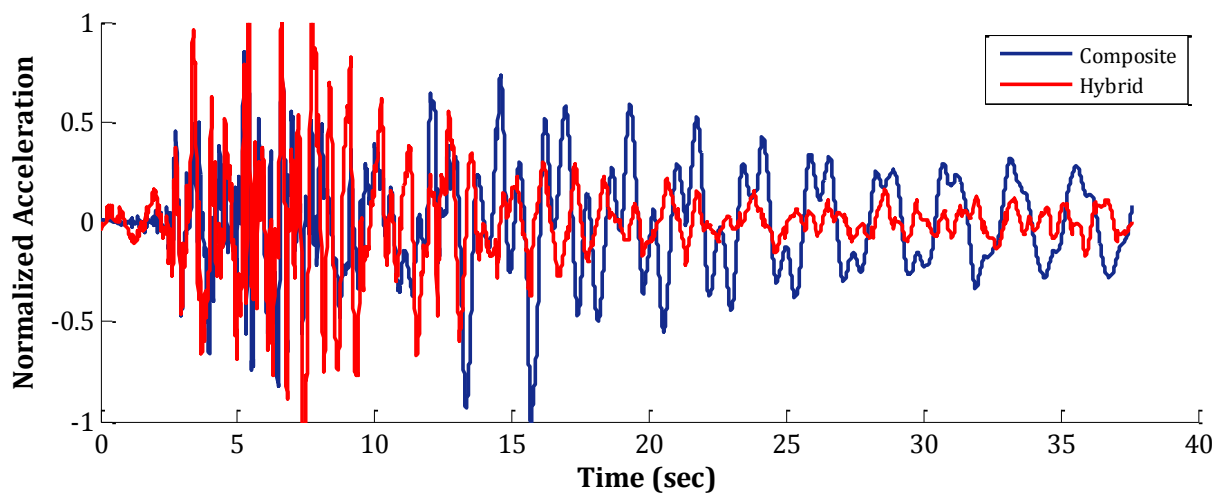


Figure 5-1 Response spectra of (a) near field records and (b) far field records compared to maximum considered earthquake

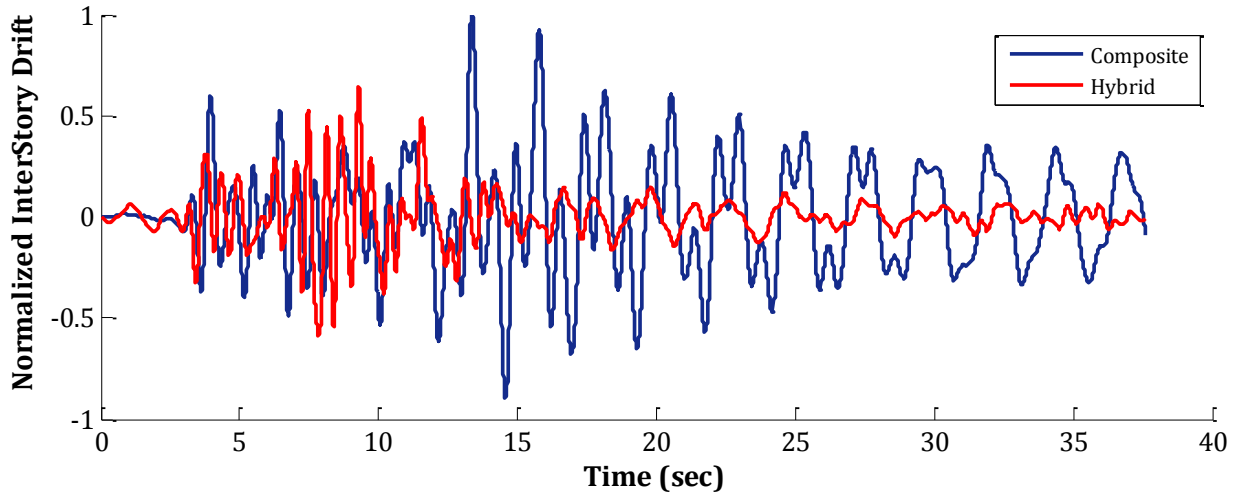
5.3 Responses of structures

The displacement, velocity, and acceleration of each degree of freedom of each structure are found for each earthquake loading over the entire time history of the event. From this large volume of data, the interstory drift and relative displacement of the slabs can be found. Since the size of data to be analyzed is very large, the story with largest excitation is the focus of the analysis in this investigation. This is consistently the tallest story of the structures, composite and hybrid design. This allowed the analysis to focus on a single degree of freedom for each parameter. The parameters of interest that are specifically targeted are the accelerations and interstory drift of the frame of the structure. The acceleration and interstory drift of each structure is plotted for a single earthquake history. The results of the rest of the earthquakes are compiled in figures that demonstrate the performance of the hybrid structure compared to the composite structure.

Figure 5-2 (a) shows the accelerations of the hybrid four story structure and the composite four story structure. This hybrid structure has the same design parameters as the optimized four story structure found in chapter 4. These accelerations are the response of the Imperial Valley earthquake of 1979 recorded at Bonds Corner. It is a near field earthquake. Figure 5-2 (b) shows the interstory drifts for the same structures under the same loading. It can be seen that the maximum accelerations are similar for the hybrid and composite structures, but the acceleration throughout the response is much lower for the hybrid structure. All responses are normalized to the maximum response of the composite structure. This behavior is found in many of the responses for acceleration. As indicated in the literature review in chapter 2, the damage found in a structure is often a result of the overall energy dissipated and excitation experienced, even at lower amplitudes, rather than the peak excitations. This means that even though the maximum accelerations are not reduced drastically, the damage to the structure is reduced significantly. This particular optimization does, however, provide a structure that consistently reduced the maximum interstory drift as well as the interstory drift throughout the event. If the optimization is focused more on the acceleration, this result would likely be found for acceleration as well.



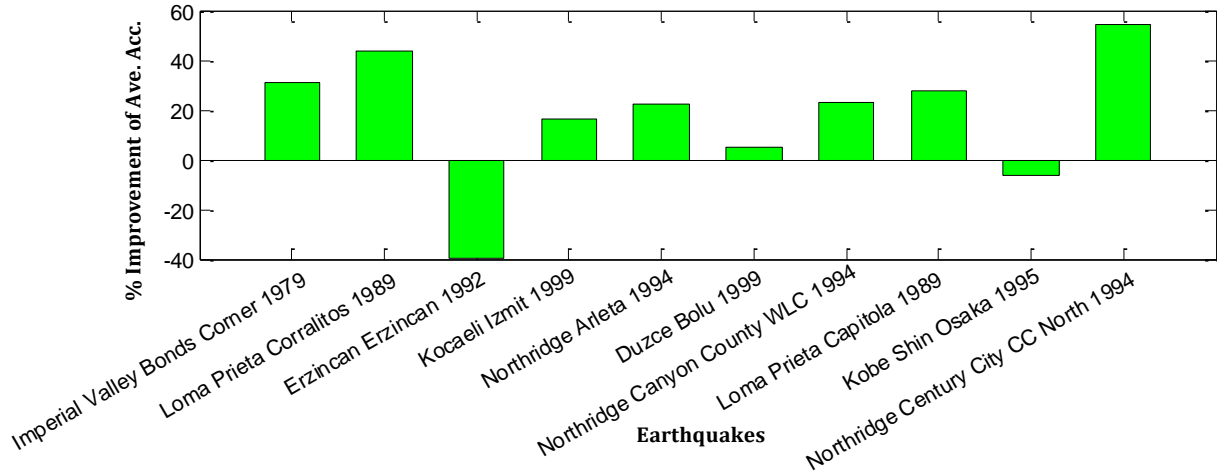
(a)



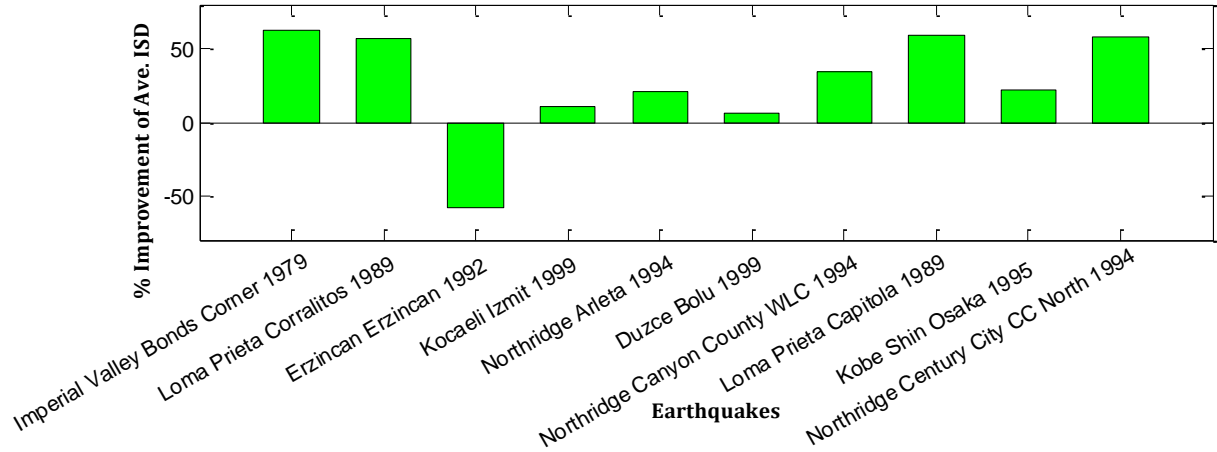
(b)

Figure 5-2. (a) Normalized Acceleration and (b) Normalized interstory drift of fourth story of optimized four story hybrid structure compared to composite four story structure under the Imperial Valley, Bonds Corner earthquake of 1979

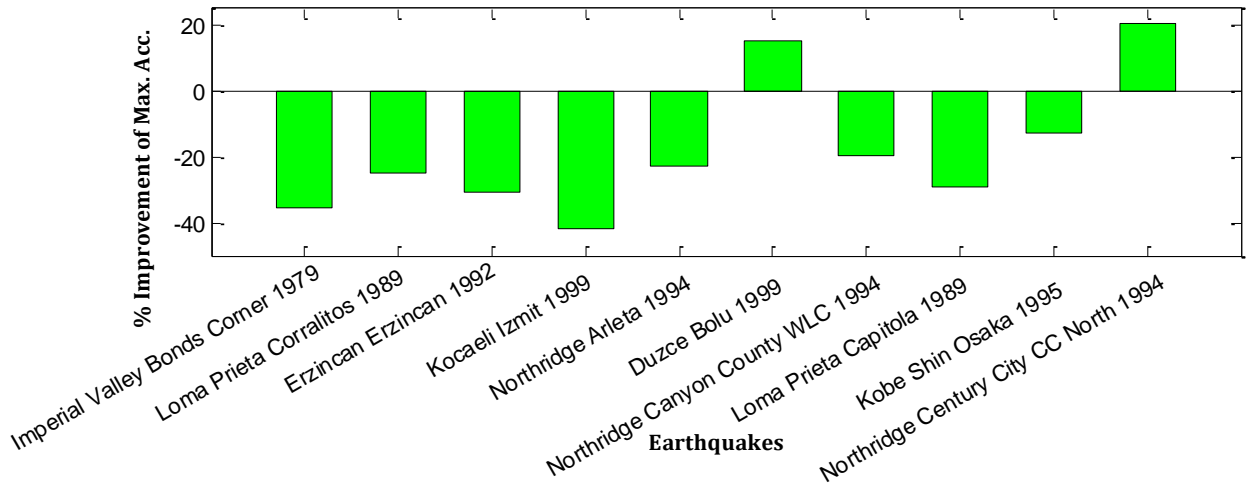
Figure 5-3(a) shows a complete assessment of the average absolute accelerations of the four story hybrid structure compared to the composite for each earthquake tested. Figure 5-3 is the percent of improvement seen in the hybrid structure compared to the composite. The first five earthquakes from left to right are near field earthquakes. The last five are far field. Figure 5-3 (a) shows that as much as 55% improvement is seen in the average acceleration. Two of the ten earthquakes have negative results, however. Figure 5-3 (b) shows the improvement of the average absolute interstory drifts of the same structure. All but one earthquake response is improved significantly. Figures 5-3 (c) and (d) show the same information as (a) and (b) but show maxima instead of averages. This is less conclusive because it may only represent a single instant in time. But the accelerations show very negative results in the maximums even though the average accelerations are very promising. The best improvement is only about 20% and improvement is only seen for two responses. Negative results by as much as 40% are seen. The maximum interstory drifts gave largely positive results again. The responses of some earthquakes are improved by as much as 50% with only two responses giving negative results.



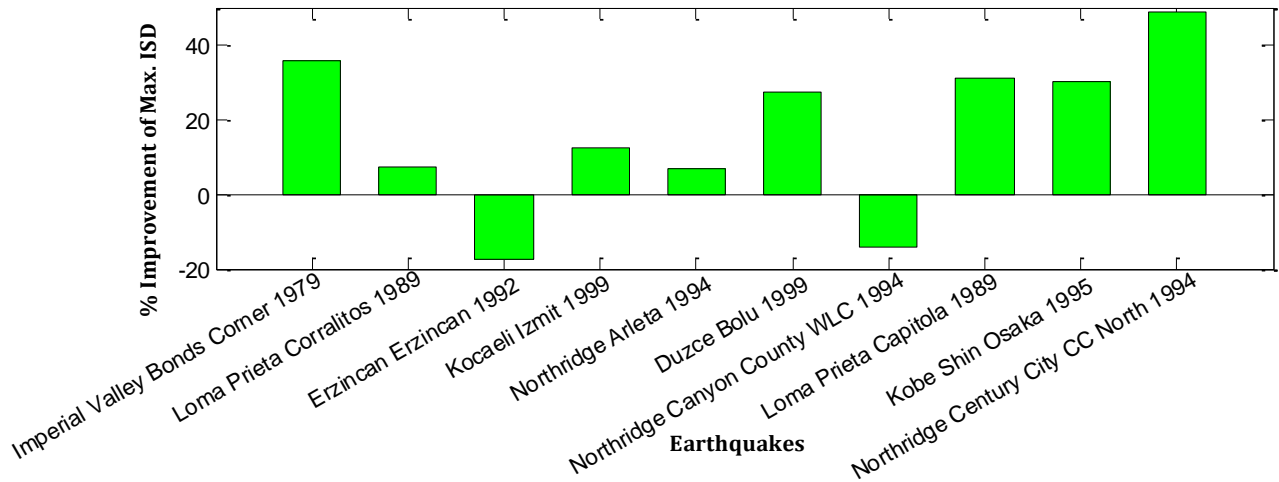
(a)



(b)



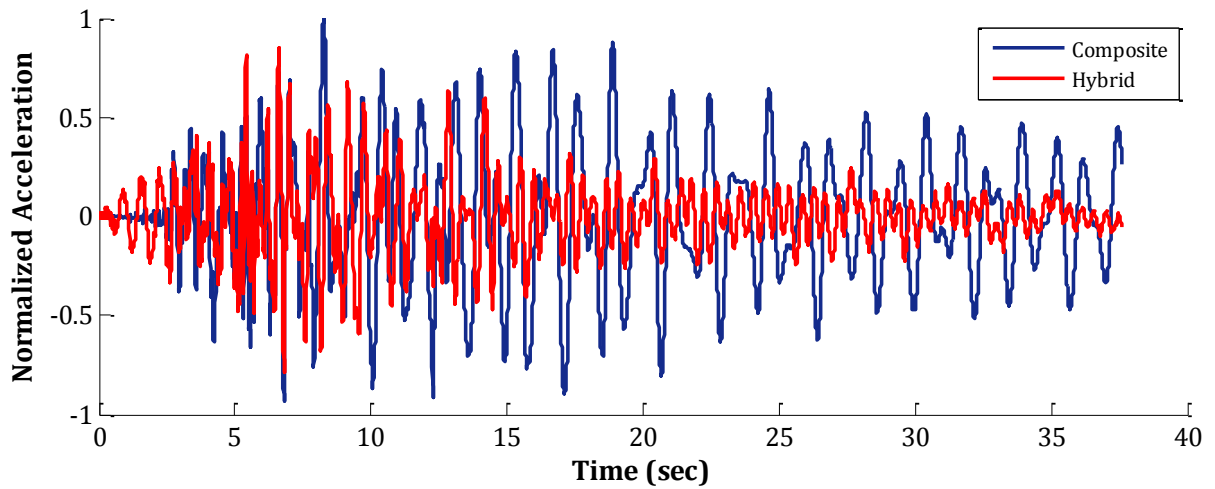
(c)



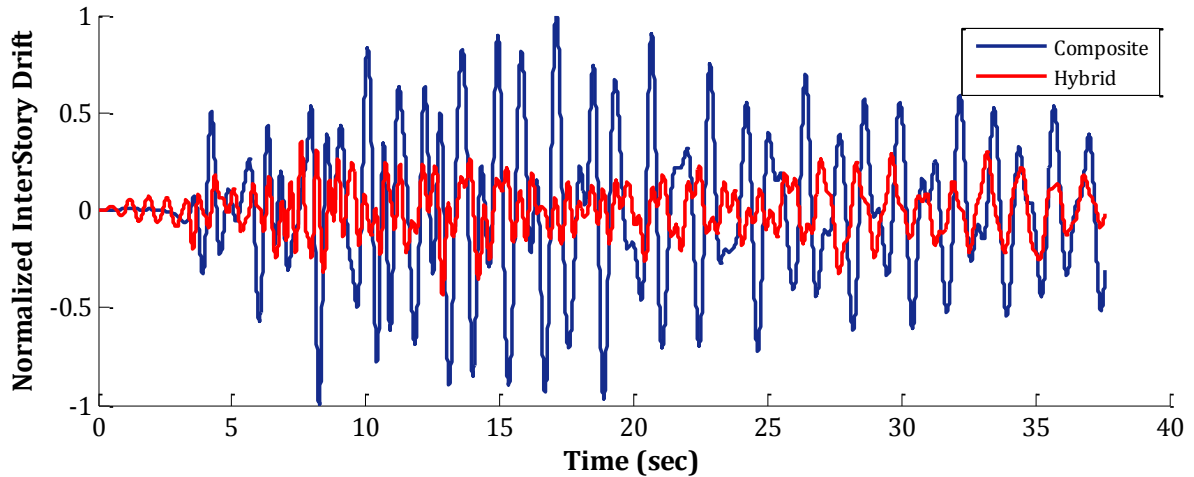
(d)

Figure 5-3. Percent Improvement of the fourth story of optimized four story hybrid structure versus composite four story structure over various earthquake loads for (a) the average acceleration (b) average interstory drift (c) maximum acceleration (d) maximum interstory drift

Figure 5-4 (a) and (b) represent the same information as Figure 5-2 (a) and (b) but for a seven story structure. The same earthquake response, Imperial Valley of 1979 at Bonds Corner, is shown. The seven story design is the same structure optimized in Chapter 4. This, again, shows little improvement in the maximum acceleration, but great improvement in the maximum interstory drift and overall acceleration and interstory drift.



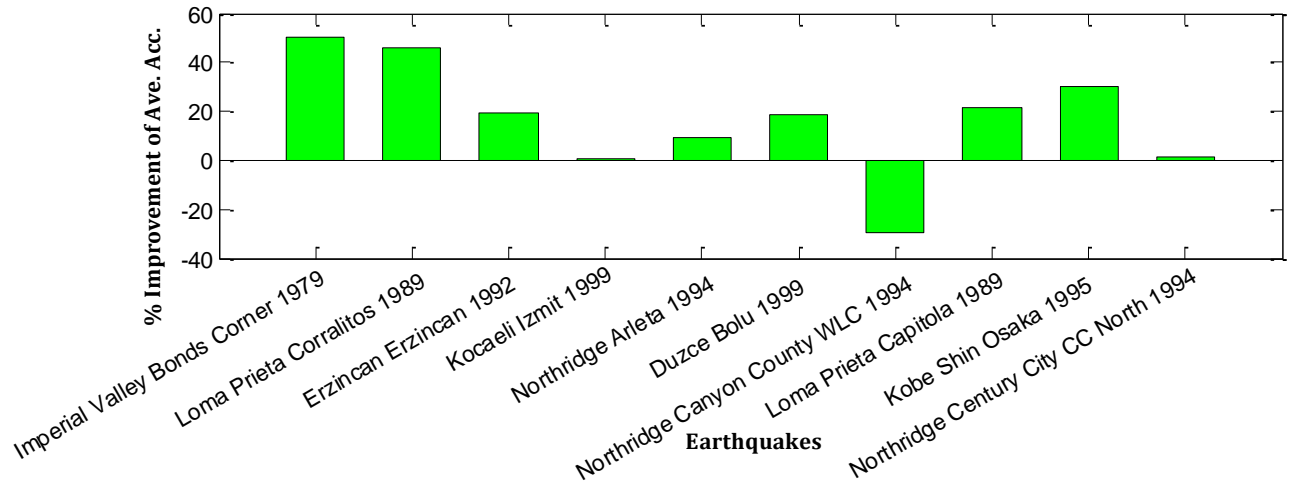
(a)



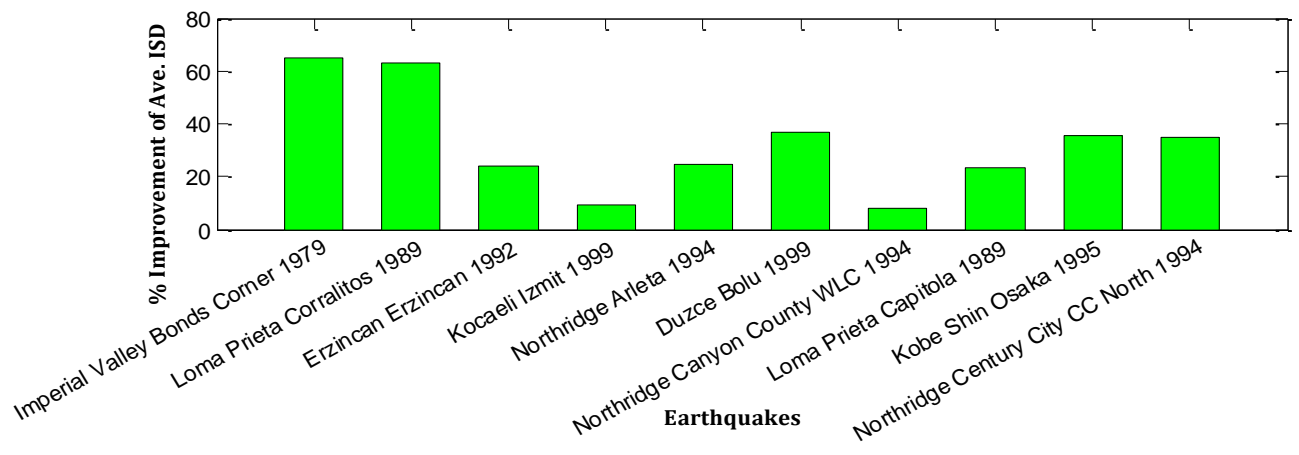
(b)

Figure 5-4. (a) Normalized Acceleration and (b) Normalized interstory drift of seventh story of optimized seven story hybrid structure compared to composite seven story structure under the Imperial Valley, Bonds Corner earthquake of 1979

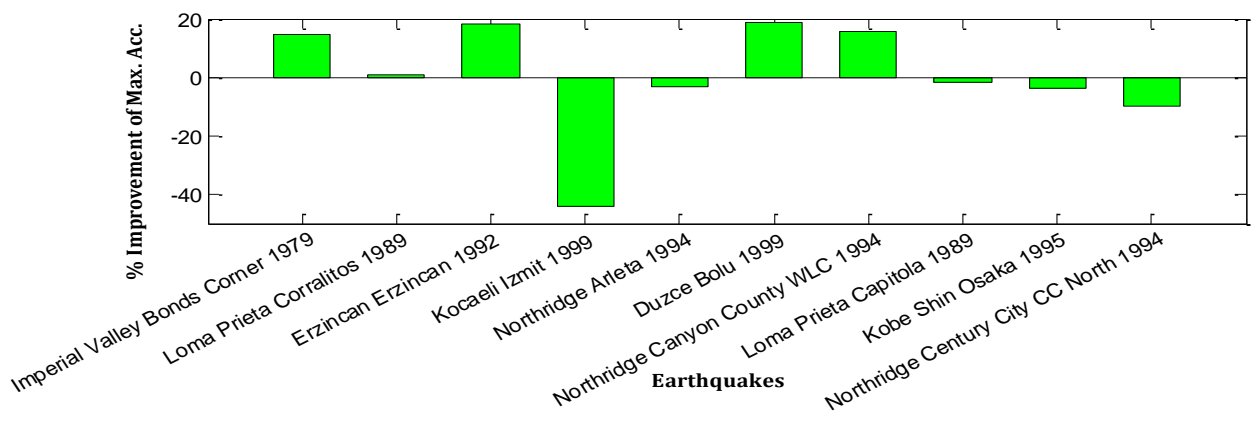
Figure 5-5 (a), (b), (c), and (d) represent the same data as Figure 5-3 (a), (b), (c), and (d) respectively but for the seven story design. Figure 5-5 (a) shows up to 50% improvement of the average acceleration and negative results for only one earthquake response. Figure 5-5(b) demonstrates improvement of average interstory drift for the responses to every single earthquake and by as much as 60%. Figure 5-5(c) shows slight improvement for the maximum accelerations for four of the responses and negative results for the other six. Only one of these earthquakes shows significant loss in effectiveness. Figure 5-5 (d) gives improvement of the maximum interstory drift for all but one response. The best response showed nearly a 60% improvement.



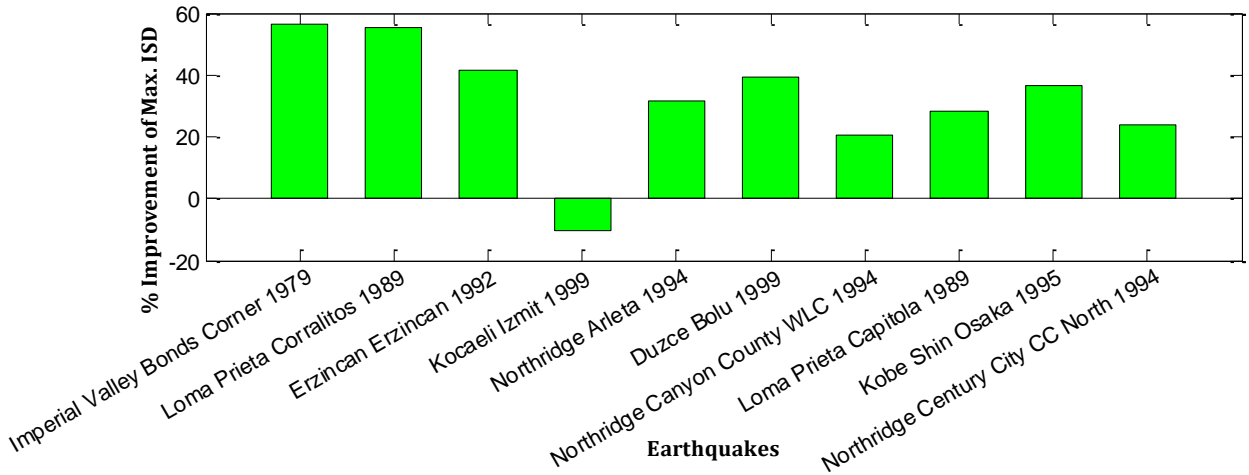
(a)



(b)



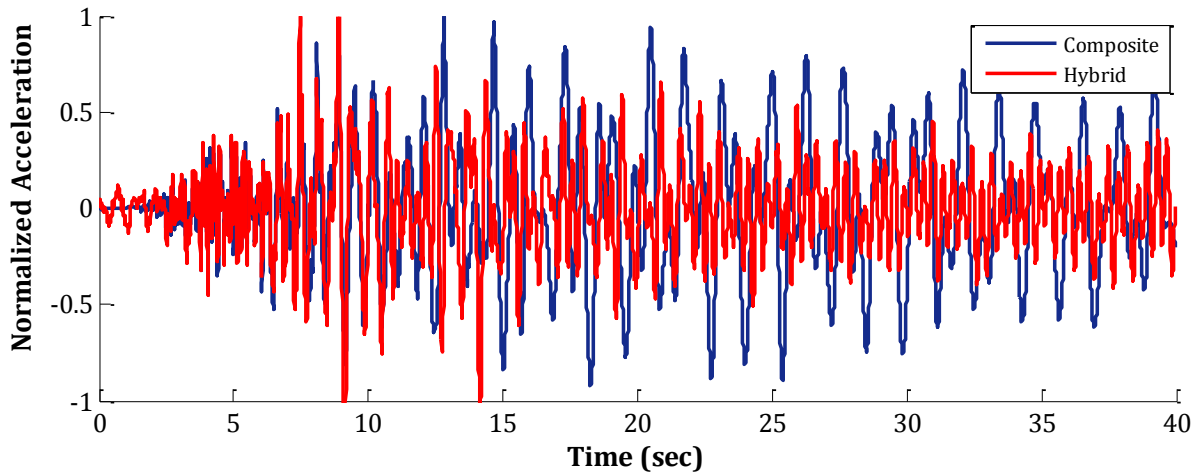
(c)



(d)

Figure 5-5. Percent Improvement of the seventh story of optimized seven story hybrid structure versus composite seven story structure over various earthquake loads for (a) the average acceleration (b) average interstory drift (c) maximum acceleration (d) maximum interstory drift

Figure 5-6 gives the same information as Figure 5-2 and 5-4, but for the Loma Prieta earthquake of 1989 recorded in Capitola and for the response of the ten story, optimized, structure from Chapter 4. In Figure 5-6 (a), no improvement can be seen in the maximum acceleration for this response, but the average acceleration shows improvement through time. Figure 5-6 (b) shows drastic improvement in all aspects of the interstory drift of the structure.



(a)

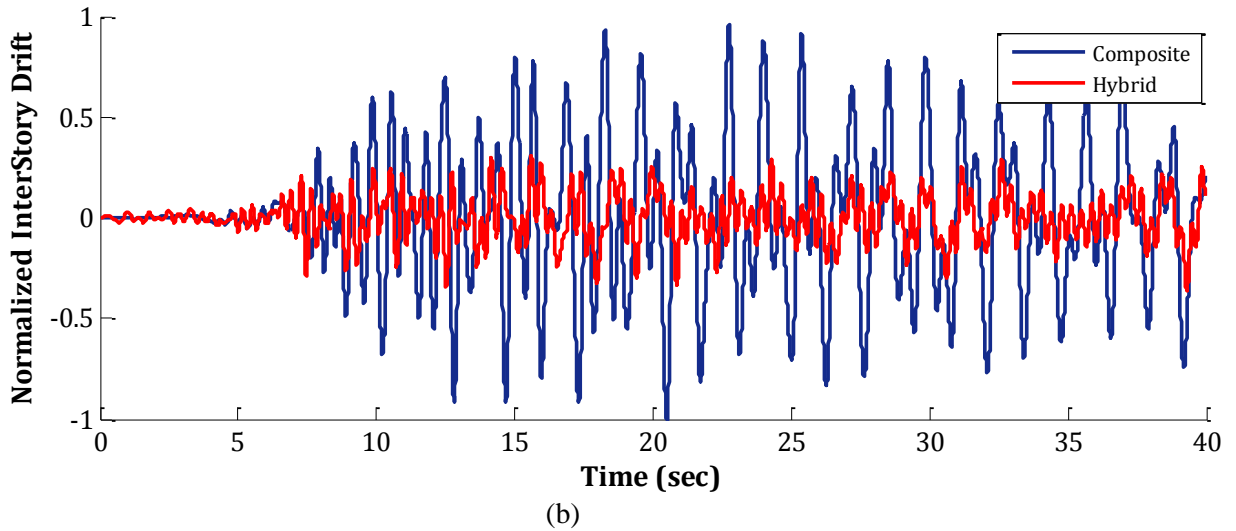
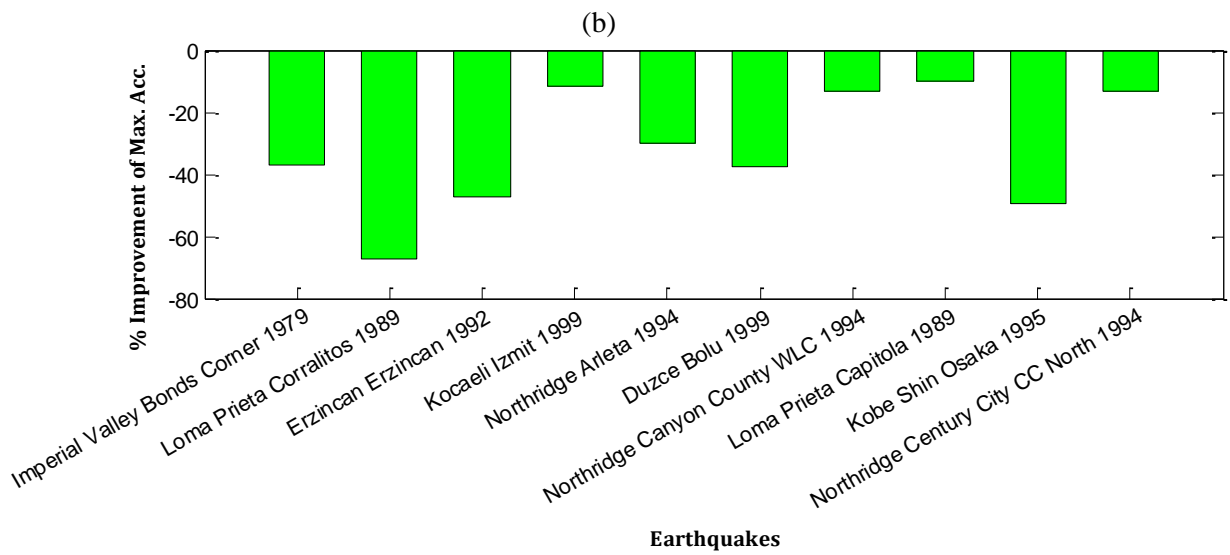
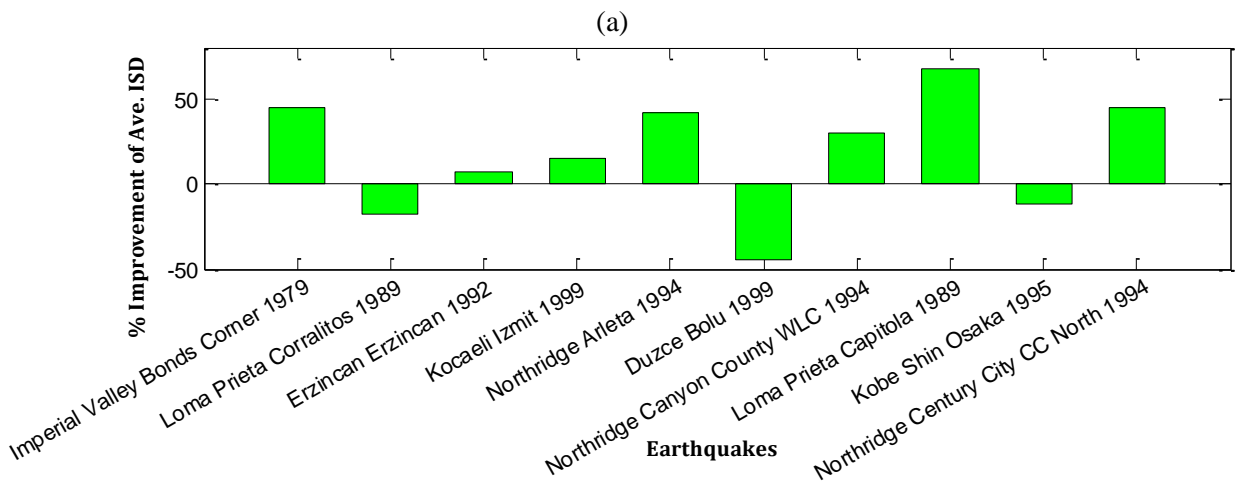
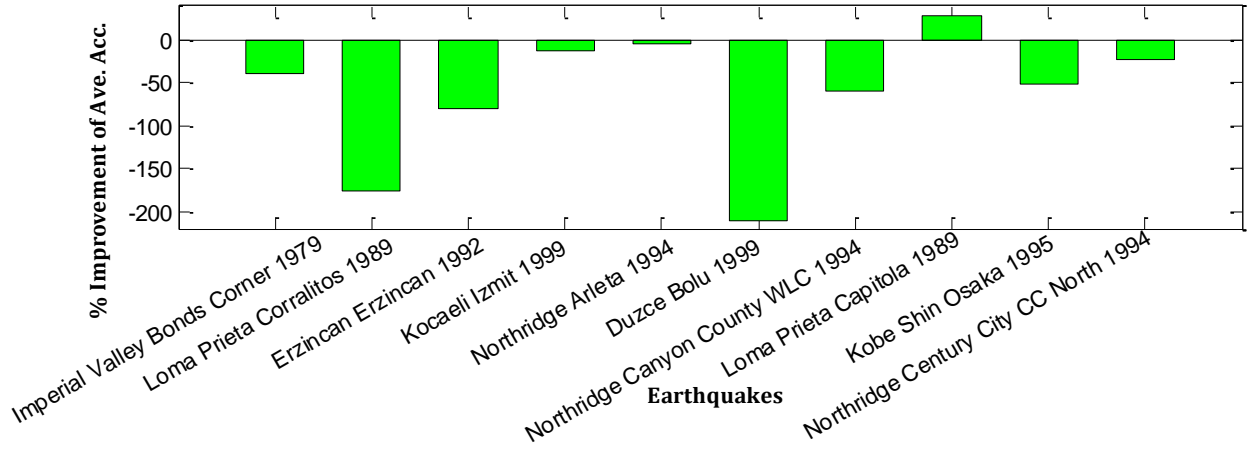
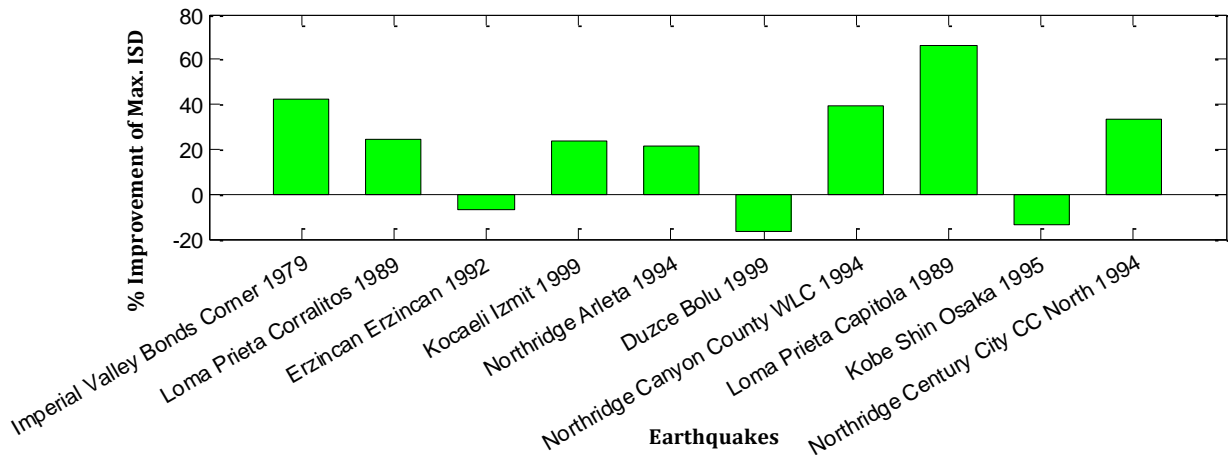


Figure 5-6. (a) Normalized Acceleration and (b) Normalized interstory drift of tenth story of optimized ten story hybrid structure compared to composite ten story structure under the Loma Prieta Capitola earthquake of 1989

Figure 5-7 shows the same information as Figure 5-3 and Figure 5-5 but for the ten story structure. Figure 5-7 (a) shows improvement in only a single response for the average acceleration and as much as 200 percent deterioration of performance in the worst response. Most are not as drastic. Figure 5-7 (c) shows worse responses for every earthquake in maximum acceleration. As described earlier this is not as important as the average. But when it is by over 60% this is a cause for concern. Though not ideal, the positive aspect of the results is that the interstory drift is still much improved for most responses. Figure 5-7 (b) shows improvements by as much as 55% and only two structures with negative results for average interstory drift. Figure 5-7 (d) improvements of over 60% in maximum interstory drift. There is improvement in every response but three. The worst negative result is only about -20%. So though the accelerations of the structure are high, the interstory drifts are very low.





(d)

Figure 5-7 Percent Improvement of the tenth story of optimized ten story hybrid structure versus composite ten story structure over various earthquake loads for (a) the average acceleration (b) average interstory drift (c) maximum acceleration (d) maximum interstory drift

5.4 Summary and Conclusions

The most important aspect to consider when analyzing these results is that they are optimized for parameters such as slab acceleration, global frame drift, and relative slab drift in addition to frame acceleration and interstory drift that are shown here. The additional parameters are not represented in this chapter. If optimization focused on acceleration, solely, the improvements would likely be much higher. However, improvement is important in all of these parameters and none can be neglected.

As is the point of testing many earthquakes over a range of frequencies, some of the events appear to induce near resonant excitations in the hybrid structure. These excitations result in responses much worse than the composite because the hybrid has a shifted resonant frequency. Many of the drastic improvements are likely due to the resonant frequency of the composite structure being excited. The important consideration is that the worst possible response of the proposed hybrid system is still drastically better than the worst possible response of the

composite structure in terms of displacement and acceleration. This is demonstrated by Figure 4-11 through 4-13 in chapter 4. These figure show that even away from resonance the response is not improved for the hybrid. The lack of improvement over many frequencies can be mitigated by energy dissipation. One consideration that must be remembered is that no damping device is being utilized in this experiment. If it is, the response over all frequencies would be reduced. This would broaden the range of responses that would be improved by the hybrid system.

Overall, most of the responses are improved by the hybrid system and the interstory drifts are especially improved. Only a few responses showed worse results, likely due to the proximity of the earthquakes primary frequency to the resonant frequency of the hybrid structure. The second important point is that the average improvement results are more important since the damage a structure experiences is more heavily influenced by the total excitation on the structure rather than just the maximum responses. The initial results of this system are very promising. Assessing the other parameters would be important for future research.

6. CONCLUSIONS

6.1 Summary of Current Work

The need for seismically resistant and near damage-free structures is well documented. Beyond designing structures that have the ability to withstand seismic events, society needs designs that prevent damage. Damage is not the total compromise of the structural integrity of a building. It is not even just cracks in the foundation. Though both of those are important reasons to design better structures and would save millions of dollars, damage can even be as little as fatigue in the members leading to reduced strength. This reduced strength, even at low vibrations can, over time, render a building unsafe without being noticed. To maintain a building's integrity, any and all energy must be deflected or dissipated.

Achieving the above mentioned performance targets is rather difficult. Base isolation must be harnessed to stay upright, thus transferring energy to the structure. Tuned mass dampers are severely limited. The most promising ideas are coming from innovative researchers who are applying unrelated ideas to the topic to find solutions. Engineers actually designing structures that allow relative motion of parts of the structure itself are finding promising results. And this is only one direction which research is leading.

The objective of this thesis is to find a solution to maintain a structure's integrity during seismic events. Find a method of designing a structure to reduce any and all demands. This is to be done by isolating the floor slabs of a structure to remove them from the inertia that is mobilized by seismic events. The large mass ratio that can be achieved by this strategy should, theoretically, create a greatly stabilized system. The equations of motion are developed and

included all components necessary to design a feasible structure, including a sloped support to center the slab back into place, bumpers to protect the structure from the motion of its slabs, and even the friction of the sliding surfaces themselves. The goal of this thesis is to design a program that could be applied to structures of any size. The final objective is to demonstrate the effectiveness of this system over many excitations. The proposed hybrid system creates an isolation system by isolating the floor slabs of a structure and allowing them to displace relative to the structure. The slabs re-center with the use of a sloped surface and bumpers protect the frame and slab from damaging contact. These aspects cause interaction and relative displacements between the slab and the frame. The interaction induces behaviors similar to TMD systems. These factors and the presence of friction forces between the supporting frame and floor slab provide a hybrid type system that utilizes aspects of many different vibration control systems.

The equations of motion for proposed hybrid system are developed, numerically solved, and its performance tested. One real advantage of this system is the simplicity. Depending on what goals the designer desires for the optimization, the system can be adjusted. Because of the large mass ratio it can be effective over many performance parameters at once. The redundancy of the stiffness between the frame and the slab offers flexibility in design as well.

6.2 Summary of Findings

Once optimized, the overall response showed an improvement of over 40% compared to a composite system. When each individual parameter is tested, the drift of the structure and interstory drift reflected the same improvement of approximately 40%. Acceleration response

showed an interesting difference. The acceleration of the slab, which would only affect the inhabitants and equipment in the building, does not improve. However, the acceleration of the structure is reduced by over 60%. This would drastically reduce the demand on the frame of the structure. The relative displacement of the slabs appeared to be high. However, it is difficult to judge this value because if compared to a regular structure, the relative displacement is zero. It does not appear that the relative displacement is outside of any feasible range.

The simplicity of this system is one of its great strengths. Though the specifics of constructing such a structure are not included, it would not be difficult. The repair would be even easier. The most difficult construction aspect is likely the curved support for the slabs. Beyond that, with the right design, this system should be effective in both primary directions. The stiffness of the bumpers can be optimized separately for each direction, and with proper design it would be effective both directions. One way to alleviate any problems that this may create is built into the design of the system. Two of the optimized parameters affect the stiffness between the slab and the structure. One is the slope of the curve and another is the stiffness of the bumpers. If the slope needs adjusting, one only needs to change the stiffness of the bumpers and the desired curvature can be achieved. If the results do not appear to have improved enough, it is stated that no damping devices are added to this system. If damping devices are added between the slab and the structure the results drastically improve. This simple addition could make this design superior to other systems.

The only limitations of this system are found in the materials used to build the design parameters. There is a lower limit on the radius of curvature of the structure, but that can be adjusted with the bumper stiffness as explained above. The limits on the bumper depend on the material properties being used. If a higher stiffness value is required, then more bumpers can be

added. The limitations on the friction coefficient lie, again, in the materials used as contact surfaces. There is a wide variety of possible friction values and should not be difficult to design.

Compared to most vibration control systems, this design offers similar or better results. What is unique about the system is that there are no damping devices contributing to energy dissipation. If these are to be included in the system the results would be even better.

6.3 Future Research

Adjustments could be made to the proposed hybrid system. For example, as the damage assessment literature review indicated, proper damage control should be focused on the total energy imposed on the structure. If a comprehensive damage evaluation could be calculated this would be an ideal optimization parameter for design. Instead of focusing on the drift and the accelerations which are easy to quantify and visualize, the energy and damage should be the focus of the optimization.

Once these results are quantified, these designs should be built in a computer model. A finite element design in a program such as ABAQUS should be tested over these same seismic events. The structure should be designed to match the optimized structure found by the optimization of the program in this thesis. The results of these tests should either validate the findings of the design or point out flaws, leading to their corrections.

Depending on the desired results, the design could be expanded as well. As discussed before, damping devices could be added to improve energy dissipation and reduce the response of the structure over all frequencies of excitation. Though this would be a simple addition and require minimal derivation or changes to the calculations, this thesis is focused on the isolation effects

and demonstration of the ability of this system without excess energy dissipation. Combining this design with energy dissipation appears to have great possibilities.

Another expansion on the design would be to test the bidirectional abilities of the system. It should not be difficult to design one set of parameters in one direction, and another set in the other. Friction may have to be constant and the radius may have to be relatively large, but otherwise the bumpers should not impose any difficulties. This ability would greatly increase the applicability of this system to the real world.

Multi-hazard applications would be the most intriguing of all research expansions. Adjusting the equations of motion to accommodate wind loads in place of seismic loads would not be difficult to do. The same design could be optimized for wind loading just as it is for seismic loading. This design, being simple and robust, should be useful for any loading for vibration control. Certain differences are apparent. But the adjustability of this system should be enough to accommodate wind design.

The potential of this proposed hybrid system under earthquake excitation can be extended to the case of multi-hazard mitigation. For example, if one could optimize for both wind and seismic loading simultaneously and attempt to find a design that reduces the overall responses of both loadings, the result would be ideal. The necessity of multi-hazard design, especially in the realm of wind and seismic design, is becoming glaringly apparent. In areas such as Japan, both hazards present enormous threats to society. Though design code should be changed, designing a structure to mitigate excitations from both hazards in the same design would be revolutionary. The simplicity and robustness of this system, stemming from a very high mass ratio, should give this design that possibility.

The most obvious and final step of this research should be to test it in the real world. Building a structure and applying the hybrid design to the slabs should be tested on a shake table. A structure of any size could be designed and tested. Once the seismic testing is completed, wind tunnel testing could be done as well. If all research points towards progress, this would be the next step.

REFERENCES

- Almazán, J. L., De la Llera, J. C., Inaudi, J. a., López-García, D., & Izquierdo, L. E. (2007). A bidirectional and homogeneous tuned mass damper: A new device for passive control of vibrations. *Engineering Structures*, 29(7), 1548–1560. doi:10.1016/j.engstruct.2006.09.005
- ASCE. Seismic Design Criteria (2005).
- ASCE. Seismic Design Requirements for Building Structures (2005).
- Bhaskararao, A. V., & Jangid, R. S. (2006). Seismic analysis of structures connected with friction dampers. *Engineering Structures*, 28(5), 690–703. doi:10.1016/j.engstruct.2005.09.020
- Boyer, C. B. (1968). *A History of Mathematics* (1st Editio.). New York: Wiley.
- Chai, Y. H., Romstad, K. M., & Bird, S. M. (1995). Energy-Based Linear Damage Model for High-Intensity Seismic Loading. *Journal of Structural Engineering*, 121(May), 857–864.
- Chopra, A. K. (1995). *Dynamics of Structures*.
- Chulahwat, A. (2013). *Structural System with Suspended and Self-Centered Floor Slabs for Earthquake Resistance*. Colorado State University.
- Chung, W.-J., Yun, C.-B., Kim, N.-S., & Seo, J.-W. (1999). Shaking table and pseudodynamic tests for the evaluation of the seismic performance of base-isolated structures. *Engineering Structures*, 21(4), 365–379. doi:10.1016/S0141-0296(97)00211-3
- Connor, J. (2003). *Introduction to Structural Motion Control* (1st Editio.). New York: Prentice Hall.
- Connor, J. J. (2003). Tuned Mass Damper Systems. In *Introduction to Structural Motion Control* (2nd ed., pp. 217–285).
- Constantinou, M. C., Soong, T. T., & Dargush, G. F. (1998). *Passive Energy Dissipation Systems For Structural Design and Retrofit* (1st Edtion.). Buffalo: Multidisciplinary Center for Earthquake Engineering Research.
- Den Hartog, J. P. (1940). *Mechanical Vibrations* (2nd Editio., p. 436). New York: McGraw Hill.
- Eartherton, M., Hajjar, J., Deierlein, G., Ma, X., & Krawinkler, H. (2010). Hybrid Simulation Teting of a Controlled Rocking Steel Braced Frame System. In *Proceedings of the 9th U.S. National and 10th Canadian Conference of Earthquake Engineering*. Toronto.

- Elenas, a, & Meskouris, K. (2001). Correlation study between seismic acceleration parameters and damage indices of structures. *Engineering Structures*, 23(6), 698–704. doi:10.1016/S0141-0296(00)00074-2
- Elgamal, A. (n.d.). Assignment for MDOF System & Modal Analysis. In *MDOF System & Modal Analysis* (Vol. 2, pp. 1–5).
- Feng, M. Q., & Mita, A. (1995). Vibration Control Of Tall Buidlings Using Mega Subconfiguration. *Journal of Engineering Mechanics*, 121(10), 1082–1088. doi:10.1061/(ASCE)0733-9399(1995)121:10(1082)
- Gerges, R. R., & Vickery, B. J. (2005). Optimum design of pendulum-type tuned mass dampers. *The Structural Design of Tall and Special Buildings*, 14(4), 353–368. doi:10.1002/tal.273
- Gewei, Z., & Basu, B. (2010). A study on friction-tuned mass damper: harmonic solution and statistical linearization. *Journal of Vibration and Control*, 17(5), 721–731. doi:10.1177/1077546309354967
- Ghobarah, A., Abou-Elfath, H., & Biddah, A. (1999). Response-Based Damage Assessment of Structures. *Earthquake Engineering and Engineering Seismology*, 28(4), 79–104.
- Gray, B. M., Christopoulos, C., Ph, D., Eng, P., Packer, J., & Gray, M. (2012). A New Brace Option for Ductile Braced Frames. *Modern Steel Construction*, 40–43.
- Hanselman, D. C., & Littlefield, B. (2005). *Mastering MATLAB 7*. Upper Saddle River: Prentice Hall.
- Hansen, N. (2011). *The CMA Evolution Strategy : A Tutorial*.
- Hoshimura, K. (2005). *Covariance Matrix Adaptation Evolution Strategy for Constrained Optimization Problem*. University of Kyoto.
- Housner, G. W., Bergman, L. A., Caughey, T. K., Chassiakos, A. G., Claus, R. O., Masri, S. F., ... Yao, J. T. P. (1997). Structural Control: Past, Present, And Future. *Journal of Engineering Mechanics*, 123(September), 897–971.
- Huang, M. J., Malhotra, P. K., & Shakal, A. F. (1993). Analysis of Records from Four Base-Isolated Buildings During Low Levels of Ground Shaking. *Applied Technology Council*, 1(17), 319–330.
- Johnson, E. A., Ramallo, J. C., Spencer, B. F., & Sain, M. K. (1998). Intelligent Base Isolation Systems. In *Second World Conference on Structural Control* (pp. 1–10).
- Joshi, A. S., & Jangrid, R. S. (1997). Optimum Parameters of Multiple Tuned Mass Dampers for Base-Excited Damped Systems. *Journal of Sound and Vibration*, 202(5), 657–667.

- Kelly, J. M. (1986). Aseismic base isolation : review and bibliography. *Soil Dynamics and Earthquake Engineering*, 5(3), 202–216.
- Kelly, J. M. (1998). Base Isolation : Origins and Development. *National Information Service for Earthquake Engineering*, 8–13.
- Kelly, J. M., & Beucke, K. E. (1983). A Friction Damped Base Isolation System with Fail-Safe Characteristics. *Earthquake Engineering and Structural Dynamics*, 11(1), 33–56.
- Kravchuk, N., Colquhoun, R., & Porbaha, A. (2008). Development of a Friction Pendulum Bearing Base Isolation System for Earthquake Engineering Education. In *Proceedings of the 2008 American Society for Engineering Education Pacific Southwest Annual Conference* (pp. 1–16).
- Lee, J., & Fenves, G. L. (1998). Plastic-Damage Model for Cyclic Loading of Concrete Structures. *Journal of Engineering Mechanics*, 124(8), 892–900. doi:10.1061/(ASCE)0733-9399(1998)124:8(892)
- Lee, S., Woo, S., Cho, S., & Chung, L. (2008). Computation of Optimal Friction of Tuned Mass Damper for Controlling Base-Excited Structures. *ICCES*, 8(3), 115–120.
- Li, C., & Zhu, B. (2006). Estimating double tuned mass dampers for structures under ground acceleration using a novel optimum criterion. *Journal of Sound and Vibration*, 298(1-2), 280–297. doi:10.1016/j.jsv.2006.05.018
- Lourenco, R. (2011). *Design , Construction and Testing of an Adaptive Pendulum Tuned Mass Damper* By. University of Waterloo.
- Mahoney, M., & Hanson, R. D. (2009). Quantification of Building Seismic Performance Factors. *FEMA P965*, (June).
- Matta, E., & De Stefano, A. (2009a). Robust design of mass-uncertain rolling-pendulum TMDs for the seismic protection of buildings. *Mechanical Systems and Signal Processing*, 23(1), 127–147. doi:10.1016/j.ymsp.2007.08.012
- Matta, E., & De Stefano, A. (2009b). Robust design of mass-uncertain rolling-pendulum TMDs for the seismic protection of buildings. *Mechanical Systems and Signal Processing*, 23(1), 127–147. doi:10.1016/j.ymsp.2007.08.012
- Mohebbi, M., Shakeri, K., Ghanbarpour, Y., & Majzoub, H. (2012). Designing optimal multiple tuned mass dampers using genetic algorithms (GAs) for mitigating the seismic response of structures. *Journal of Vibration and Control*, 1–21. doi:10.1177/1077546311434520
- Mokha, B. A., Constantinou, M., & Reinhorn, A. (1990). Teflon Bearings in Base Isolation. I: Testing. *Journal of Structural Engineering*, 116, 438–454.

- Moon, K. S. U. N. (2010). Vertically Distributed Multiple Tuned Mass Dampers in Tall Buildings: Performance Analysis and Preliminary Design. *The Structural Design of Tall and Special Buildings*, 19, 347–366.
- Nakamura, S. (1995). *Numerical Analysis and Graphic Visualization with MATLAB*. Upper Saddle River: Prentice Hall.
- Newmark, N. M. (1959). A Method of Computation for Structural Dynamics. *Journal of the Engineering Mechanics Division*, (July), 67–94.
- Ormondroyd, J., & Den Hartog, J. P. (1928). The Theory of Dynamic Vibration Absorber. *ASME Journal of Applied Mechanics*, 50(7), 9–22.
- PEER Ground Motion Database. (2010). Berkeley, CA. Retrieved from <http://peer.berkeley.edu/>
- Ramallo, J. C., Johnson, E. A., & Jr, B. F. S. (2002). “ Smart ” Base Isolation Systems. *Journal of Engineering Mechanics*, 128(10), 1088–1099.
- Randall, S. E., Halsted, D. M., & Taylor, D. L. (1981). Optimum vibration absorbers for linear damped systems. *ASME Journal of Mechanical Design*, 103, 908–913.
- Saatcioglu, M., & Ozcebe, G. (1989). Response of Reinforced Concrete Columns to Simulated Seismic Loading. *Structural Journal*, 86(1), 3–12.
- SeismoSoft. (2013). SeismoSignal. Retrieved from <http://www.seismosoft.com/en/SeismoSignal.aspx>
- Setareh, M., Ritchey, J. K., Baxter, A. J., & Murray, T. M. (2006). Pendulum Tuned Mass Dampers for Floor Vibration Control. *Journal of Performance of Constructed Facilities*, 20(February), 64–73.
- Sladek, J. R., & Klingner, R. E. (1993). Effect of Tuned-Mass Dampers on Seismic Response. *Journal of Structural Engineering*, 109(8), 2004–2009.
- Spencer, B. F. J., & Sain, M. K. (1997). Controlling Buildings: A New Frontier in Feedback. *IEEE Control Systems*, (December), 19–35.
- Stephens, J. E., & VanLuchene, R. D. (1994). Integrated Assessment of Seismic Damage in Structures. *Computer-Aided Civil and Infrastructure engineering*1, 9(2), 119–128.
- Suidan, M., & Eubanks, R. (1971). *Cumulative Fatigue Damage in Seismic Structures*. University of Illinois, Champaign. Retrieved from http://www.iitk.ac.in/nicee/wcee/article/5_vol2_2792.pdf
- Tazarv, M. (2011). Linear Time History Analysis of MDOF Structure by Mode Superposition Method using Newmark’s Beta Method. Retrieved from <http://alum.sharif.edu/~tazarv/>

- Tedesco, J. W., MacDougal, W. G., & Ross, C. A. (1999). *Structural Dynamics: Theory and Applications* (1st Editio.). Menlo Park: Addison Wesley Longman Inc.
- Tsai, H., & Lin, G. (1993). Optimum Tuned-Mass Dampers for Minimizing Steady-State Response of Support-Excited and Damped Systems. *Earthquake Engineering and Structural Dynamics*, 22, 957–973.
- Warburton, G. B. (1982). Optimum Absorber Parameters for Various Combinations of Response and Excitation Parameters. *Earthquake Engineering and Structural Dynamics*, 10(3), 381–401.
- Warburton, G. B., & Ayorinde, E. O. (1980). Optimum Absorber Parameters for Simple Systems. *Earthquake Engineering and Structural Dynamics*, 8, 197–217.
- Yashinsky, M. (2006). Earthquake Damage to Structures. In *Earthquake Engineering for Structural Design* (p. 58). Boca Raton: Taylor and Francis Group, LLC.